Correlation between the dynamic cone penetration index and the subgrade resilient modulus obtained from the Falling Weight Deflectometer

Emmanuel Okang Klu, B.Sc. Civil (Hons)
(PG 2611108)

A Thesis Submitted to the College of Engineering
Kwame Nkrumah University of Science and Technology
in partial fulfilment of the requirements for the degree of

MASTER OF SCIENCE

in

ROAD AND TRANSPORTATION ENGINEERING

Department of Civil Engineering in the
Faculty of Civil and Geomatics Engineering
College of Engineering

May, 2011

CERTIFICATION

I hereby certify that this submission is my own work towards the MSc and that, to the best of my knowledge, it contains no material previously published by another person nor material which has been accepted for the award of any other degree of the University, except where due acknowledgement has been made in the text.

EMMANUEUL OKANG KLU	....	....
(Student)	Signature	Date
Prof. S.I.K. AMPADU	....	....
(Supervisor)	Signature	Date
Prof. Mohammed Salifu	....	....
(Head of Department)	Signature	Date

ACKNOWLEDGEMENT

I wish to express my sincerest gratitude to my programme Supervisor, Dr. S. I. K. Ampadu, a Professor and Provost, School of Engineering, K. N. U. S. T., Kumasi. His invaluable contributions and useful suggestions have contributed immensely to the success of this work.

I highly appreciate the invaluable assistance given to me by Mr Emmanuel Nii Bonne-Acquah, Director of Materials, Ghana Highway Authority. I also extend my appreciation to Mr Lawrence Lloyd Lanquaye Lamptey, Pavement Manager of Materials Division, Ghana Highway Authority.

I would also like to thank all those technicians and drivers who assisted in the field data collection, especially Mr Joseph Kwamina Akromah.

Last, but not the least, I would thank my dear wife (Tina) and the children, Abel-Livingbrook Adjetey Okang and Harold Graham Klu Okang. Their patience and forbearance helped in the success of this work.

DEDICATION

To my late father Mr. Theodore Klu Adjei, who so much desired to see me come this far and beyond in my education before being called to glory by the Lord. May his soul rest in perfect peace.

And

My wife (Tina) and the Children: Abel-Livingbrook Adjetey Okang and Harold Graham Klu Okang who had to bear with my absence during this study period.

ABSTRACT

Modern pavement design characterizes the subgrade soil in terms of the resilient modulus. This parameter is determined in a non-destructive in-situ method using the falling weight deflectometer (FWD) and in the laboratory from the repeated load triaxial test. These methods however are both expensive and time consuming and are not readily available in most highway departments in developing countries. On the other hand, the simple and inexpensive dynamic cone penetrometer has been extensively used for pavement in-situ subgrade characterization. The objective of this thesis is to find a correlation between the results of the Dynamic Cone Penetrometer index, DCPI and the output of the Falling Weight Deflectometer (FWD) test for purposes of estimating the subgrade resilient modulus. The study road is a major urban arterial road in Accra with varying terrain, comprising of a hill flanked by two valleys. The study road was sectioned into three according to the terrain, i.e. section 1 and 3 are in the valley whiles section 2 is on the hill. Fifty-two FWD deflections and Dynamic Cone Penetrometer field tests were conducted at these sections. Laboratory tests, performed on soils recovered from five trial pits sunk within this varying terrain, revealed two types of soils, namely, A-2-7 soil on the hill and A-6 soil in the valley. The results of the output of the FWD sensors were analyzed and correlated with the DCP penetration index, DCPI, for the subgrade soils and the unbound material lying on the subgrade. Statistical regression model for predicting the subgrade resilient modulus was developed based on the the results of the Dynamic Cone Penetrometer index, DCPI and the output of the Falling Weight Deflectometer (FWD) test for the subgrade soils. This was extended to the unbound material overlying the subgrade soil. The statistical regression model for predicting the resilient modulus based on the field tests of FWD and DCP penetration index results were developed on section by section basis for the subgrade soils and also for the unbound material. Combined sections with similar soil characteristics were also considered for both the subgrade and the unbound material. The model correlates the subgrade resilient modulus to the DCP penetration index, DCPI. Poor agreement were obtained between the resilient modulus of the of subgrade soils (A-6 and A-2-7) on the study road and the DCP penetration index, DCPI.

TABLE OF CONTENT

LIST OF TABLES

LIST OF FIGURES

LIST OF PHOTOGRAPHS

CHAPTER 1

1.1 Background

Subgrade material characterization plays an important role in the design, construction and maintenance of roadways. For this purpose, pavement engineers require assessment of the pavement structure and the characterization of the in-situ subgrade soils along alignment of the design road. Both destructive and non destructive tests can be conducted on the subgrade soils for characterization of the alignment soils.

The resilient modulus is an important parameter used to characterize the subgrade soil for the design and rehabilitation of roads. The resilient modulus is obtained through performance of laboratory repeated triaxial test on undisturbed subgrade soils or performing the falling weight deflection test (FWD) directly on the design road. The undisturbed soil used in the laboratory may be disturbed in some way during the sampling and handling process. The FWD testing has proven to be successful measuring the structural properties of the pavement in terms of the resilient modulus. The FWD has several desirable features which makes it favored over the laboratory repeated triaxial loading test. First, the load magnitude can be selected to match a typical wheel load expected on the designed road. Secondly, the pulse duration of the FWD is similar to that from a moving vehicle. Also, the deflections obtained from the FWD are highly accurate and absolute. Lastly, the FWD test can be performed at desired road locations and at selected distances. However, the use of FWD to evaluate pavements is limited to those agencies in countries that can afford the cost of acquiring the equipment. Also trained personnel are required to perform and analyzed the results of the FWD test. The cost of performing the test is very high especially on network level.

The Dynamic Cone Penetrometer (DCP) test in some instances has been used to characterize the pavement properties and the subgrade soils in particular for design and rehabilitation of roads in terms of the CBR values. The DCP test is easy to acquire by any road agency and the test can be performed by anybody trained within a short time. The data is easily analyzed using any curve plotting software. The DCP test is rapid, inexpensive and can be performed in inaccessible areas. Attempts have been made to convert the CBR values into resilient modulus using correlations for design purposes.

However, these correlations have various limitations. For example, the correlations are valid for the type of material location of the researcher. Also, the correlations are limited to particular CBR range and certain soil types.

Thus a research in finding a correlating between the FWD subgrade resilient modulus readings and the DCP penetration values using soils typical to this sub region will be helpful to agencies that do not have the equipment for performing the resilient modulus test.

1.2 Objective of Study

The objective of this study is to establish a correlation between the FWD subgrade resilient modulus and the Dynamic Cone Penetrometer penetration values (mm/blow) for the purpose of predicting the subgrade resilient modulus from the DCP penetration index D. Also to compare the developed model with other established correlations. The developed model would be used to predict the sugrade modulus from the DCP penetration index D.

Specifically, the study will

1. Determine the resilient modulus of the various pavement layer over a stretch of road using the FWD.
2. Determine the DCP penetration profile of the various pavement layers over the same stretch of road.
3. Develop a mathematical correlation between the FWD resilient moduli and DCP penetration indices.

1.3 Justification of Study

The cost of undertaking a Falling Weight Deflectometer test for structural classification of roads is $1000 a day. This is high for developing countries. Analysis of the deflected values using the back-calculation requires experts and specialised personnel with knowledge in the analysis software. Laboratory repeated load triaxial test (RLT) requires well-trained personnel and expensive laboratory equipment and it is also considered relatively time-consuming.

On the network level for road appraisal purposes, road agencies need to classify the structural conditions of the various sections of roads at the minimum cost within the shortest time interval.

The DCP equipment, relatively simple in design and operation, has been used successfully by pavement engineers for the characterization of pavement soils over the years.

Researchers such as Chen et al. (2001) used the Dynamic Cone Penetrometer penetration rates (mm/blow) to calculate the CBR which is to estimate the subgrade modulus. The relationship is

M_R (MPa) = 17.58 x CBR …………………………… (1)

This yield results comparable to subgrade resilient modulus. But this is said to have reasonable results only for fine grained soils with a soaked CBR of 10 or less. The objective of this study in finding a correlation between the FWD subgrade resilient modulus and the DCP penetration values (mm/blow) would assist pavement engineers carry out a quick structural classification of the various roads in the entire net work for budgeting purposes. It would also be of help to those developing countries who could not acquire the FWD equipment as a result of cost implications. Thus the determination of a correlation of FWD deflection and the Dynamic Cone Penetrometer penetration values (mm/blow) for the prediction of the subgrade resilient modulus would go a long way to assist road agencies in selecting roads for rehabilitation or up grading at the least cost. The results of this research is anticipated to provide a relatively simple, rapid, cost-effective and repeatable approach to estimate the resilient modulus of subgrade soils for new pavement design and for pavement overlay design.

1.4 Scope of Study

The scope of this study includes delineating the study road into sections according to the topography. The scope of the study also includes conducting field and laboratory tests at the identified sections. The field test involves conducting fifty two FWD and DCP field tests at 100m intervals and excavating five trial pits at these three sections along the study road. The laboratory tests involves performance of Atterberg limit test and sieve analysis on subgrade soils recovered from the trial pits at the three sections on the study for classification.

The wet sieve analysis includes the hydrometer test for the classification of the study road soils. The undisturbed samples were used to determine the dry density of the in-situ soil.

The scope of the study also includes using statistical analyses to develop models for the prediction of the FWD reading of the resilient moduli from the DCP penetration index.

These prediction models have been used to correlate the FWD readings of the moduli for the unbound materials and the subgrade soils with the DCP penetration values separately at the depth of occurrence of these materials.

1.5 Thesis Outline

This thesis is divided into five Chapters. Chapter one is the introduction. Chapter two covers the literature review. It includes definition of the resilient modulus, methods of measuring the resilient modulus, some known correlations that exist between the DCP penetration index and the back-calculated resilient modulus.

Chapter three describes the procedure used for FWD and Dynamic Cone Penetrometer data acquisition as well as the laboratory tests conducted on the recovered subgrade soils. It also describes how the field data has been analyzed.

Chapter four presents the discussion of results of test data for the FWD and the DCP conducted at the project road for establishing a correlation for this thesis report. Finally, the recommendations, and conclusions of this thesis are presented in Chapter five.

CHAPTER 2: LITERATURE REVIEW

2.1 Soil Resilient Modulus, M_R

2.1.1 Definition of Soil Resilient Modulus, M_R

The concept of a resilient modulus of a material was originally introduced by Seed et al in 1962. The resilient modulus of pavement materials has been the subject of extensive research since that time. The main purpose is to use the resilient modulus parameter as input for pavement design, since the resilient modulus test simulates the pavement behavior under dynamic traffic load.

The term resilient modulus, M_R, describes the recoverable effects of soils and other unbound materials when an applied dynamic load at the point of application has been removed. It is well known that most pavement materials are not elastic, and experiences some permanent deformation after a number of load applications. The term is also used to separate out the component of soil behaviour which is elastic though non-linear from plastic component, where strains are non recoverable. Under stress conditions, the resilient modulus, M_R, is defined as the ratio of stress due to dynamic load to recoverable or resilient axial strain. Under dynamic condition, the resilient modulus, M_R, is defined as the deviatoric stress divided by the recoverable strain.

$$M_R = \frac{\sigma_d}{\varepsilon_r} \qquad \text{..} \ (2)$$

where ε_r is the recoverable axial strain

σ_d = P/A = stress due to dynamic load, deviator stress ($\sigma_1 - \sigma_3$),

P = applied axial load

A = the cross sectional area

ε_r = D/Lg = recoverable or resilient axial strain

D = axial deformation

Lg = gauge length.

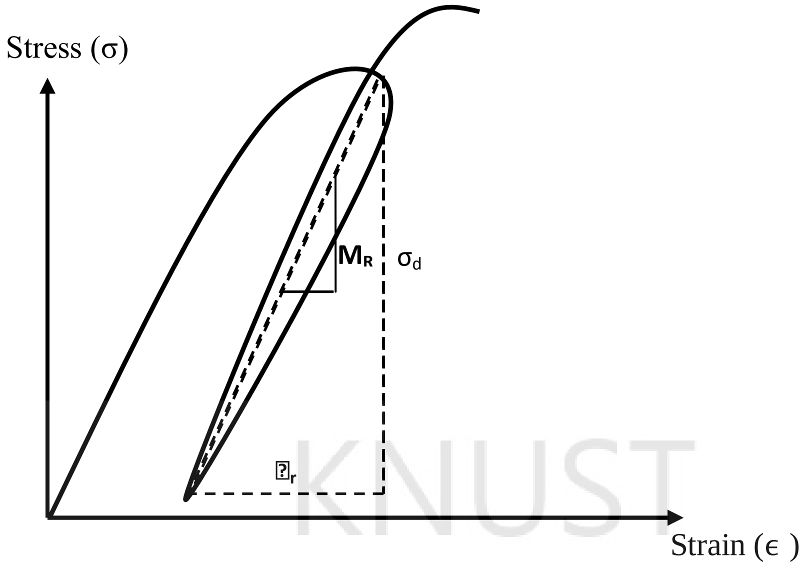

Figure 1: Illustration of Definition of Resilient Modulus

Because the applied load is usually small, the resilient modulus test is a non destructive test, and the sample can be used for many tests under different loading and environmental conditions.

Two methods are used in the prediction of the resilient modulus of the soil both for design of a new road or design of overlay for rehabilitation of in service road. These methods are

i) Laboratory repeated triaxial test, conducted on remoulded soil samples or on undisturbed soil recovered from the field.

ii) Non-destructive in-situ deflection test conducted on the in service road to predict the structural capacity and structural integrity of the pavement.

The laboratory repeated triaxial test is conducted for coarse grained soils and fine grained soils. The test method is different for each type of soil. The stress state and stress sequence are also different for each type of soil.

The in-situ non-destructive test for the determination of the resilient modulus is obtained from the performance of Falling Weight Deflectometer Test (FWD) and its variations and modifications. The moduli of the pavement materials are predicted from the deflection bowl through iteration known as back-calculation.

2.1.2 Laboratory Method of Measuring Resilient Modulus

The type and the duration of loading used in the repeated load test should simulate that actually occurring in the field.

When a wheel load is at a considerable distance from a given point in the pavement, the stress at that point is zero. When the load is applied directly above the given point, the stress at this point is high. It is therefore reasonable to assume the stress pulse to be a haversine or triangular loading, the duration of which depends on the vehicle speed and the depth of the point below the pavement surface (Huang, 2004.)

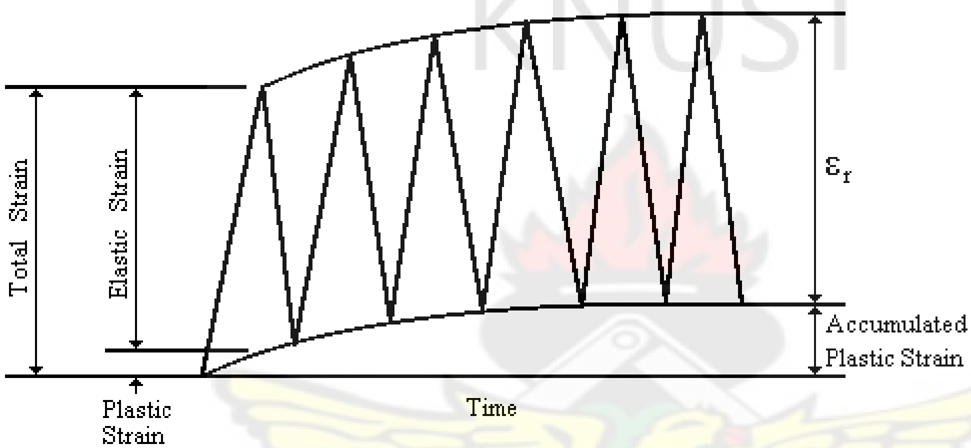

Figure 2: Strain under repeated loads (Huang, 1993)

In the laboratory cyclic triaxial test, the sample is initially subjected to a hydrostatic confining pressure (σ_c), which induces an initial strain ($\square_o$). This initial strain is unmeasured in the test, but it is assumed the same in all directions for isotropic material behavior. The axial stress is then cycled at a constant magnitude ($\Delta\sigma$), which during unloading induces the cyclic resilient axial strain ($\Delta\square$). To simulate the dynamic loading condition as observed in the field due to traffic, the stress $\sigma_1 - \sigma_3$ (known as deviatoric stress or pressure) is made pulsating. This dynamic nature of triaxial testing is intended to match loading and the unloading durations in the same way as they occur in the in-service road. Deformation of the sample occurs when the load is applied to it, and recovery takes place when the load is removed. Dynamic triaxial testing on soil or granular material shows that a fraction of the total strain is unrecoverable, called permanent deformation, even when the load is removed.

Permanent deformations are prominent when the sample is subjected to a large number of load repetitions.

The triaxial state of stress condition in the laboratory load repeated test is illustrated below. The resilient modulus under the test conditions is given as

$$M_R = \frac{\sigma_1 - \sigma_3}{\varepsilon_{re}} \quad \ldots\ldots\ldots\ldots\ldots\ldots\ldots\ldots\ldots\ldots \quad (3)$$

where ε_{re} is the recoverable strain

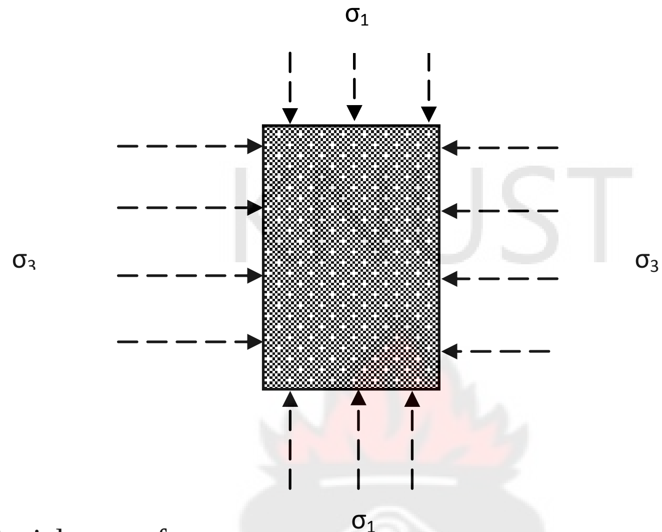

Figure 3: A triaxial state of stress

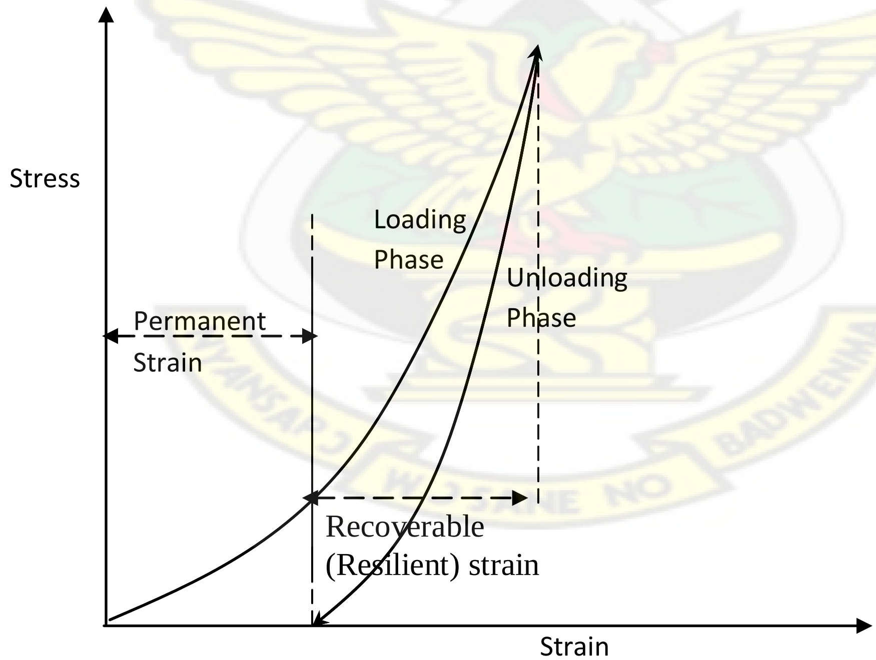

Figure 4: Recoverable and permanent strain in dynamic triaxial loading

The standard test for the laboratory determination of the resilient modulus is contained in AASHTO T307

2.1.3 The Insitu Methods of Determining Resilient Modulus

2.1.3.1 Light Weight Falling Weight Deflectometer

Light Falling Weight Deflectometer (LFWD) is a portable falling weight deflectometer that has been developed in Germany as an alternative in-situ testing device to the plate load test. Different types of LFWD exist in the market. Three main types of LFWD have been used in previous studies; they are the German Dynamic Plate (GDP), the Transport Research Laboratory (prototype) Foundation Tester (TFT), and the Prima 100 LFWD.

Generally, the LFWD consists of a loading device that produces a defined load pulse, a loading plate, and one center geophone sensor (electric deflectiondata device) to measure the center surface deflection. Prima 100 has been recently developed and marketed by Carl Bro Pavement Consultants (previously Phφnix). Figure 5 shows the Prima 100, light falling weight deflectometer equipment. Table 1 describes a comparison between the different types of LFWD. All types exhibit many similarities in their mechanics of operation although there are many differences in design and mode of operation, which lead to variations in the measured results.

Figure 5: Prima 100, light falling weight deflectometer

The Prima LFWD weighs 26 kg (57.2 lbs) and has a 10 kg (22 lb) falling mass which impacts a spring to produce a load pulse of 15-20 milliseconds. For safe operation, the drop weight is supported with a transportation-lock pin and guide rod with stabilizer. Prima 100 has a load range of 1-15 kN (i.e. up to 450 kPa with its 200 mm diameter loading plate). It measures both force and deflection, utilizing a velocity transducer with a deflection range of 22 mm (Fleming et al., 2000).

Table 1: Specification for different types of LFWD (Fleming 2001)

Model	Plate Diameter (mm)	Mass		Total load pulse (ms)	Deflection Transducer		Stress Range (kPa)
		Falling Weight (kg)	pulse		Type	On plate Ground	
GDP	300	10	17	18±2	Accelerometer	Plate	100
TFT	200, 300	10	20	15 - 25	Velocity	Ground	< 120
Prima 100	200,300	10,20	16	15 - 20	Velocity	Ground	< 200

During any test operation, the center deflection (δc) of the loading plate is measured and used to estimate the LFWD elastic stiffness modulus (ELFWD). The expression used to calculate ELFWD is similar to the one used to calculate the surface modulus of a layered media assuming a uniform Poisson's ratio (μ), and constant loading on an elastic half space (Boussinesq elastic half space). This expression is described by Equation 4 below:

$$ELFWD = \frac{2(1-\mu^2)\sigma R}{\sigma_c} \qquad \text{.. (4)}$$

where,

σ = the applied stress

σ_c = deflection measured under the plate

μ = Poisson's ratio

R= the plate radius

A complete analysis of the LFWD field data can provide an estimate of the linear elastic response of the individual material making up the pavement structure and its supporting layer.

Therefore, it is well suited for application in the quality control and quality assurance procedures for the construction of pavement layers and other geo-materials. However, there are currently limited published data relating to its efficiency (Fleming et al., 2000).

2.1.3.2 Falling Weight Deflectometer (FWD)

The Falling weight deflectometer is a non destructive test equipment for highways and airfields. It is used to determine the moduli of pavement layers by inducing an impulse load on the surface and measuring deflections with geophones. The FWD is trailer towed equipment which consists of a drop weight mounted on a shaft with geophones and a central plate which induces the load waves into the pavement layer structure. The drop weight is hydraulically lifted to the predetermined height of 510 mm. The weight is usually dropped onto a 300 mm diameter loading plate resting on a 5.6 mm thick rubber buffer, which is usually used to improve the uniformity of loading stress distribution over the whole loading plate area. The impact of the weight is capable of producing load waves approximately half-sinusoidal with loading time of 25 microseconds into the pavement. Uneven road surfaces are made even by using uniformly graded sand prior to lowering the loading plate onto the road surface.

The waves are picked by the geophones and recorded as deflections by the computer which are processed into moduli through back-calculation. The FWD field test information is stored in Microsoft Access database.

The moduli are determined from deflection measurements using iterative back-calculation computer programs. In general, a modulus determined by FWD will be higher than a modulus determined from cyclic triaxial resilient modulus tests. Thus, AASHTO recommends a correction of 0.33 to 0.5 be applied to moduli determined by FWD.

2.1.4 Analysis of FWD Test Results

2.1.4.1 Pavement Structure

The general principle in pavement modeling is that layers of similar properties are combined into one layer.

The material and thickness of the individual pavement layer along the road under study has to be known. This is done normally by referring to construction and maintenance records.

In the absence of this, the thickness of individual layers is determined through;

i) sinking of trial pits at intervals along the road under study,

ii) using ground penetrating radar system or

iii) using dynamic cone penetrometer equipment.

A flexible pavement is normally modeled as a three-layer structure with all asphalt materials (.i.e. bound materials) combined into one top layer, the base and sub-base as the second layer (Unbound materials), and the subgrade as the third layer.

A rigid pavement is normally modeled as a two-layer structure with the concrete slab as the top layer and the sub-base combined with the subgrade to form the second layer.

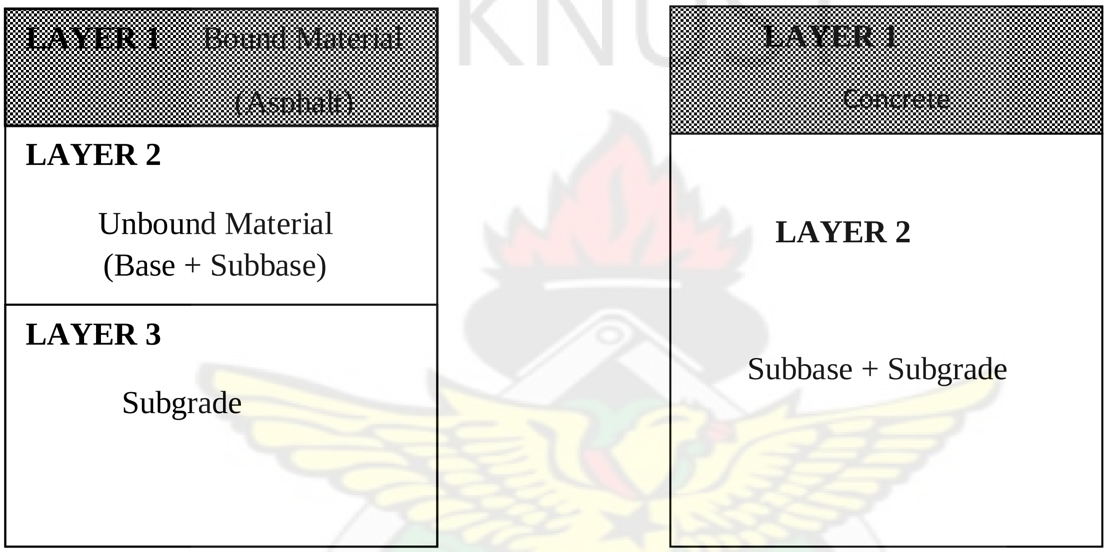

(a) Flexible Pavement (b) Rigid Pavement

Figure 6: Pavement structure model as used in ELMOD software analysis

Sometimes the above standard models may not give reasonable results, e.g., a sub-base modulus lower than that of the subgrade. The reason may be due to a non-linear subgrade modulus, normally increasing with depth. The subgrade modulus may also be stress dependent, usually the modulus increases as the deviator stress on the subgrade decreases. Hence, the subgrade modulus measured under the load centre is smaller than that measured at some distance away from the load.

A third reason may be the presence of an effective rigid layer at a certain depth in the subgrade. To achieve a more reasonable backcalculation result, the subgrade may be further divided into two layers, with a layer just beneath formation level of thickness 500 – 1000 mm on top of a semi-infinite bottom layer. (Hong Kong, Highway Department, 2009).

Backcalculation of Pavement Layer Moduli

One of the most useful applications of FWD testing is to back-calculate the moduli of pavement layers including the subgrade. The basic procedure is to measure the pavement deflection basin normally with seven sensors at different offsets from a load plate.

Using the FWD deflection, the subgrade modulus is back-calculated using the software Elmod 5 provided by Dynatest (the FWD supplier). This software uses the Boussinesq equations to calculate the deflection of the pavement. The deflection is the sum of the deformations in the pavement layers including the subgrade.

The deflection is proportional to the stiffness of the layer. The surface modulus at a distance 'r' roughly reflects the surface modulus at the same equivalent depth z = r. The subgrade modulus, E, is calculated using the furthest deflection from the load plate with the following equation:

$$E = \frac{(1-\mu^2)\sigma_0 a^2}{d_i r_i} \quad \text{..............................} \quad (5)$$

where:

μ = Poisson's ratio (0.35)

σ_o = Load plate load

a = Load plate radius (mm)

d_i = Deflection of geophone i

r_i = Radial distance to geophone i

Then the E-moduli of the bearing courses are calculated by iteration.

The iteration is discontinued when satisfactory conformity between the measured and calculated deflection has been obtained. The theoretical base of the calculations implies that the E-values decrease by at least a factor of three down through the road layers.

Then using the design layer thicknesses or thickness measured from the field, a mathematical model (typically a linear-elastic program) is run numerous times, varying the moduli value of each layer.

The process is stopped when an acceptable match is obtained between the theoretically calculated and measured deflection bowls. A variety of methods based on layer elastic theory have been developed to backcalculate layer moduli. Different programs may apply different principles.

ELMOD uses an approximate method based on Boussinesq's equations and Odemark's method of equivalent thickness to estimate the layer moduli. ELMOD 5 uses an equivalent thickness methodology incorporated in a deflection basin best-fit routine to compute the resilient modulus (M_R) of the subgrade using the last deflection sensors and the pavement layer moduli. ELMOD 5 considers the depth to bed rock and the nonlinear behavior of the subgrade in its calculations. Poisson's ratio is recommended in the range of 0.30 to 0.50 (AASHTO, 1993). To account for the difference between the back-calculated M_R and the design M_R , the M_R computed is multiplied by an adjustment factor C whose value is not greater than 0.33. AASHTO (1993) also recommends correcting this value of M_R for use in flexible pavement designs by employing the following equation:

$M_{R\ corrected} = M_R / 3$ ……………………………… (6)

Several parameters influence the backcalculated moduli, for example, seed moduli, number of layers, layer thickness, and depth to rigid layer. In most instances, it is preferred not to analyze a system with more than three or four layers.

The theories that are being used by ELMOD 5 are outlined below:

Boussnesq's Equations

The 'Radius of curvature' method adopted by ELMOD makes use of the Boussinesq's equations. Boussinesq developed a set of equations to calculate the stress, strain and displacement conditions in a homogeneous, isotropic, linear elastic semi-infinite space under a point load. The stress, strain and displacement conditions under a uniform load can be found by integration.

At the depth 'z' below the centerline of a uniform circular load 'σ_0' with radius 'a', the stress, strain and displacement are given by the following:

$$\sigma_z = \sigma_o \times \left\{ 1 - \frac{1}{\left[1 + \left(\frac{a}{z} \right)^2 \right]^{3/2}} \right\} \quad \ldots\ldots\ldots\ldots (7)$$

$$\sigma_r = \sigma_t = \sigma_0 \times \left\{ \left(\frac{1+2\mu}{2} \right) - \frac{(1+\mu)}{\left[1 + \left(\frac{a}{z} \right)^2 \right]^{1/2}} + \frac{\left(1/2 \right)}{\left[1 + \left(\frac{a}{z} \right)^2 \right]^{3/2}} \right\} \quad \ldots\ldots\ldots\ldots (8)$$

$$\varepsilon_z = (1+\mu) \times \frac{\sigma_0}{E} \times \left\{ \frac{z/a}{\left[1 + \left(z/a \right)^2 \right]^{3/2} - (1-2\mu) \times \left\{ \frac{z/a}{\left[\left[1 + \left(z/a \right)^2 \right]^{\frac{1}{2}} - 1 \right]} \right\}} \right\} \quad \ldots\ldots\ldots (9)$$

$$d_z = (1+\mu) \times \sigma_0 \times \frac{a}{E} \times \left\{ \frac{1}{\left[1 + \left(\frac{z}{a} \right)^2 \right]^{1/2} + (1-2\mu) \times \left\{ \left[1 + \left(\frac{z}{a} \right)^2 \right]^{1/2} - z/a \right\}} \right\} \quad \ldots\ldots\ldots (10)$$

$$R = E \times \frac{\frac{a}{\left[\left(1 - \mu^2 \right) \times \sigma_0 \right]}}{\left\{ 1 + \left[1 + \frac{3/2}{(1-\mu)} \right] \times \left(\frac{z}{a} \right)^2 \right\} | \times \left[1 + \left(\frac{z}{a} \right)^2 \right]^{5/2}} \quad \ldots\ldots\ldots\ \ldots\ldots\ldots\ \ldots\ldots\ldots (11)$$

$$\varepsilon_r = \frac{z}{2/R} \ldots\ldots\ldots\ldots\ldots\ldots\ldots\ldots\ldots\ldots\ldots\ldots\ldots(12)$$

where

σ_z = vertical stress;

σ_r = radial stress;

σ_t = tangential stress;

ε_z = vertical strain;

ε_r = horizontal strain;

d_z = vertical displacement;

R = radius of curvature;

E = modulus;

μ = Poisson ratio.

The horizontal strain at the bottom of a bituminous layer, often the critical strain in the pavement structure, can be found by first calculating the radius of curvature of the plane at the bottom of Layer 1. (Highways Department, June, 2009).

Odemark's Method of Equivalent Thickness

Boussinesq's equations are only applicable to a homogeneous layer. In practice, most pavement structures are not homogeneous but are layered systems.

Odemark developed an approximate method to transform a system consisting of layers with different moduli into an equivalent system where the thicknesses of the layers are altered but all layers have the same modulus. This is known as the Method of Equivalent Thickness.

The transformation assumes that the stiffness of the layer remains the same, i.e.

$$\frac{I \times E}{\left(1-\mu^2\right)} \qquad \text{remains constant}$$

where

I = moment of inertia

E = layer modulus, and

μ = Poisson ratio.

Since I is a function of the cube of the layer thickness, the equivalent thickness transformation for a layer with thickness = h_1, modulus = E_1, and Poisson ratio μ_1 into a layer with equivalent thickness = h_e, modulus E_2, and Poisson ration μ_2 may be expressed as follows:

$$\frac{\left(h_1^{\,3} \times E_1\right)}{\left(1-\mu_1^{\,2}\right)} = \frac{\left(h_e^{\,3} \times E_2\right)}{\left(1-\mu_2^{\,2}\right)} \quad \text{..(13)} \qquad \text{or}$$

$$h_e = h_1 \times \left[\frac{E_1/_{E_2} \times \left(1-\mu_2^{\,2}\right)}{\left(1-\mu_1^{\,2}\right)}\right]^{1/3} \quad \text{..(14)}$$

Since this is an approximate method, an adjustment factor 'f' is applied to the right hand side of the above equation to obtain a better agreement with elastic theory. The value of 'f' which ranges between 0.8 – 1.0, depends on the layer thicknesses, modular ratios, Poisson ratios and the number of layers in the pavement structure. Furthermore, the Poisson ratio for all pavement materials can be assumed to be the same, usually equal to 0.35.

The equivalent thickness equation can therefore be expressed as:

$$h_e = f \times h_1 \times \left[\frac{E_1}{E_2}\right]^{1/3} \quad \text{..(15)}$$

In the analysis of a multi-layer pavement structure with known layer moduli, the layers can be successively transformed into an equivalent system with a homogeneous layer modulus equal to the modulus of the semi-infinite subgrade layer by applying Odemark's method. Boussinesq's equations can then be applied to calculate the stress, strain and displacement conditions within the equivalent layered system. In analyzing FWD data, the process is reversed by using the surface displacements measured at varying distances under a plate load to 'backcalculate' the moduli of individual pavement layers. The backcalculated modulus is often called the effective modulus because the value represents the effect of the layer within the whole pavement structure. This may be different from the modulus obtained if the layer is evaluated in isolation, such as in the case of testing a cored sample in the laboratory (Hong Kong, Highway Department, 2009).

Surface Modulus

The surface modulus is the ‘weighted mean modulus’ of the semi-infinite space calculated from the surface deflection using Boussinesq’s equations. The surface modulus at a distance ‘r’ roughly reflects the surface modulus at the same equivalent depth z = r.

If the subgrade is a linear elastic semi-infinite space, the surface modulus should be the same at varying distances. If a stiff layer is present, the surface modulus at some distance should become very large. ELMOD 5 begins the process by estimating the subgrade modulus using the outer deflections since these are almost entirely controlled by the subgrade.

The change in moduli with varying distances from the load centre is used to check whether a stiff layer is present at some depth.

This can be checked by calculating the ‘surface modulus’ as follows:

$$E_0(0) = 2\times(1-\mu^2)\times\sigma_0\times\frac{a^2}{d_0(0)} \qquad (16)$$

and

$$E_o(r) = (1-\mu^2)\times\frac{\sigma_0\times a^2}{[r\times d_0(r)]} \qquad (18)\ \text{(Valid for r > 2a)}$$

where

$E_0(r)$ = surface modulus at distance r;

μ = Poisson ratio of the subgrade (normally = 0.35);

σ_0 = uniform stress on the plate;

a = radius of the loading plate;

r = distance from the centre of load; and

$d_0(r)$ = surface deflection at distance r.

Note that the equation for $E_0(r)$ is only valid for r > 2a.

Subgrade Non-Linearity

If a stiff layer is not detected, ELMOD 5 calculates the subgrade non-linearity coefficients ‘C’ and ‘n’ using the following equation:

$$E_0 = C\times(\sigma_1/\sigma)^n \qquad (17)$$

where

E_0 = surface modulus;

σ_1 = major principal stress;

σ = reference stress, normally 160 MPa;

C = constant; and n = negative constant.

Normally, 'C' decreases linearly with increase in moisture content. 'n' may be taken as a measure of the non-linearity. If n is zero, the subgrade is linearly elastic and as 'n' decreases, the non-linearity becomes more and more pronounced.

Iteration

With the 'Radius of Curvature' method, ELMOD 5 uses the centre deflection and the curvature of the deflection basin under the loading plate to determine the moduli of the top layer, and the intermediate layers if they are present. The subgrade modulus under the load centre is adjusted according to the estimated stress level, and the outer deflections are checked.

If adjustments are necessary, the layer moduli are then recalculated. The 'Deflection Basin Fit' method goes one step further by closely matching the calculated deflection profile and the measured deflection profile. The percentage difference between the calculated value and the measured value can be specified as the convergence criteria in the iteration (Hong Kong, Highway Department, 2009).

2.1.5 Calibration of the FWD

There are two types of calibration on the geophones, namely:

1. Relative calibration, and
2. Reference, calibration

The relative calibration of the geophones is used to ensure that all the geophones on a given FWD are in calibration with each other. As such, it serves as the final step in the overall calibration process and as a quick means to verify periodically that the geophones are functioning properly and consistently.

2.1.5.1 Reference Calibration

The Reference Calibration is performed to ensure that the geophones on the FWD are performing correctly. The Reference Calibration is done at a calibration center.

This is done by placing the deflection sensors from the Falling Weight Deflectometer, along with reference accelerometer, in a large stand. A series of drops are performed, where the reference accelerometer and the sensors from the FWD sees the same deflections.

After one trial is done, the sensors are rotated relative to the accelerometer and a second trial is completed. The results from this Reference Calibration are used to create a series of interim gain factors for the deflection sensors. A third and fourth trial may be needed in some cases.

2.1.5.3 Relative Calibration

After the reference calibration, a Relative Calibration is done to improve the precision of the deflection sensor calibration. Also a Relative Calibration procedure reveals if the gain of a geophone is out of range. To accomplish this, a large number of drops are done with the FWD to tighten up the data. These results are used to produce the final gain factors for the FWD.

The Relative Calibration is done using a Relative Calibration stand supplied by the FWD manufacturer. The sensors are stacked vertically in the stand, one above the other so that all the sensors are subjected to the same pavement deflection.

Relative Calibration assumes that mean deflection as determined from stimulation measurements by the full set of deflection sensors, yields accurate estimates of the true deflection. This assumption requires that the deflection sensors must have first been subjected to the reference calibration procedure. The process involves rotation of each geophone through every position in the calibration stand. Each combination of geophones is considered as a ‘set’ and the number of ‘set’ is equal to the number of geophones. A test point is chosen to ensure that a minimum geophone deflection of 300-400μm is achieved. This point is marked onto the pavement to ensure that the calibration stand for all “set” is located exactly on this point. In this regard, error between different ‘set’ will be minimised.

The required order of the movement of the seven (7) geophones is given below.

Set	Order (Highest to lowest in calibration stand)
1.	1-7
2.	2-7, 1
3.	3-7, 1-2
4.	4-7, 1-3
5.	5-7, 1-4
6.	6-7, 1-5
7.	7, 1-6

It is very important that the geophones have to be rotated correctly. Also spare geophones do not need to be calibrated until they are in active use. When relative calibration is done with reference calibration, the Relative Calibration procedure should be repeated twice. (Hong Kong, Highway Department, 2009).

2.2 Application of FWD

The FWD is used to provide non-destructive evaluation of the structural capacity of pavements for overlay design purposes.

It has proven to be a good non-destructive test for pavement structure assessment mainly because of its speed, better simulation of traffic loading, and results that can directly be applied in structural design (Fleming et al., 2000).

Current research on FWD, suggests that the FWD can be used in the quality control during construction of pavement layers. Zaghloul and Saeed (1996) suggested an empirical approach to set FWD target deflections. In this approach trial sections are constructed and FWD tests are performed at locations showing acceptable density levels to determine the required target deflections. They also suggested that the quality control and quality assurance procedures that include dividing pavement sections into homogenous segments, and FWD tests conducted on each layer, then statistical tests should be conducted on measured deflections in order to evaluate the construction quality and to identify weak points.

Furthermore, Rogers et al. (2000) performed tests using FWD to determine the relation between the stiffness and the dry density of a base course layer. Their test results showed that although the stiffness increased during the initial compaction passes, adequate stiffness development took place only when the density is close to its maximum value at the optimum moisture content. Based on this result, they suggested that there is no evident correlation between dry density and the stiffness measured by FWD. Although the FWD is classified as a suitable device for stiffness measurements, it is sometimes considered unnecessarily complicated for base and sub-base testing (Fleming, 2000). In addition, the use of the FWD to evaluate the pavement structure during construction of subgrade, subbases, and base layers is faced with some problems. One of these problems is that pavement layers which are under construction are not as accessible to FWDs as for completed roads.

Another drawback of using FWD for monitoring the load carrying capacity of a pavement structure under construction is that the uneven surface causes tilting of the deflection sensors. Tilting in excess of a certain value leads to inaccurate deflection measurement that cannot be used in back calculation (Gurp et al., 2000).

2.3 Dynamic Cone Penetrometer (DCP)

2.3.1 History of DCP

The DCP is simple, economical, requires minimum maintenance, easy to transport to site, and provides continuous measurements of the in-situ strength of pavement section and the underlying subgrade layers without the need for excavating the existing pavement as in the California Bearing Ratio test. The test can be performed and the data analyzed by trained personnel within minutes of training.

The idea for the development of the DCP was proposed by Scala from Australia in the year 1956. Later in the year 1969, Van Vuuren from South Africa developed a new DCP equipment. This new equipment has a drop weight heavier than the Scala device. Also it has a shorter drop height. Van Vuuren DCP equipment was shown to be suitable for soils with CBR values ranging from 1 to 50.

The DCP equipment which has been adopted by many countries was developed by Kleyn also from South Africa. His equipment is a modified version of the Van Vuuren DCP equipment and was used for the evaluation of pavements.

The dynamic cone penetrometer (DCP) device developed by the British Transport Research Laboratory consists of a cylindrical rod with a cone tip that is driven into the soil by repeatedly dropping an 8kg weight from a height of 575mm. The cone tip is both 300 or 600 angle and a 20mm-diameter base.

Disposable tips can be used in which the tip remains in the soil when the rod is extracted. The cumulative penetration is measured and recorded with the number of blows. Penetration readings are typically measured for each blow in soft soils and every 5 or 10 blows in stiffer soils. Penetration readings of 20 blows that result in minimum or less penetration is record as refusal to penetration and the test is terminated. The DCP penetration ratio is defined by the slope of the curve relating the depth of penetration to the number of blows at a given linear depth range. For rehabilitation or reconstruction design, only small cores (diameter as little as 25.4mm) need to be drilled through the pavement surface to expose the underlying unbound materials for DCP investigation.

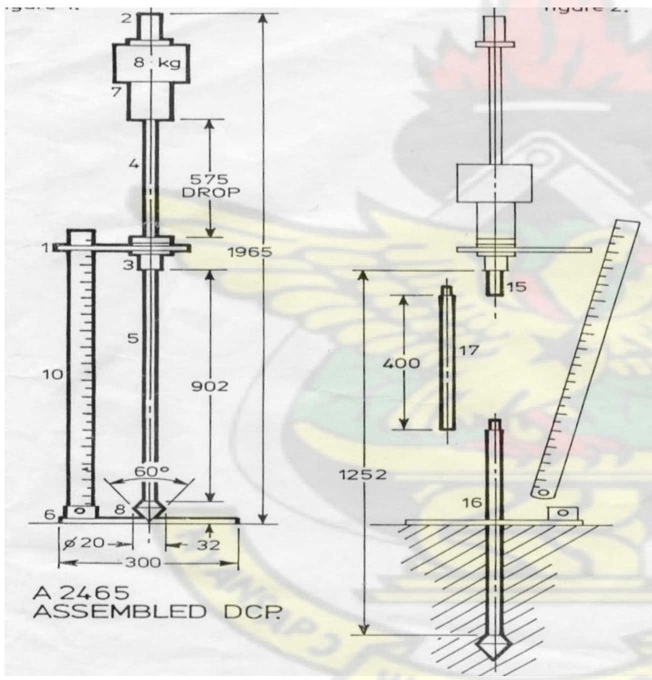

Figure 7: DCP test equipment of TRRL Model A2465 used in the study

2.3.2 Applications of the DCP

DCP tests are designed to estimate the structural capacity of pavement layers and embankments. The DCP has the ability to verify both the level and uniformity of compaction, which makes it an excellent tool for quality control of pavement construction. In addition, it can also be used to determine the tested layer thickness (Chen et al., 2001).

DCP and CBR

Livneh et al. (1989) demonstrated that results from penetration tests correlate well with the in-situ CBR values. In addition, they indicated that the layer thickness obtained from DCP tests matches that obtained in the test pits, and concluded that the DCP tests are a reliable alternative for pavement evaluation. Harrison (1986) also found that there is a strong correlation between CBR and DCP penetration ratio in log-to-log form. He reported that CBR-DCP relationship is not affected by changes in moisture content and dry density. Table 2 is a summary of DCP - CBR correlations which have been developed by various researchers.

Table 2: DCP-CBR Correlations

Correlation	Material tested	Equation Reference
log(CBR) = 2.56 - 1.16 log (DCPI)	Granular and cohesive	Livneh (1987)
log(CBR) = 2.55 - 1.14 log (DCPI)	Granular and cohesive	Harison (1987)
log(CBR) = 2.45 - 1.12 log (DCPI)	Granular and cohesive	Livneh et al. (1992)
log(CBR) = 2.46 - 1.12 log (DCPI)	Various soil types	Webster et al. (1992)
log(CBR) = 2.62 - 1.27 log (DCPI)	Unknown	Kleyn (1975)
log(CBR) = 2.44 - 1.07 log (DCPI)	Aggregate base course	Ese et al. (1995)
Log(CBR) = 2.60 - 1.07 log (DCPI)	Aggregate base course and cohesive	NCDOT (Pavement, 1998)
Log(CBR) = 2.53 - 1.14 log (DCPI)	Piedmont residual soil	Coonse (1999)

Chen et al. (2001) also indicated that the DCP can be useful when the Falling Weight Deflectometer (FWD) back-calculated resilient moduli is not accurate, such as when the asphalt concrete layer thickness is less than 75mm or when bedrock is shallow. During the past decade, the DCP test has been correlated to many engineering properties such as the CBR, shear strength of granular materials, and most recently, the subgrade resilient modulus (M_R) and elastic Modulus (E_s) and soil classification. In addition, many studies attempted to determine whether there is a reasonable correlation between the DCP penetration rate (PR) and in-place compaction density. Most results of DCP testing on cohesive and selected granular materials showed too much variability to practically apply a correlation. However these studies demonstrated that properly compacted granular base materials exhibit very uniform penetration rate (PR) values.

DCP and Compaction Control

Due to the ability of the DCP equipment to provide continuous record of relative soil strength with depth, it can be used for compaction control in pavement construction. The DCP test allows the detection of pockets of low levels of compaction deeper in road pavements (Ampadu and Arthur, 2002). By plotting a graph of penetration index versus depth, one can observe the profile showing layer depths and strength condition.

Because of the DCP's proven capability as an effective tool in the assessment of the in situ strength of sub base/base materials and subgrade it can be used for QC/QA in highway construction.

Historically, the compaction levels of pavement subgrade and base layers have been determined by means of in-place density testing. In an effort to determine whether there is a reasonable correlation between the DCPI and in-place compaction density of cohesive and select backfill materials, some testing has been recently performed on these materials to determine if such a correlation exits. Most results of DCP testing have indicated too much variability in DCP results to practically apply a correlation (Burnham, 1997). Siekmeier et al. (1999), as part of the Minnesota Department of Transportation study, investigated the correlation between DCP results and compaction of soils consisting of mixture of clayey and silty sand fill. They first correlated DCPI to the CBR. CBR was then related to the modulus using published relationships. They examined the relations between the modulus and percent compaction. It was concluded that a good correlation did not exist between the DCP results and percent compaction, partly because a typical range of soil mixtures at the site was not truly uniform. However, the results of Ampadu and Arthur (2002) showed a good correlation between DCPI and percentage compaction of lateritic gravel used as a subbase for a road pavement.

DCP and Bearing Capacities

DCP as an in-situ penetration test has been widely used in geotechnical and foundation engineering for site investigation in support of analysis and design. It has been used successfully in estimating the CBR value of subgrade soils for pavement design and construction. Some attempts have been made to determine the allowable bearing capacities of shallow foundations.

Ampadu (2005) correlated the allowable bearing stresses computed from the Terzaghi's equations with DCP results with two lateritic soils.Sanglerat (1972) used a semi-emperical approach to derive an equation for computing the allowable stress from the DCP readings. Sowers and Hedges (1966) produced a correlation between the DCP readings and the SPT N-values. Ampadu and Dzitse-Awuku (2009) correlated the DCP test results with the bearing capacity of a model ground for shallow foundation in the laboratory.

DCP application in Quality Control of Granular Base Layer Compaction

The Minnesota Department of Transportation suggests this application to reduce testing time and effort while providing more consistent quality control of base layer compaction (Burnham, 1977). Using this procedure, immediately after the compaction of each layer of granular base material, DCP tests are conducted to insure that the DCPI is less than 19 mm per blow (0.75 inches per blow). The DCPI limiting value is valid for all freshly compacted base materials. The DCPI dramatically decreases as the materials "setup time" increases and under traffic loading. Using this method, the DCP testing will only indicate those adequately compacted base layers that pass. Test failure, however, must be confirmed by other methods such as the nuclear gauge or the sand cone density method. Based on general agreement between the DCPI and percent compaction, the Minnesota Department of Transportation has revised the limiting penetration rate to the following (Siekmeier et al., 1998):

a) 15 mm/blow in the upper 75 mm (3.0 in)

b) 10 mm/blow at depths between 75 and 150 mm (3 and 6 in) and

c) 5 mm/blow at depths below 150 mm (6 in).

They concluded that the penetration rate is a function of moisture content, set-up time, and construction traffic, and that accurate and repeatable tests depend on seating the cone tip properly and beginning the test consistently.

They recommended the following:

a) the test be performed consistently and not more than one day after compaction while the base material is still damp.

b) the construction traffic be distributed uniformly by requiring haul trucks to vary their path.

c) at least two dynamic cone penetrometer tests be conducted at selected sites within each 800 cubic meters of constructed base course.

They proposed a Penetration Index Method (Trial Mn/DOT Specifications 2211.3C4) which described a step-by-step procedure for determining the pass and fail tests (Siekmeier, et al. 1998). Siekmeier et al. (1999) also studied the correlation between DCP results and compaction of soils consisting of sand and gravel mixture with less than 10-percent fine.

They first correlated DCPI to the CBR. CBR was then correlated to the modulus using published relationships. They examined the relations between the modulus and percent compaction. It was concluded a good correlation existed between the DCP results and percent compaction.

2.3.3 Factors affecting DCP test results

Material Effects

Several investigators have studied the influence of several factors on the DCPI. Kleyn and Savage (1982) showed that moisture content, gradation, density, and plasticity were important material properties influencing the DCPI. They concluded that for fine-grained soils, moisture contents, soil classification, dry density and confining pressures influence the DCPI. For coarse-grained soils, coefficient of uniformity and confining pressures were important variables. Hassan (1996) performed a study on the effects of several variables on the DCPI. The higher the moisture content the higher the penetration rate. Penetration rate tends to be higher in granular materials than on fine – grained soils.

The lower the density of the soil, the higher the penetration rate. Plasticity affects the penetration rate of any soil. Soils with high plasticity tend to have finer soil particles present whilst soils with low plasticity have coarse-grained soil particles with little fines.

At given moisture content, the penetration rate of soils with higher plasticity increases with moisture content and decreases with decrease in moisture content.

Vertical Confinement Effect

Livneh, et al. (1995) performed a comprehensive study of the vertical confinement effect on dynamic cone penetrometer strength values in pavement and subgrade evaluations.

The results have shown that there is no vertical confinement effect by rigid pavement structure or by upper cohesive layers on the DCP values of lower cohesive subgrade layers. In addition, their findings have indicated that no vertical confinement effect exists by the upper granular layer on the DCP values of the cohesive subgrade beneath them. There is, however, vertical confinement effect by the upper asphaltic layers in the DCP values of the granular pavement layers.

These confinement effects usually result in a decrease in the DCP values. Any difference between the confined and unconfined values in the rigid structure or in the case of granular materials is due to the friction developed in the DCP rod by tilted penetration or by a collapse of the granular material on the road surface during penetration.

Side Friction Effect

The DCP equipment has cone tip diameter bigger than the attachment rod to minimize rod friction when penetrating the soil. Whenever the DCP device is not completely vertical while penetrating the soil, the penetration resistance would be high due to side friction. This apparent higher resistance may also be caused when penetrating in a collapsible granular material. This effect is usually small in cohesive soils. Livneh (2000) suggested the use of a correction factor to correct the DCP/CBR values for the side friction effect.

2.4 DCP Penetration Resistance and Resilient Modulus

Many researchers have developed correlations between resilient modulus (M_R) and Dynamic cone penetration rates. Hassan (1996) developed a simple regression model correlating DCPI with M_R for fine grained soils at optimum moisture content:

M_R = 7013.065 - 2040.783*ln (DCPI) ………………………… (18)

where

DCPI is expressed in inches/blow; and M_R is in psi

Based on the DCP tests and CBR-DCP relationships developed in Malaysia during the 1987 National Axle Load study Chai, et al (1998) proposed the following model to determine the subgrade elastic modulus:

$$E = 17.6 \times \left(\frac{269}{DCP} \right)^{0.64} \quad \ldots\ldots\ldots\ldots\ldots\ldots\ldots\ldots\ldots\ldots\ldots \text{(19)}$$

where

DCP = blows/300mm penetration and

E is in-situ subgrade modulus in MN/m^2

They also developed a relationship between the back-calculated modulus and the DCP value in the following form:

$E_{(back\text{-}calculation)} = 2224 \times (DCP)^{-0.996}$ ……………………………… (20)

where

$E_{(back\text{-}calculation)}$ = Backcalculated subgrade modulus (MN/m^2)

Jianzhou, et al (1999) used FWD deflection data and DCP results to develop a relationship between the DCPI and backcalculated subgrade moduli as follows:

$E(back\text{-}calculated) = 338 \times DCPI^{-0.39}$ ……………………………… (21)

E = back-calculated elastic modulus in MPa

DCPI is expressed in mm/blow

De Beer proposed a simple correlation between elastic modulus and DCP-PR that has the following form:

$\text{Log}(Es) = 3.05 - 1.07 \times \text{Log}(PR)$ ……………………………… (22)

where

PR is penetration ratio (mm/blow) and

E_s is elastic modulus (MPa).

George and Uddin (2000) conducted a comprehensive study to correlate the DCPI values to the laboratory resilient modulus.

They proposed two different models based on their investigation, one for coarse grained soils and another for fine grained soils.

The following are the proposed models.

For fine grained soils (Cohesive soils)

$$M_R = \left(\frac{DCPI}{\log C_u}\right)^{a_1} \left(\gamma_{dr}{}^{a_2} + \left(\frac{LL}{w_c}\right)^{a_3}\right) \qquad \ldots\ldots\ldots\ldots\ldots\ldots\ldots\ldots\ldots\ldots\ldots\ldots\ldots (23)$$

where

MR = Resilient modulus in MPa,

DCPI = penetration Index, mm/blow,

W_c= Actual moisture content, %

LL = liquid limit in %

γ_{dr}= Density ratio, i.e. field density/maximum dry density

C_u = coefficient of uniformity

a_0, a_1, a_2 and a_3 are regression coefficients.

For Coarse grained soils (Granular soils)

$$M_R = a_0 \left(\frac{DCPI}{\log c_u}\right)^{a_1} \left(w_{cr}{}^{a_2} + \gamma_{dr}{}^{a_3}\right) \qquad \ldots\ldots\ldots\ldots\ldots\ldots\ldots\ldots\ldots\ldots\ldots\ldots\ldots (24)$$

MR = resilient modulus in MPa

DCPI = dynamic cone penetration index in mm/blow

c_u = coefficient of uniformity

w_{cr} = moisture ratio, field moisture/optimum moisture

γ_{dr} = density ratio, field density/maximum dry density

a_o,a_1,a_2 and a_3 are regression coefficients.

The 1993 AASHTO Guide for Design of Pavement Structures has adopted equations (27) and (28) proposed by Huekelom and Klomp (1962) for calculating subgrade resilient modulus (MR) from CBR values as follows:

MR (psi) = 1500 * CBR or ……………………………… (25)

MR (MPa) = 10.34 * CBR ……………………………. (26)

The resilient moduli from which this correlation was developed ranged from 750 to 3000 times the CBR. Also, the formula is limited to fine-grained soils with a soaked CBR of 10 or less (Chen et al., 2001). Powell et al. (1984) suggested another relationship between subgrade resilient modulus and CBR as follows:

$$MR\ (psi) = 2550 \times CBR^{0.64} \text{ or} \quad \ldots\ldots\ldots\ldots\ldots\ldots\ldots\ldots\ldots\ldots\ldots\ (27)$$

$$MR\ (Mpa) = 17.58 \times CBR^{0.64} \quad \ldots\ldots\ldots\ldots\ldots\ldots\ldots\ldots\ldots\ldots\ldots\ (28)$$

Other equations related the DCP Penetration Rate (PR) with the subgrade modulus directly.

Pen (1990) suggested the following two relationships between the subgrade's elastic modulus (Es) in (MPa) and PR in (mm/blow) as

$$Log\ (Es) = 3.25\text{-}\ 0.89 * Log\ (PR) \quad \ldots\ldots\ldots\ldots\ldots\ldots\ldots\ldots\ldots\ldots\ldots\ (29)$$

$$Log\ (Es) = 3.652\text{-}1.17 * Log\ (PR) \quad \ldots\ldots\ldots\ldots\ldots\ldots\ldots\ldots\ldots\ldots\ldots\ (30)$$

CHAPTER 3: METHODOLOGY

3.1 Study Road Selection

The study road is a 5.3km two lane surface treated road located in the south eastern part of the Greater Accra Region of Ghana. It is an urban minor arterial connecting regional road N4.

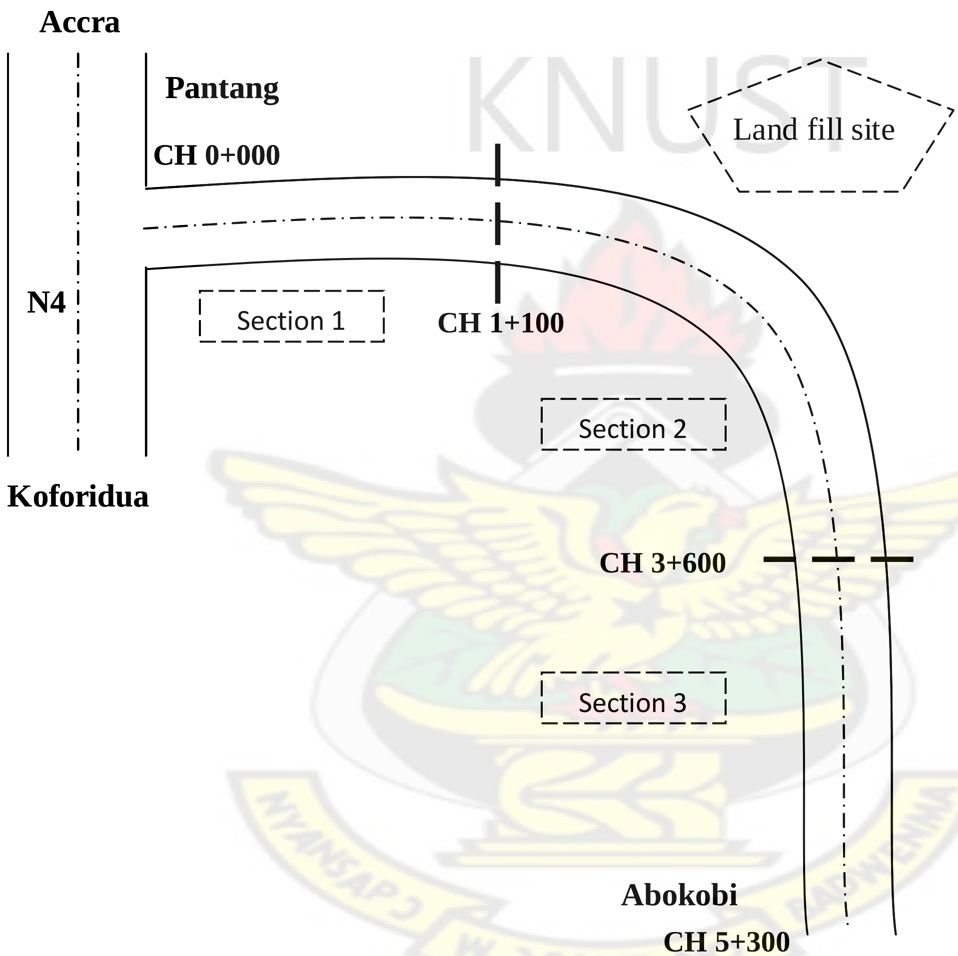

Figure 8. Sketch of the study road

The study road traverses both a hill and valley, which informed the selection of the sections for the thesis project. The road was divided into three different sections according to the grade. Two sections lies in low grade section (valley) whiles one section lies in high grade section (Hill). Field and laboratory testing programmes were performed at located sections of the road.

The field tests involved performance of FWD and DCP, excavation of trial pits to establish pavement layer thicknesses, and taking of undisturbed samples using core cutters. Disturbed samples were recovered from the trial pits for laboratory testing.

The laboratory testing programme involved performance of Atterberg limit test and sieve analysis (wet) on the recovered samples based on BS 1377, Part 2, 1990. The classification of the soil was based on AASHTO M145.

The FWD/DCP test locations on the study road was marked with white paint at intervals of 100m using hand held measuring cycle pushed along the shoulder of the road. The FWD and the DCP tests were conducted in the outer wheel path at these marked locations in the direction of Abokobi.

Photo 1 Marking of the study road for FWD/DCP tests

Photo 2 Marking of the study road in progress

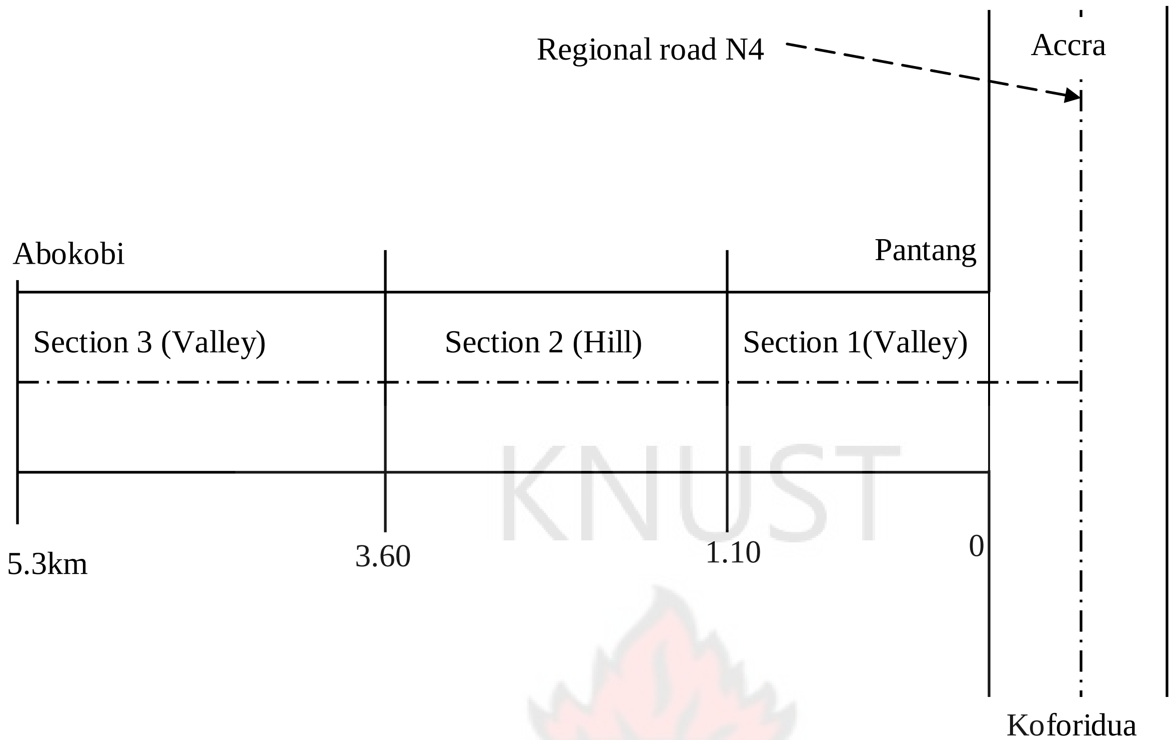

Figure 9: Sketch of study road showing the delineated test sections

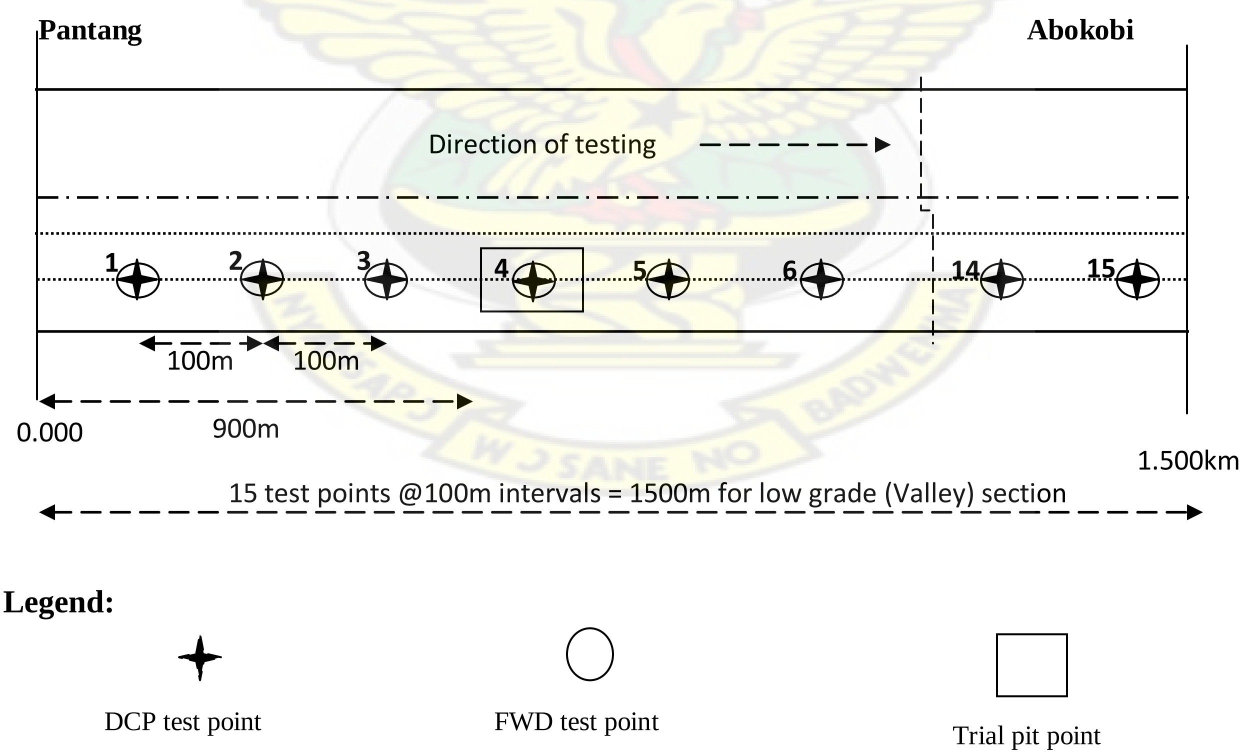

Figure 10. Sketch of test points at a typical section of the study road

3.2 FWD Test

3.2.1 FWD Equipment

The FWD system used in this study is the Dynatest model 8000 (Figure 7). It consists of three main components:

• the loading system

• the deflection measuring sysytem

• the processing system

The Dynatest 8002E FWD is a trailer mounted FWD consisting of a 155 kN drop weight mounted on a vertical shaft, towed by a vehicle. The drop weight is hydraulically lifted to predetermined height of 510 mm. The weight is dropped onto a 300 mm diameter loading plate resting on a 5.6 mm thick rubber buffer, which is usually used to improve the uniformity of loading stress distribution over the whole loading plate area. The impact of the falling weight produces impact loads approximately half-sinusoidal wave, and having a loading time of 25 micro-seconds applying impulse loading to a circular plate in contact with the pavement surface.

Embedded in the load plate is a load cell which measures the load applied during test. The deflection system consists of seven geophones. The geophones measure the deflections on the pavement surface due to the applied load. They are positioned at 0, 305, 457, 610, 914, 1219, 1524 mm away from the center of the loading plate. A suitable hole is provided in the center of the loading plate such that the center deflection may also be measured. The load cell and seismic deflection transducers are connected to sockets in a protective Trailer Connection Box on the trailer.

A transducer holder is also provided for each of the seven geophones. They are in movable holders along a 2.45 m raise/lower bar, for precise deflection basin measurements. The output of the geophones is stored in the Dynatest 8600 System Processor.

The Dynatest 8600 System Processor is a microprocessor based control and signal processing unit that connects the FWD trailer with the computer. It controls the FWD operation, performs scanning, conditioning and further processing of the geophone signals and monitors the status of the FWD unit to ensure correct measurements. The application of the loading is remotely controlled by the operator.

Figure 11. Dynatest Model 8000 (FWD) set up used in this study

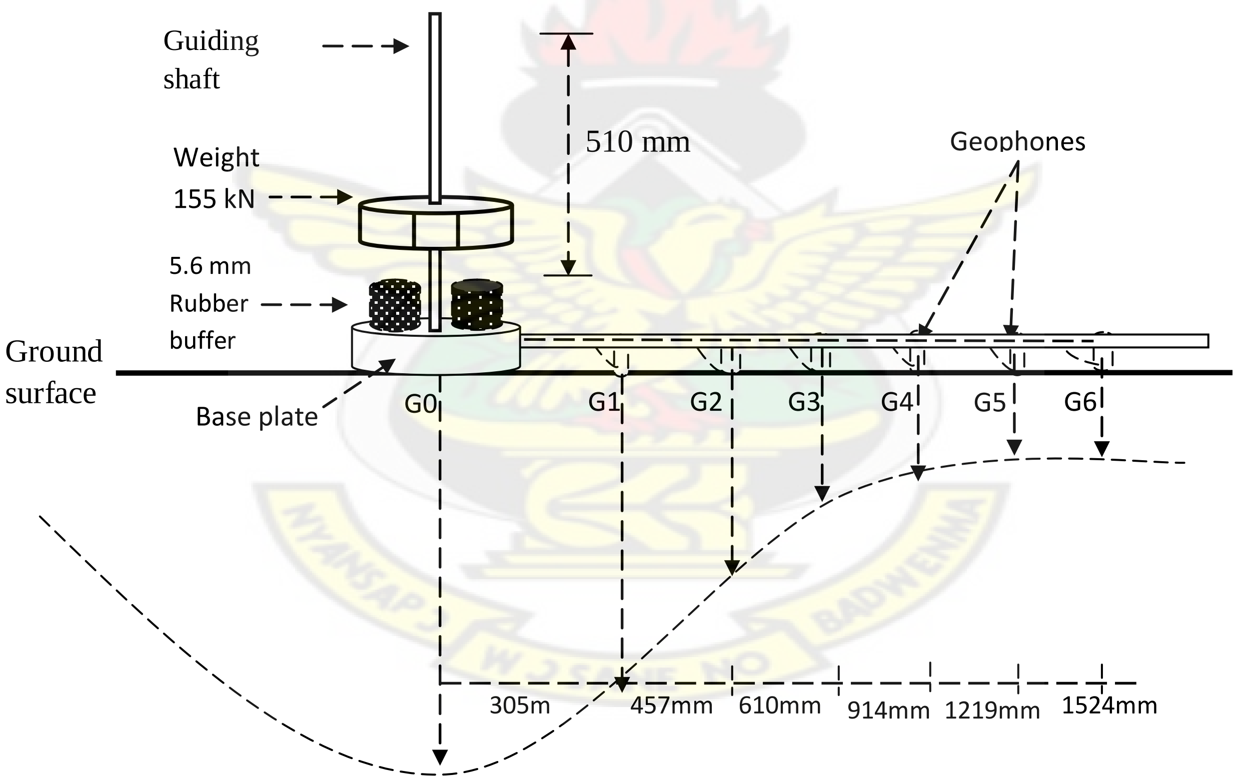

Figure 12. Typical Dynatest deflection basin with sensor configuration

The FWD also incorporates a distance measuring instrument meter. It automatically measures the chainage of testing points.

Attached to the FWD equipment are an air-temperature sensor and an infra red surface temperature transmitter. The air-temperature sensor is a measuring probe recording the air and in-situ pavement temperatures. Besides, the FWD trailer is equipped with a non-contact infra red surface temperature transmitter for recording pavement surface temperature.

3.2.2 FWD Field Test

The field testing of FWD started from Pantang at chainage 0+000 and ended at Abokobi at chainage 5+300. The performance of the FWD testing started with the traffic in both directions being stopped a distance away from the test location by traffic control men in both lane of the road. This action was to prevent the interference of vibration of passing vehicle with the impulse from the FWD testing. The FWD equipment was towed into position on the first test mark.

The FWD geophones were lowered onto the road through a command from the computer mounted inside the towing car. The test load was lifted hydraulically through a command from the computer to a height of 510 mm then left to fall freely under gravity on to rubber bumpers, transmitting the pulse load onto the road into the pavement. This was repeated at each point. The generated pulses were detected or picked up by the various geophones which were relayed to the computer linked to the geophones. The generated pulses resulting in deflection bowl of the pavement determined from measurement of peak deflection at the centre of the loading plate and at seven radial positions by the seven geophones were stored in the computer. The lowered geophones were lifted up, locked in position and towed to the next test point.

Photo 3 FWD equipment in position for the deflection test

Photo 4 Towing the FWD test equipment to position

3.3 DCP Test

The DCP test was performed at 100m intervals at the same locations where the FWD tests had been conducted. The number of test points was equivalent to the number of FWD tests.

The test was conducted by dropping the weight from 575 mm height and recording the number of blows versus depth. The assembled DCP equipment was put in place at the test location of the FWD. The DCP equipment is operated by three operators. One operator held the equipment vertical while the other raises the hammer to a height and left to fall freely on to the anvil. The third operator records the penetration with depth. This exercise continues until all the lower rod of the DCP has penetrated the pavement layers. The equipment was removed to the next test point where the FWD test has been performed.

Photo 5 Performing DCP test on study road using DCP TRL equipment

3.4 Trial Pitting

Five trial pits were excavated along the project road. The trial pits were spaced approximately 900m apart. The pits were manually excavated. The surface treatment was removed before excavating the base. In the process of excavation of the various pavement materials, all layers encountered were separated for identification.

The separations were possible because the various layer boundaries were clearly visible and the colours of the layers were distinct. The disturbed subgrade material encountered in all the pits were taken for laboratory testing after the pit logging had been completed. Undisturbed samples were taken from the subgrade layer using core cutter.

Photo 6 Open trial pit on study road (Ch 0+600)

Photo 7 Open trial pit on study road (Ch 2+400)

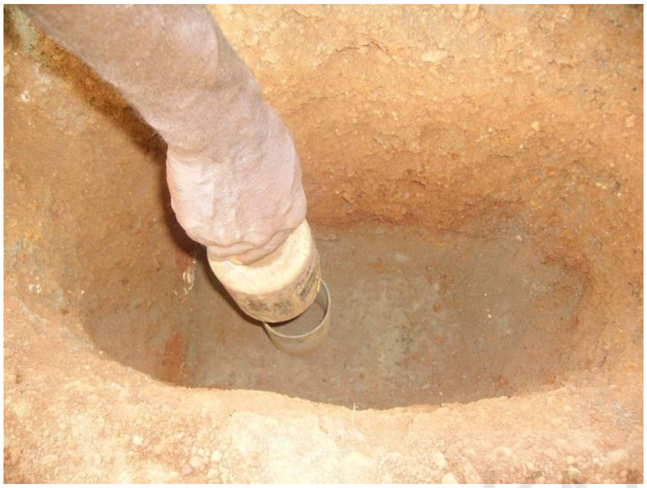

Photo 8 Taking undisturbed soil sample (Ch2+400)

Photo 9 Weighing undisturbed sample in the laboratory for density determination

3.5 Laboratory Test

In the laboratory, some of the samples recovered from the various trial pits were used for moisture content determination. The remaining samples were air dried for the determination of Atterberg limit test using the Casagrande open cup method and wet sieve analysis (including hydrometer test) based on BS 1377 Part 2, 1990. The fraction passing BS sieve 0.425mm was used for the Atterberg limit tests. The soil samples were classified using the AASHTO method of classification. The in-situ dry densities of the subgrade materials were determined using the cored undisturbed soil samples. In the determination of the dry density of the subgrade soils, the trimmed cores were weighed individually. With the known volume of the core cutters, the wet densities of the soils were determined.

The determined moisture contents were used in the determination of the dry densities of the samples. The detailed laboratory grading and Atterberg limit test results are presented in Appendices A and B.

CHAPTER 4: DISCUSSION OF TEST RESULTS

4.1 The Study Road

The study road is a minor arterial 5.2km in length which links a major arterial regional road N4 connecting the Greater Accra regional capital to Koforidua the regional capital of Eastern region. The road lies in the warm savanna climate of the Greater Accra Region in the southern part of Ghana. This road is a double surface treated road which traverses two different terrains. One part of the road lies in lowland whiles the other part lies on a highland. The road carries about two hundred vehicular traffic per day. The vehicular traffic is made up of mainly private cars, mini buses, and occasionally, tipper trucks. The road has undergone only one major rehabilitation since its construction. This rehabilitation was in the form of widening to accommodate traffic diverting onto the road as a result of the construction of new estate housing units. Not much routine maintenance had been done on the road.

4.2 Road Pavement Structure

Two pavement structures were identified on the study road. The first, consisting of base lying directly on the subgrade was identified in low grade areas. The second, consisting of base, subbase overlying the subgrade was also identified on high grade area of the study road. The logs of the trial pit are given in Appendix C. The two layer system is found at Ch 0+100 – 1+100 (section 1) and 3+600 - 5+200 (section 3). The three layer structure is located at 1+200 - 3+500 (section 2), sandwiched between the two layer systems on the study road. Inspection of the trial pit indicates pavement structure of varying thicknesses. The base course for the two layer structure at chainage 0+100 – 1+100 (section 1) and chainage 3+600 – 5+200 (section 3) were of thickness 150mm and 200mm. The base and the subbase layer thickness for the three layer structure at1+200 - 3+500 (section 2) are 200mm and 400mm respectively.

The two layer structure for sections 1 and 2 consisted mainly of a lateritic gravel base lying on silty CLAY subgrade. The AASHTO classification of the subgrade is A-6. The three layer structure consisted of lateritic gravel base, lateritic gravel subbase and silty gravelly sand subgrade.

The AASHTO soil classification of the subgrade soil underlying the three layer structure is A-2-7. The plots of the grading of the various subgrade soils are presented in Figure 13 below.

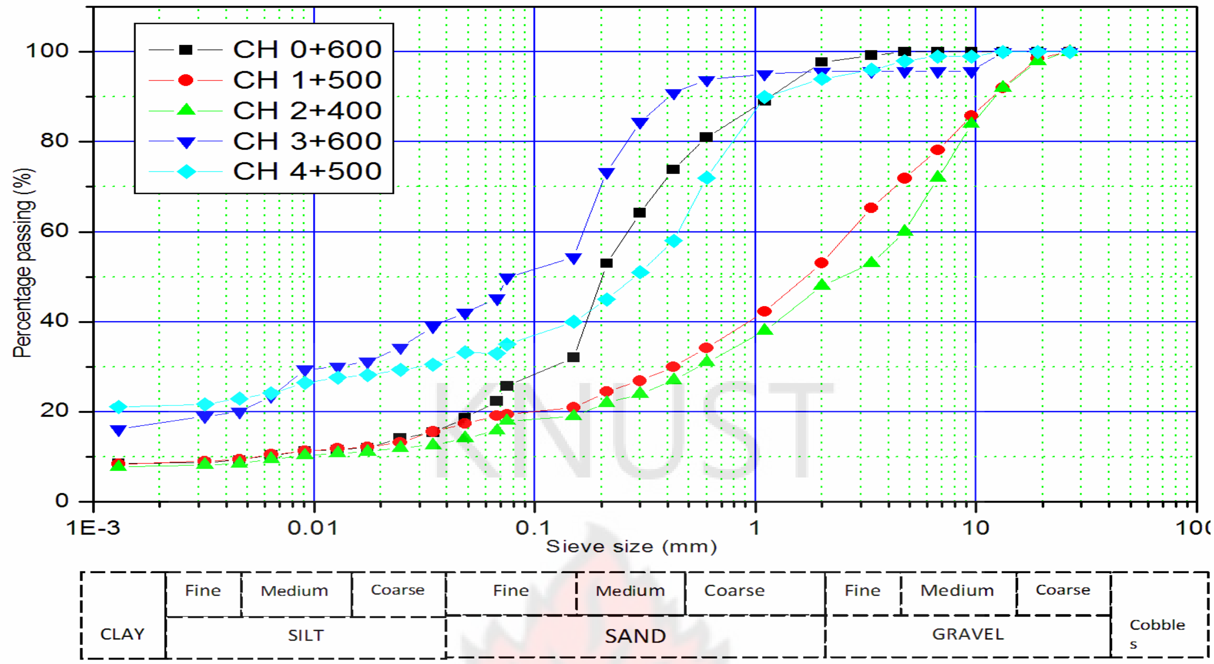

Figure 13: Grading curves for the subgrade soils on the study road.

The summary of the various laboratory test results are presented in Table 3 below.

Table 3: Summary of laboratory test results for the subgrade soils.

Test Section	Chainage	Passing #200 (%)	Liquid Limit (%)	Plastic Limit (%)	Plasticity Index (%)	Natural Moisture Content (%)	Field Dry Density Kg/m^3	AASHTO Soil Classification
Section 1 (Valley)	0+600	25.7	32.0	13.0	19.0	4.3	1936	A - 6
	1+500	30.8	36.3	20.7	16.0	3.5	1834	A - 6
Section 2 (Hill)	2+400	17.6	23.1	12.6	11.0	3.6	1833	A-2-7
Section 3 (Valley)	3+600	49.9	43.9	23.2	20.6	5.5	1836	A - 6
	4+500	33.1	32.0	16.8	15.0	4.8	1995	A - 6

The summary of the thicknesses of the various pavement layers encountered on the study road are indicated in Tables 4, 5 and 6.

Table 4: Trial pit log for chainage 0+000 – 1+100 (section 1)

Layer Thickness (m)	**Layer Designation**	**Layer Description**	**Field description**
0.00 – 0.15	1	Base	Lateritic gravel
0.15 – 0.35	2	Subgrade	Silty clay (A-6)

Table 5: Trial pit log for chainage 1+200 – 3+500 (section 2)

Layer Thickness (m)	**Layer Designation**	**Layer Description**	**Field description**
0.00 – 0.20	1	Base	Lateritic gravel
0.20 – 0.40	2	Subbase	Lateritic gravel
0.40 – 0.80	3	Subgrade	Silty gravelly sand(A-2-7)

Table 6: Trial pit log for chainage 3+600 – 5+200 (section 3)

Layer Thickness (m)	**Layer Designation**	**Layer Designation**	**Field description**
0.00 – 0.20	1	Base	Lateritic gravel
0.20 – 0.35	2	Subgrade	Silty clay (A-6)

4.3 FWD Analysis

The output of the FWD sensors is shown in Appendix D. Tables D_1 to D_7 are the road pavement deflection values registered at the various geophone positions. Two load drop tests were conducted on the road pavement at each FWD locations. The output the deflection test shows the number of load drops used for the test, the force impacted on the load plates and the stresses induced in the pavement structure.

The first drop test was the sitting blow, whiles the second load drop test was the actual deflection test. The results of the second load drop test were used in the back-calculation for the moduli of the pavement layer.

The ELMOD 5 pavement analysis software was used in the analysis of the FWD deflection data. The back-calculation procedures used by ELMOD 5 starts with “seed” values of moduli for each pavement layer. The peak applied dynamic load is represented by a static load on the surface, and a static deflection basin is calculated for the pavement model layers. A comparison is made of the calculated deflection basin with the measured deflection basin. Differences are used to guide adjustment of moduli in various layers, and another set of deflection is calculated for the model. A Poisson’s ratio of 0.35 was used for the calculation of the subgrade M_R. The comparison-adjustment-recalculation procedure is carried out until the calculated deflections are as close as possible to the measured peak dynamic deflections. The result is a set of moduli for the layers of the model that gives a calculated static deflection basin close to the measured dynamic deflection basin.In the ELMOD analysis, the road was delineated according to the topography and the soil type encountered along the study road. Two moduli layer system was observed in the analysis of the pavement structure. This is as a result of the software modelling the base or the combination of the base and subbase as one bound layer and the subgrade as the other layer.

The thin double surface treatment acting as a waterproofing layer was not considered as structurally contributing to the strength of the pavement and hence not considered in the ELMOD analysis. The output of the ELMOD 5 programme is presented in Tables 7 to 9.

H_1 is the thickness of the unbound layer from the trial pit log used as input used for back-calculation of the resilient modili. E_1 and E_2 are the resilient moduli for the bound and subgrade soils respectively. Co and N are the subgrade non-linear properties. N is the measure of non-linearity. N equals to zero indicates linearly elastic subgrade property and a decreasing N results in pronounced non-linearity of the subgrade. The maximum and minimum values of the subgrade non-linear properties, Co and N for the three sections are shown in Table 10.

Table 7: Output of Elmod 5 for section 1

Chainage	Layer Thickness (mm) H1	H2	H3	H4	Moduli (MPa) E1	E2	E3	E4	E5	Non Linear Properties CO	N
0.000	150				1906	141				164	-0.151
99.900	150				1619	69				91	-0.352
199.500	150				1454	105				144	-0.300
299.900	150				288	349				349	0.000
399.500	150				1714	171				234	-0.265
499.600	150				683	97				144	-0.293
599.600	150				2660	130				162	-0.270
699.700	150				943	61				82	-0.303
800.000	150				1191	476				525	-0.058
899.500	150				1209	135				163	-0.164
1000.000	150				844	126				126	0.000
1100.100	150				920	204				207	-0.008

Table 8: Output of Elmod 5 for section 2

Chainage	Layer Thickness(mm) *H1*	H2	H3	H4	Moduli (MPa) E1	E2	E3	E4	E5	Non-Linear properties CO	N
1200.000	400				512	236				236	0.000
1300,000	400				331	29				22	-0.594
1400.000	400				445	55				42	-0.361
1500.000	400				352	44				30	-0.565
1600.000	400				602	126				126	-0.297
1700.000	400				212	36				36	-0.564
1800.000	400				607	102				98	-0.268
1900.000	400				763	100				91	-0.339
2000.000	400				837	215				217	-0.200
2100.000	400				573	51				41	-0.727
2200.000	400				692	261				261	0.000
2300.000	400				638	46				34	-0.846
2400.000	400				677	62				51	-0.411
2500.000	400				606	43				32	-0.666
2600.000	400				571	72				65	-0.368
2700.400	400				338	12				5	-1.428
2800.000	400				741	64				51	-0.748
2900.000	400				557	63				56	-0.324
3000.000	400				538	35				25	-0.565
3100.000	400				340	123				123	0.000
3200.000	400				511	61				55	-0.227
3300.000	400				494	48				40	-0.483
3400.000	400				445	192				192	0.000
3500.000	400				388	43				38	-0.476

Table 9: Output of Elmod 5 for section 3

Chainage	Layer Thickness (mm) H1	H2	H3	H4	Moduli (MPa) E1	E2	E3	E4	E5	Non linear Properties CO	N
3600.000	200				429	73				80	-0.108
3700.500	200				493	75				87	-0.177
3800.000	200				626	135				135	0.000
3900.000	200				978	130				147	-0.158
4000.000	200				412	84				96	-0.231
4100.000	200				636	22				20	-0.843
4200.000	200				1035	112				124	-0.150
4300.000	200				881	157				191	-0.193
4400.000	200				613	116				131	-0.123
4500.000	200				603	150				154	-0.029
4600.000	200				895	279				296	-0.050
4700.000	200				985	55				67	-0.401
4800.000	200				484	240				240	0.000
4900.000	200				773	123				153	-0.221
5000.000	200				737	117				139	-0.333
5100.000	200				854	190				234	-0.183
5200.000	200				748	181				227	-0.198

Table 10: Subgrade non-linear properties

Section	Maximum C_o Value	Minimum C_o Value	Maximum N Value	Minimum N Value
1	525	82	0	-352
2	261	5	0	-1.428
3	296	20	0	-0.843

4.4 DCP Results

The numerical values and the plots of all the DCP test results are presented in Appendix E.

The Microcal Origin Pro 7 statistical analysis software was used in the analysis of the DCP data. The DCP data was keyed into a Microsoft excel sheet which was imported into the Microcal Origin Pro 7.

A table consisting of cumulated number of blows in one column and the penetration values in another column was formed. A scatter plot of the points of cumulated sum of blows against the penetration values was plotted. This shows a series of points in straight line according to changes in the layers encountered as the DCP rod was driven into the road. The cumulated number of blows plotted against the penetration curves resulted in different gradients. This implies that different layers were encountered at a DCP point.

The depth used in the determination of the penetration index for the different materials used in the correlation was selected to coincide with the depth of the layers observed in the excavated trial pits log for the materials at three sections. DCP layers within defined thicknesses were combined and the line of best fit determined. The penetration rate, PR (sometimes referred as DCP ratio, or penetration index PI) is determined. The DCP ratio is defined by the slope of the curve relating the number of blows to the depth of penetration (mm/blow) at a given linear depth range. The penetration indices were obtained for gradients of the curve of best fit line from combined layers which coincide with the thicknesses defined from the trial pits logs. The penetration indices of the subgrade material was determined from the mean weighted average of the curve of best fit line of combined layers below the bound materials obtained from the trial pit logs. In the statistical analysis for the development of the prediction model, only very few outliers were observed in the DCP data. The depths observed in the trial pits logs were also used in the analysis of the back-calculations for the determination of the moduli. Tables 11 to 13 present pavement layer thicknesses used in the analysis of the DCP for the penetration index determination.

Table 11: Layer thicknesses and DCPI values used in the DCP analysis for section 1

CHAINAGE (m)	**SECTION**	**H_1 (mm)**	**H_2 (mm)**	**$DCPI_1$ (mm/blow)**	**$DCPI_2$ (mm/blow)**
0+100	1	150	672	1.84	3.455
0+200		150	752	2.67	2.65
0+300		150	837	1.41	3.257
0+400		150	810	3.411	2.42
0+500		150	797	2.493	4.196
0+600		150	825	1.173	2.882
0+700		150	820	1.082	2.86
0+800		150	824	2.02	3.585
0+900		150	615	0.905	2.663
1+000		150	830	2.166	3.955
1+100		150	639	2.155	2.075

Table 12: Layer thicknesses and DCPI values used in the DCP analysis for section 2

CHAINAGE (m)	SECTION	H_1 (mm)	H_2 (mm)	$DCPI_1$ (mm/blow)	$DCPI_2$ (mm/blow)
1+200	2	400	840	2.332	3.461
1+300		400	844	5.647	3.18
1+400		400	820	4.503	9.953
1+500		400	850	2.079	5.075
1+600		400	813	2.205	4.257
1+700		400	816	5.215	8.858
1+800		400	814	4.228	8.854
1+900		400	825	1.831	7.547
2+000		400	732	2.25	4.579
2+100		400	814	3.418	6.206
2+200		400	819	3.553	3.54
2+300		400	809	2.87	3.777
2+400		400	806	1.834	3.223
2+500		400	811	3.637	5.043
2+600		400	814	2.279	6.483
2+700		400	851	1.265	5.244
2+800		400	851	2.104	5.122
2+900		400	889	4.887	7.191
3+000		400	838	3.031	9.919
3+100		400	834	1.521	5.453
3+200		400	840	4.156	8.733
3+300		400	850	3.815	6.793
3+400		400	828	2.509	5.24
3+500		400	840	4.73	7.195

Table 13: Layer thicknesses and DCPI values used in the DCP analysis for section 3

CHAINAGE (m)	SECTION	H_1 (mm)	H_2 (mm)	$DCPI_1$ (mm/blow)	$DCPI_2$ (mm/blow)
3+600	3	200	828	3.554	7.934
3+700		200	818	3.147	5.354
3+800		200	828	3.738	5.299
3+900		200	825	2.151	4.262
4+000		200	826	3.244	7.904
4+100		200	848	2.439	5.067
4+200		200	846	2.53	4.516
4+300		200	824	1.53	2.853
4+400		200	818	3.7	4.339
4+500		200	796	4.737	8.145
4+600		200	800	3.144	4.793
4+700		200	830	2.992	5.5
4+800		200	835	3.672	3.423
4+900		200	673	1.611	3.891
5+000		200	683	4.873	2.394
5+100		200	683	2.08	4.618
5+200		200	683	2.522	4.736

4.5 Model Prediction

The Microcal Origin Pro 7 statistical software was used in the comprehensive analysis of the determination of the relationship between the resilient moduli of the FWD and the penetration indices of the bound and the subgrade materials. In the statistical analysis of the FWD modulus and the DCP penetration index, data points for the model prediction of the relationship between the subgrade resilient modulus and the penetration index were tested for outliers that would affect the results of the model predicted for the relationship.

The T_o - test statistics given by Equation (32) was used in the determination of the outliers.

$$T_0 = \left| \frac{x_0 - \bar{x}_n}{S_n} \right| \quad \ldots\ldots\ldots\ldots\ldots\ldots\ldots\ldots.. \quad (31)$$

where

$\bar{x}_n$ = arithmetic mean

S_n = sample standard deviations

x_o = value of the test result differing most from the mean

The value of T_o is compared with the critical values of T for the applicable value of "n", from Table 14. If the absolute value of T_o is greater than T, then xo is an outlier.

Table 14: Table of critical values for predicting outliers for n number of observations

No of observations (n)	**Critical values (T)**
4	1.46
5	1.67
6	1.82
7	194
8	2.03
9	2.11
10	2.18
11	2.23
12	2.29
13	2.33
14	2.37
15	2.41
16	2.44
17	2.47
18	2.50
19	2.53
20	2.56

This statistical test on both the FWD modulus and the DCP penetration index (DCPI) show few outliers. These were removed prior to the fitting of the curve for the regression model.

FWD resilient modulus value E_2 at a chainage location in section 1 of Table 7 is paired with a DCP penetration index, $DCPI_2$ at the same chainage in Table 11 for the plotting of the scatter diagram for the prediction of the model.

This was done in a similar manner for the FWD moduli and the DCP penetration index, DCPI for both the subgrade and the unbound materials for the other sections. For each section, the best fit linear curve was fitted to the plotted points of the FWD moduli and the DCP penetration indices in a Log-Log plot. The FWD moduli was set as the independent variable whiles the DCP penetration index were set as the dependent variable. The prediction model was performed individually for the bound and subgrade materials within the three sections. Additionally, prediction model was performed for the combined resilient modulus of the subgrade with similar soil characteristics. The prediction model for the combined unbound material was performed for the entire section by characterizing the soil to have the same properties from the visual inspection of the trial pit samples. Thus eight prediction models were obtained according to the locations of the pavement structure at the three sections observed from the topography.

4.5.1 Correlations for the Subgrade soils

The plots of the FWD subgrade resilient moduli versus the DCP penetration index are shown in Figure 13 to 16. Subgrade soils encountered in sections 1 and 3 both classify as A-6. Therefore the two sections were also combined for a combined regression.The prediction model used for fitting the results for A-6 subgrade soils was also used to fit the results of A-2-7 subgrade soils.

This was done by using the the Microcal Origin 7 Log – Log linear regression analysis. The significance of the correlations between any two variables is measured using the Pearson product-moment coefficient of correlation (r). If the value of r is zero or near zero, this indicates that there is no evidence of an apparent linear correlation present. If the value of r is positive or negative one, a perfect linear correlation does exist. Normally a correlation coefficient of greater than 0.60 is considered as significant value.

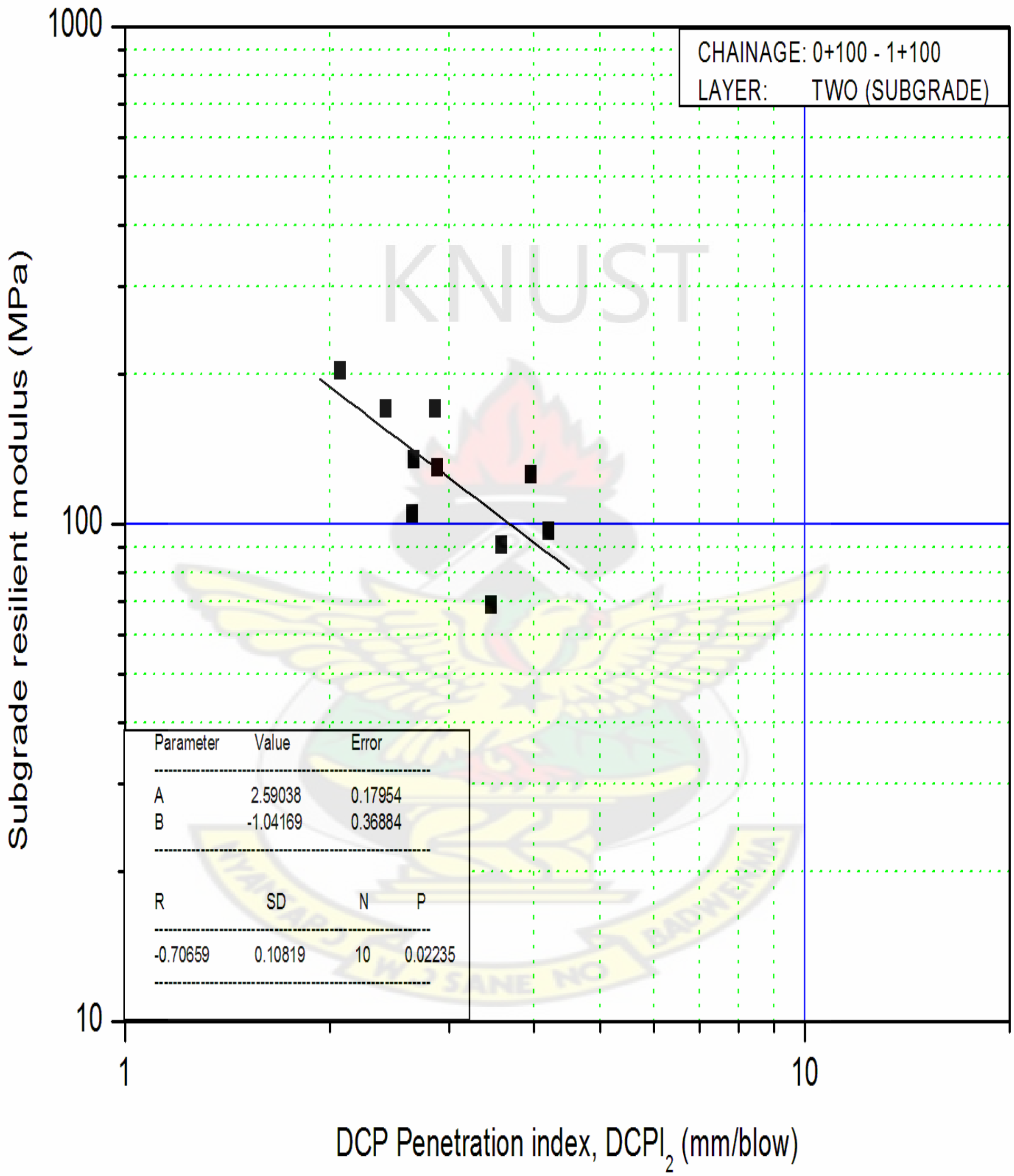

Figure 14: Plot of subgrade resilient modulus versus DCP penetration index for Section 1

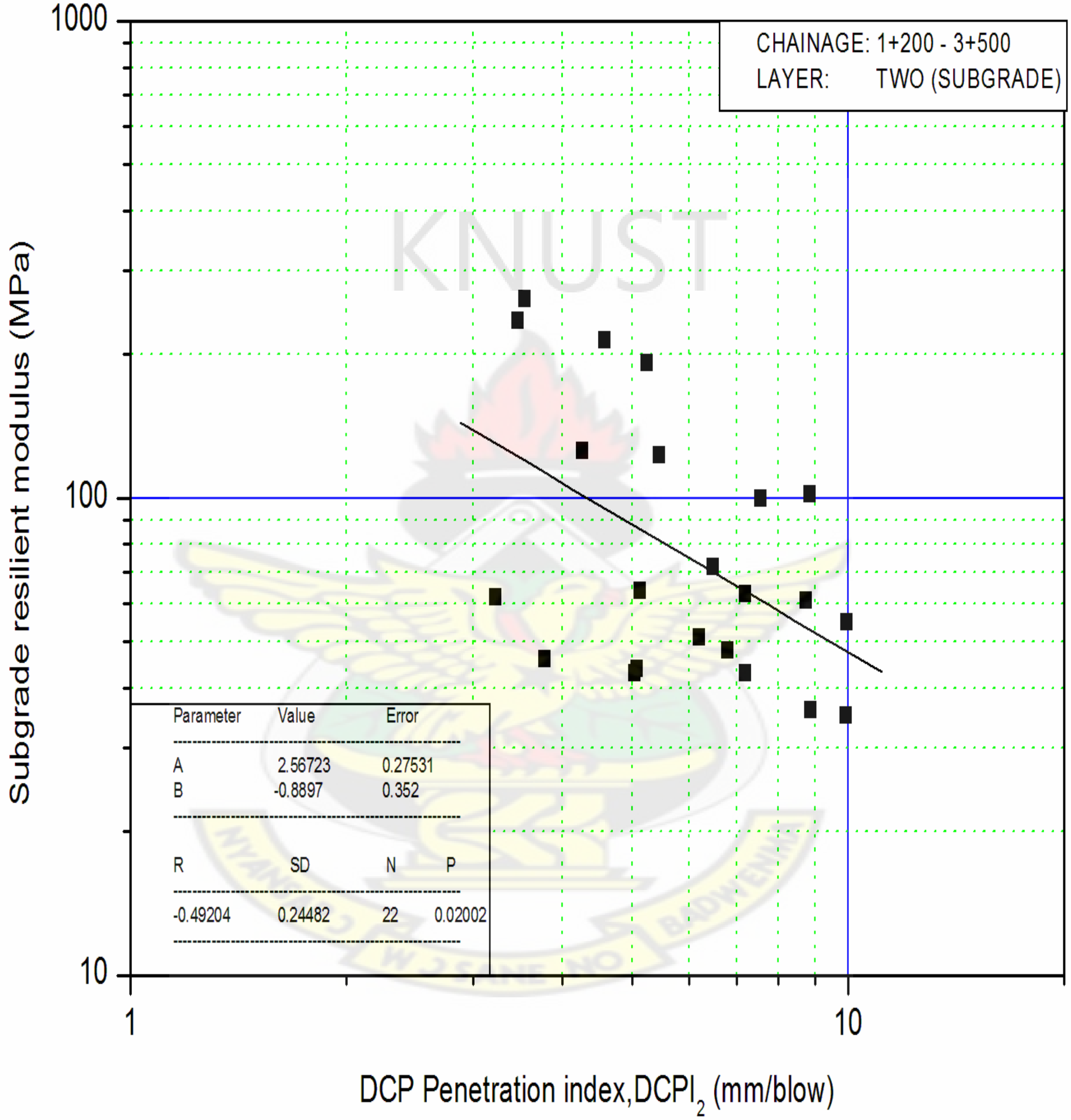

Figure 15: Plot of subgrade resilient modulus versus DCP penetration index for Section 2

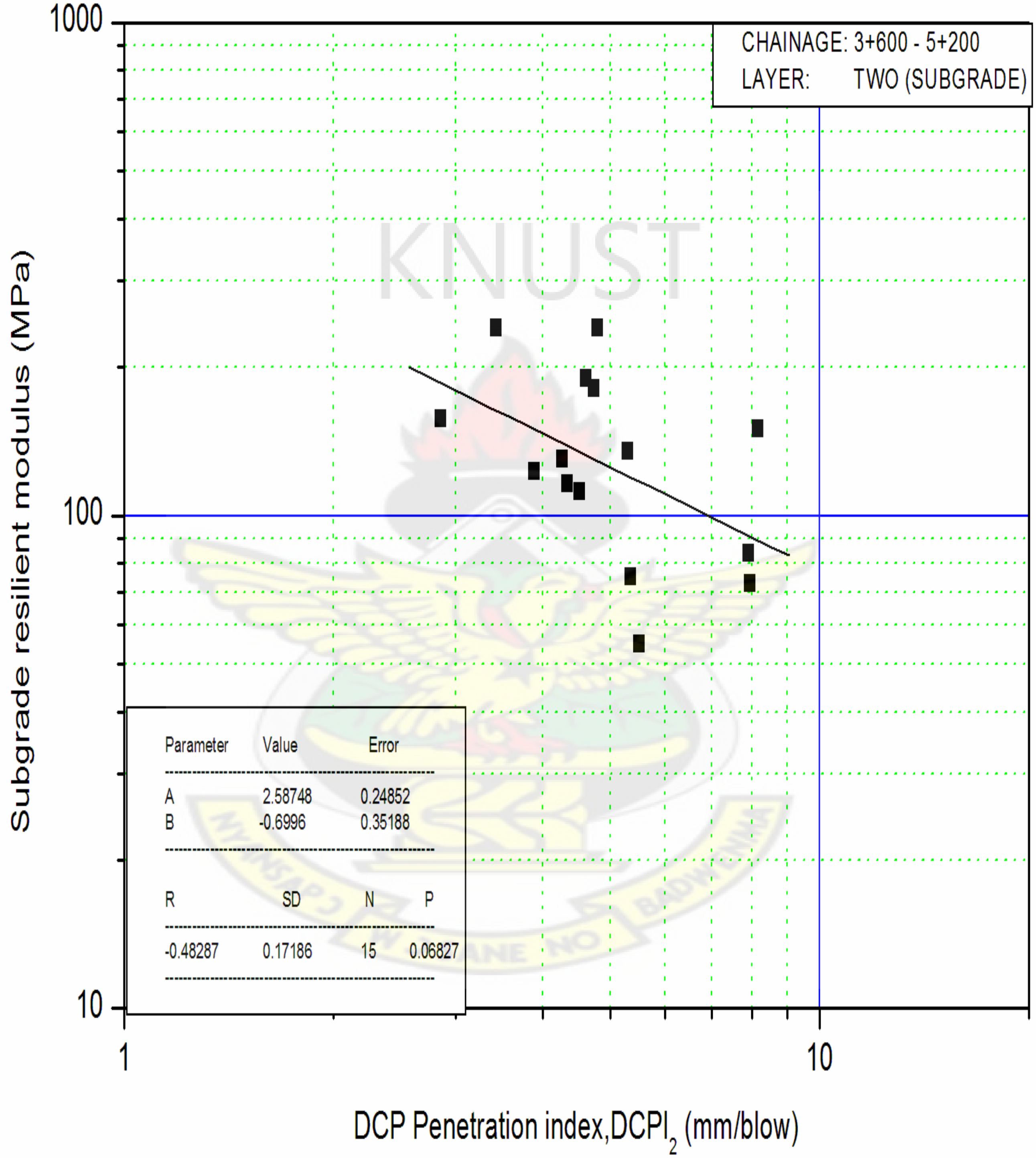

Figure 16: Plot of subgrade resilient modulus versus DCP penetration index for Section 3

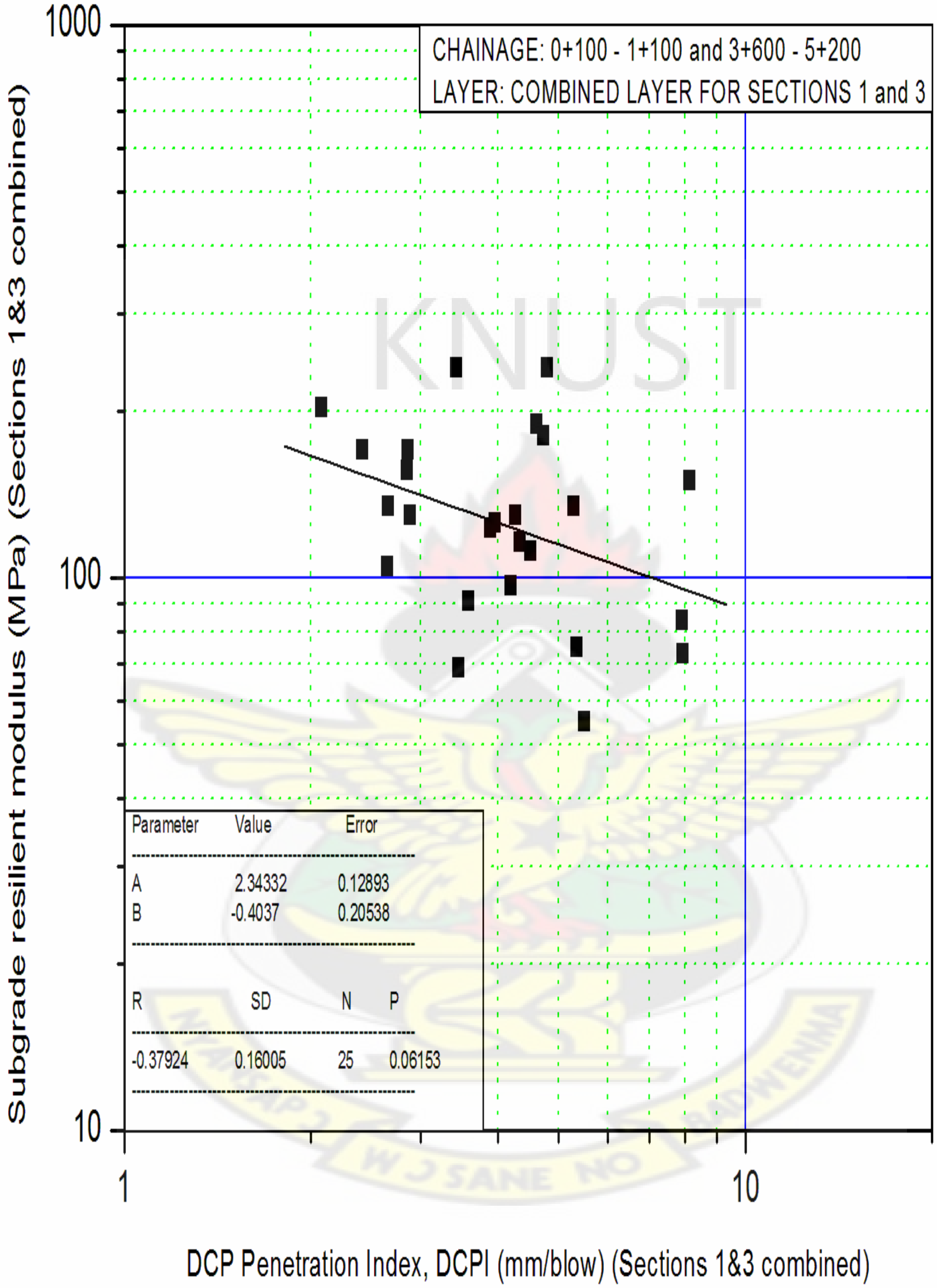

Figure 17: Plot of subgrade resilient modulus versus DCP penetration index for sections 1 and 3

The regression analysis yielded the following:

For section 1

$$\text{Log } M_R = 2.59038 - 1.04169 \text{ Log DCPI}, \; r = -0.70659 \quad \text{.......................... (32)}$$

For section 3

$$\text{Log } M_R = 2.58748 - 0.6996 \text{ Log DCPI}, \; r = -0.48287 \quad \text{.......................... (33)}$$

For section 2

$$\text{Log } M_R = 2.56723 - 0.8897 \text{ Log DCPI}, \; r = -0.49204 \quad \text{.......................... (34)}$$

The regression analysis for the two A-6 sections combined yielded the result below.

$$\text{Log } M_R = 2.34332 - 0.4037 \text{Log DCPI}, \; r = -0.37924 \quad \text{.......................... (35)}$$

The summary of the soil properties and regression model parameters of the test statistics is presented in table 15.

Table 15: Summary of soil properties and regression model parameters of test statistics for subgrade layer for the studied sections

Subgrade

Section	**Chainage (m)**	**Soil Properties**			**Fitting**			
		PI	**Fines**	**Class**	**A**	**B**	**r**	**P < 0.05**
1	0+100 – 1+100	19	26	A - 6	2.59038	-1.04169	-0.70659	0.02235
2	1+200 – 3+500	13	19	A – 2- 7	2.56723	-0.8897	-0.49204	0.02002
3	3+600 – 5+200	18	41	A - 6	2.58748	-0.6996	-0.48287	0.06827
4	Combined	-	-	(A-6)	2.34332	-0.4037	-0.37924	0.06153

Based on the results of the regression analysis, the coefficient of correlation (r) for the combined subgrade soils is above 0.4.

This shows that there is a poor correlation between DCP penetration index, DCPI and the FWD resilient modulus of the subgrade. The significance level test for p-values of 0.06 shows that there is poor collinearity among the variables used since the p-values is above 0.05.

4.5.2 Correlations for the unbound materials

The plots of the FWD subgrade resilient moduli versus the DCP penetration index are given below.

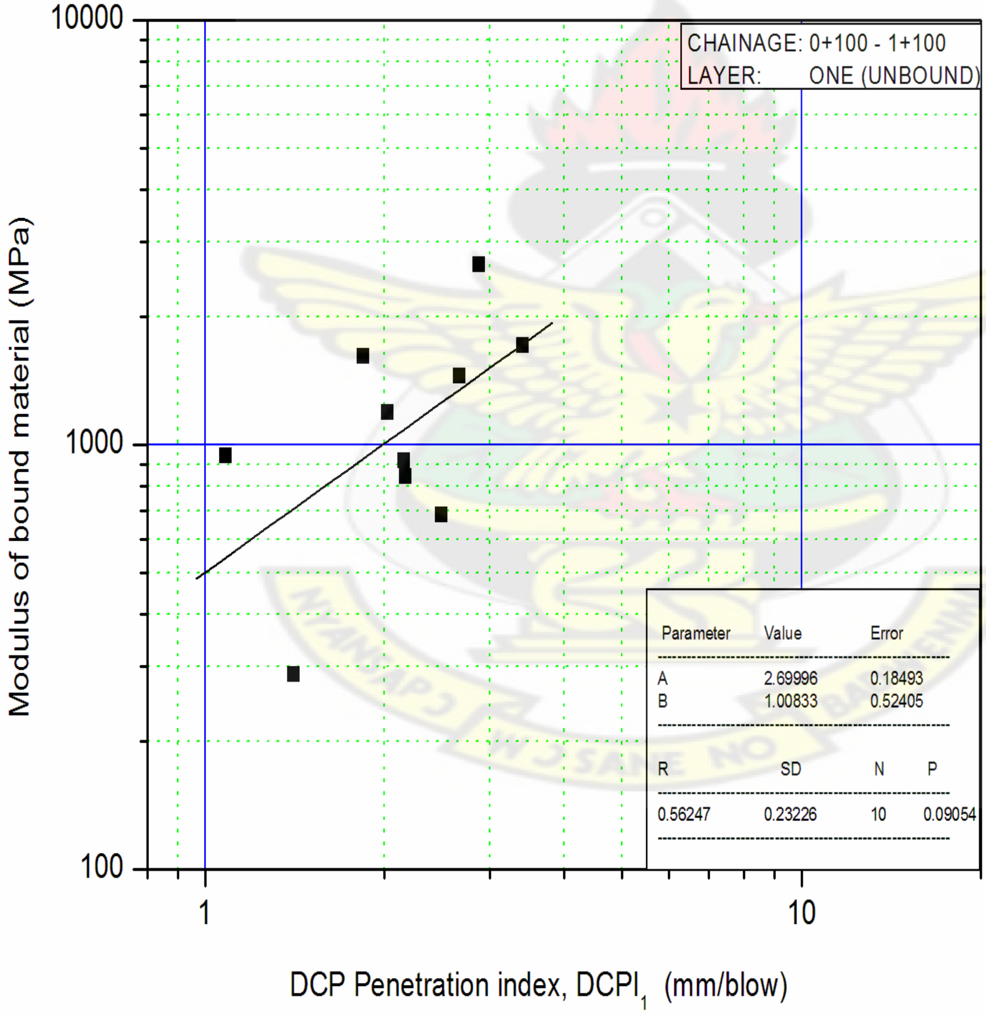

Figure 18: Plot of modulus of unbound material versus DCP penetration index for Section 1

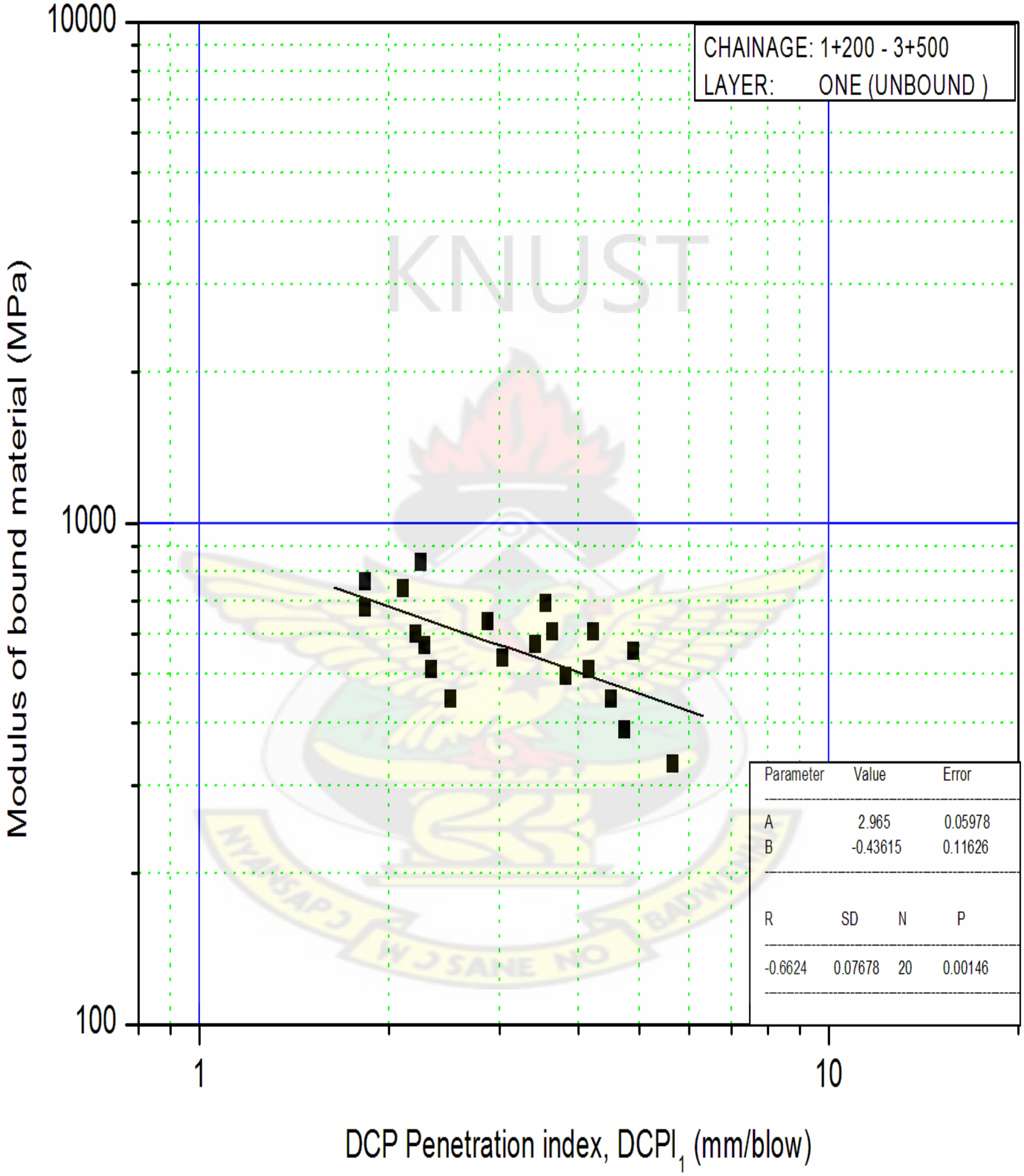

Figure 19: Plot of modulus of unbound material versus DCP penetration index, for section 2

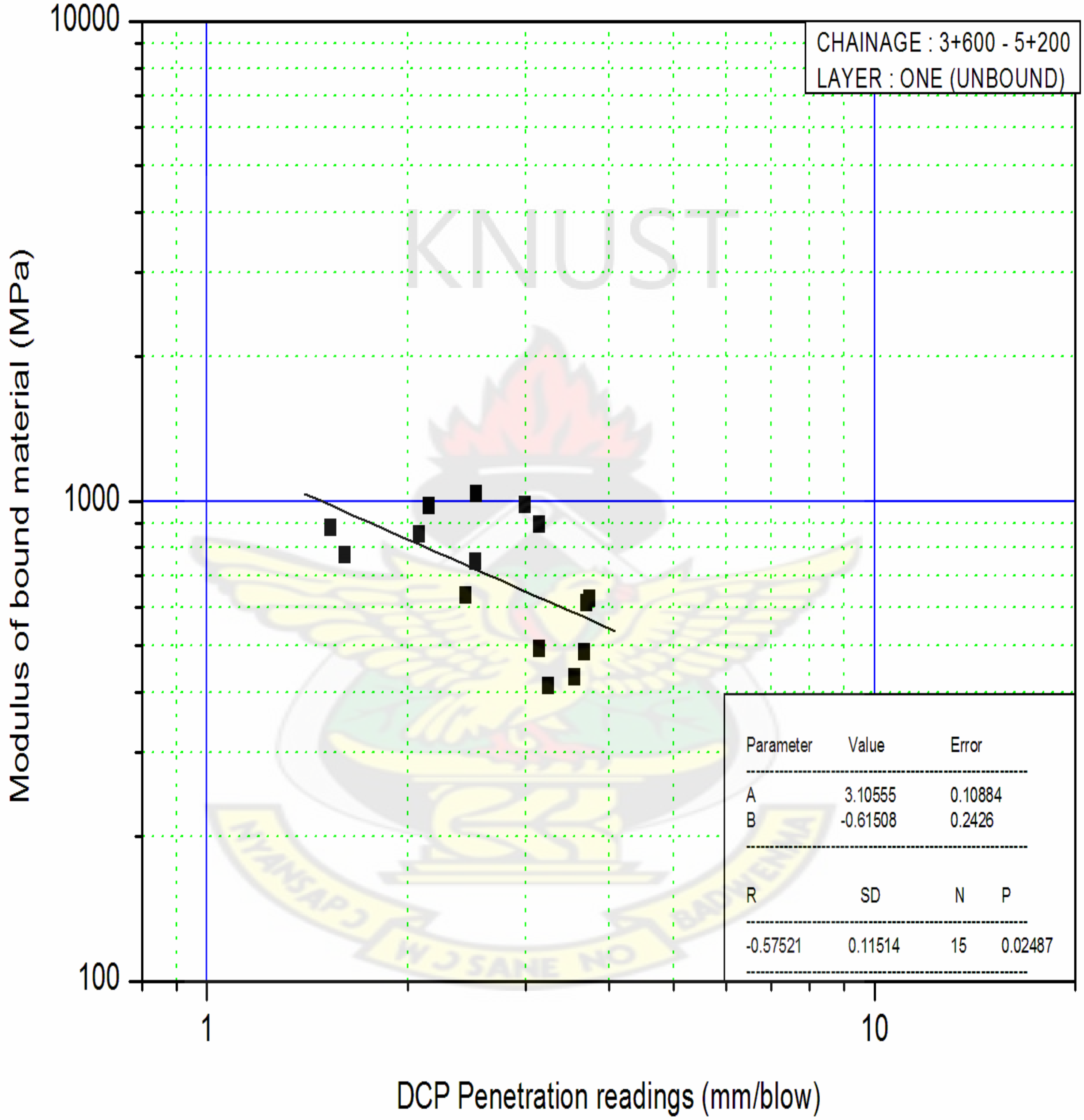

Figure 20: Plot of modulus of unbound material versus DCP penetration index for Section 3

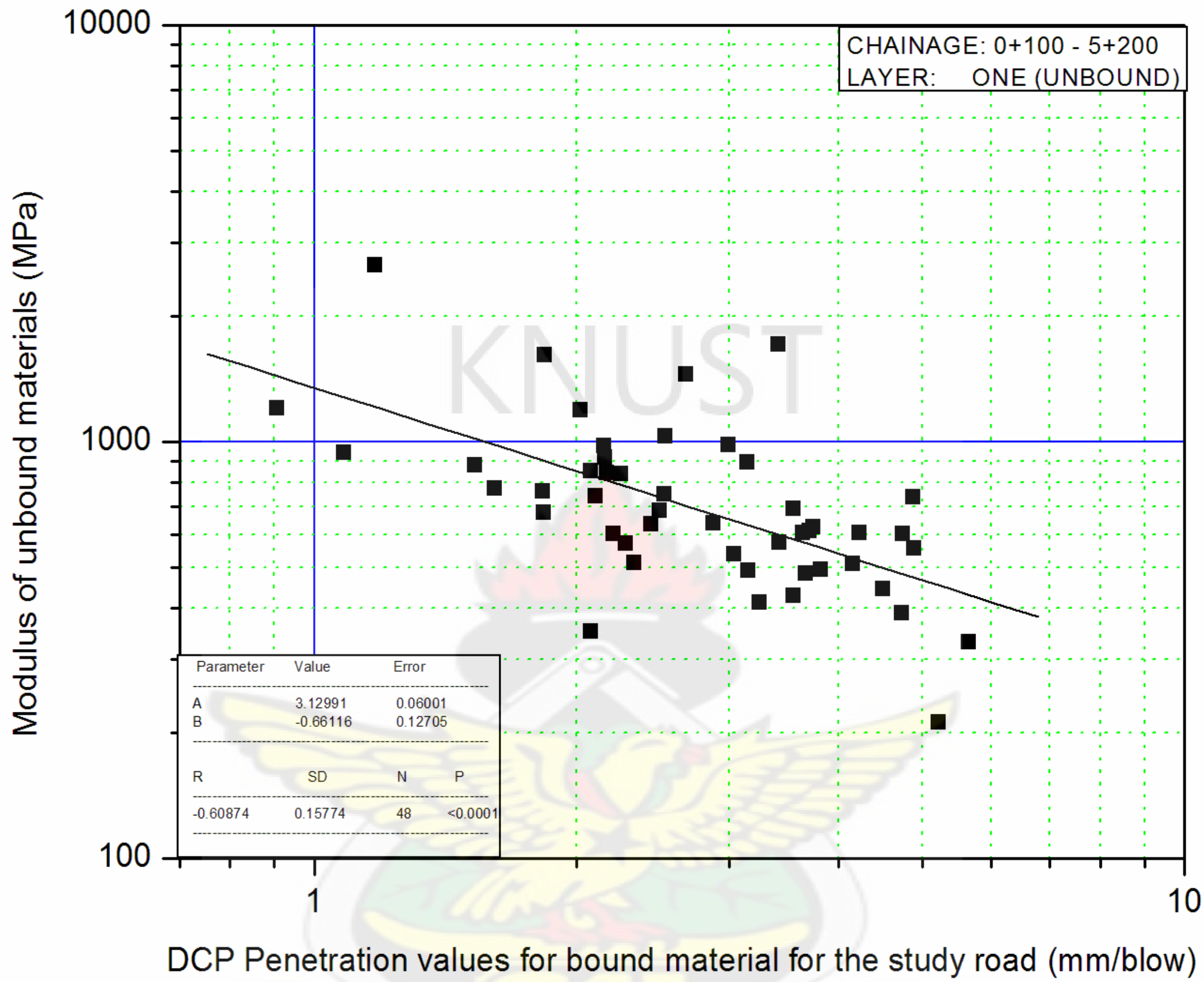

Figure 21: Plot of model equation of combined modulus of unbound materials versus DCP penetration index for Sections 1, 2 and 3

Attempts were made to fit a correlation between the unbound modulus and the DCP penetration index, DCPI.

The summary of the results is shown in Table 16. Sections 2 and 3 show a negative correlation whiles section 1 showed a positive correlation. Since no physical soil properties of the unbound material were available, it is difficult to explain the different correlations obtained. This may be attributed to the data variability, especially given the relatively thin layer thickness of 150mm for section 1 unbound material.

The unbound material was therefore combined and a correlation attempted. Table 16 shows the summary soil properties and regression model parameters of the test statistics for the unbound materials.

Table 16: Summary of soil properties and regression model parameters of test statistics of the unbound layer for the studied sections

Unbound Layer

Section	Chainage (m)	Soil Properties			Fitting			
		PI	Fines	Class	A	B	r	$P < 0.05$
1	0+100 – 1+100	-	-	-	2.69996	1.00833	0.56247	0.09054
2	1+200 – 3+500	-	-	-	2.965	-0.43615	0.66240	0.00146
3	3+600 – 5+200	-	-	-	3.10555	-0.61508	0.57521	0.02487
4	Combined unbound layers	-	-	-	3.12991	-0.66116	-0.60874	<0.0001

The regression analysis for the unbound material for the three sections 1, 2 and 3 are given below in the order as stated

$$\text{Log } M_R = 2.69996 + 1.00833 \text{ Log DCPI}, \quad r = 0.56247 \quad \ldots\ldots (36)$$

$$\text{Log } M_R = 2.96500 - 0.43615 \text{ Log DCPI}, \quad r = 0.66240 \quad \ldots\ldots (37)$$

$$\text{Log } M_R = 3.10555 - 0.61508 \text{ Log DCPI}, \quad r = 0.57521 \quad \ldots\ldots (38)$$

The regression analysis for the combined unbound materials is given as

$$\text{Log } M_R = 3.12991 - 0.66116 \text{ Log DCPI}, \quad r = -0.60874 \ldots\ldots (39)$$

CHAPTER 5: CONCLUSION AND RECOMMENDATIONS

5.1 Conclusion

This report presents the development of models in an effort to predict the resilient modulus of subgrade soils from test results of penetration index, DCPI, for the subgrade soils (cohesive, A-6 and non-cohesive, A-2-7). However, the correlation was extended to cover the prediction model for the modulus of the unbound material and the penetration index for the three sections. Field and laboratory testing programs were conducted to gather data and to classify the study road subgrade soils. The field testing program covers DCP and FWD testing. The laboratory program involves the determination of the subgrade soil physical properties .i.e. Atterberg Limit and soil Classification tests.

Comprehensive statistical analyses were conducted on the field test results (FWD and DCP) of the unbound material and the subgrade soils. Based on the results of this study, the following conclusions have been drawn:

Subgrade soils

- There exists a poor correlation between the FWD subgrade resilient modulus and DCP penetration index (DCPI) in the form of logarithmic relation for the subgrade soils.

  The equation obtained is

$$\text{Log } M_R = 2.56776 - 0.82232 \text{ Log DCPI}, \ r = 0.4$$

Unbound materials

- There exists a poor correlation between the FWD subgrade resilient modulus and DCP penetration index, DCPI, in the form of logarithmic linear relation for the unbound granular natural gravel soils,

  The equation obtained is

$$\text{Log } M_R = 3.12991 - 0.66116 \text{ Log DCPI}, \ r = 0.61$$

5.2 Recommendations

It is recommended that:

1) Further tests need to be conducted to validate the models developed in this study by conducting more field testing and including large variety of materials in the test factorial.
2) Future study should include investigation of factors such as dry density (γ_d), moisture content (w_c), liquid limit (LL), and plasticity index (PI)) which affect the resilient modulus of the subgrade soil.

REFERENCES

1. American Society of Testing Materials (2003). “Standard Test Method for Use of the Dynamic Cone Penetrometer in Shallow Pavement Applications” ASTM D 6951-03, ASTM International, West Conshohocken, PA.

2. American Society of Testing Materials (2003). “Standard Guide for Calculating In Situ Equivalent Elastic Moduli of Pavement Materials Using Layered Elastic Theory” ASTM D 5858 – 96.

3. Ampadu and Arthur, (2006). “Dynamic Cone Penetrometer in compaction Verification on a model Road Pavement” Geotechnical Testing Journal, ASTM

4. Ampadu,S.I.K and Dzitse-Awuku,D. (2009), “Model Tests for Bearing Capacity in a Lateritic Soil and Implication for the use of of the Dynamic Cone Penetrometer” Proceedings of the 17th International Conference on Soil Mechanics and Geotechnical Engineering, Alexandria, Egypt.

5. Ampadu, S.I.K (2005), Proceedings of the 17th International Conference on Soil Mechanics and Geotechnical Engineering, Osaka, Japan

6. Chai, G. and Roslie, N. (1998). “The Structural Response and Behavior Prediction of Subgrade Soils Using Falling Weight Defelectometer in Pavement Construction”, Proc. 3rd Int. Conf. on Road & Airfield Pavement Technology.

7. De Beer, M. (2000), “Use of Dynamic Cone Penetrometer in the Design of Road Structures”, Geo-techniques in African Environment, Balkema Rotterdam pp 167-176,2000

8. Fleming, P.R., Frost, M. W., Rogers, C.D.F (2000) "A Comparison of Devices for Measuring Stiffness In- situ." Proceedings of the Fifth International Conference on Unbound Aggregate In Roads, Nottingham, United Kingdom, 2000.

9. George, K.P. and Uddin, W.(2000); “Subgrade Characterization for Highway Pavement Design”. Final Report, MS-DOT-RD-00-131.

10. Hassan, A.(1996), “The Effect of Material Parameters on Dynamic Cone Penetrometer

Results for Fine-grained Soils and Granular Materials," Ph.D Dissertation, Oklahama State University, Stillwater, 1996.

11. Heukelom, W. & Klomp, A.J.G. (1962). "Dynamic Testing as a Means of Controlling Pavements During and After Construction". Proceedings of the 1st International Conference on the Structural Design of Asphalt Pavements (pp. 667-685).

12. Highway Department (2009). "Guidance Notes on Backcalculation of Layer Moduli and Estimation of Residual Life using Falling Weight Deflectometer Test Data"

13. Horak, E. (2002), "Surface Moduli Determined with the Falling Weight Deflectometer used as Benchmarking tool".

14. Jianzhou, C., Mustaque, H., and LaTorella, T. M. (1999). "Use of Falling Weight Deflectometer and Dynamic Cone Penetrometer in Pavement Evaluation", Paper Presented in the Transportation Research Board, Washington, D.C.

15. Kleyn, E.G. and Savage, P.E. "The Application of the Pavement DCP to determine the Bearing Properties and Performance of Road Pavements," International Symposium on Bearing Capacity of Roads and Airfields. Trodheim, Norway, June 1982.

16. Ksaibati, K. (1994). "Selection of subgrade modulus for pavement overlay design procedures" Subnitted to Wyoming Department of Transportation.

17. Livneh, M., Ishai, I., and Livneh, N. A. (1995). "Effect of Vertical Confinement on Dynamic Cone Penetrometer Strength Values in Pavement and Subgrade Evaluations", Transp. Res. Rec. 1473, pp. 1-9.

18. Maher,A. (2000), "Resilient Modulus Properties of New Jersey Subgrade Soils" Final Draft Report submitted to NJDOT.

19. Pen, C. K. (1990), “An Assessment of the Available Methods of Analysis for Estimating the Elastic Moduli of road pavements”, Proc. 3 rd Int. Conf. on Bearing Capacity of Roads and Airfields, Trondheim.

20. Scala, A. J. (1956). “Simple Methods of Flexible Pavement Design Using Cone Penetrometers”, New Zealand Engineering, Vol. 11, No. 2.

21. Seed, H.B., Chan, C.K., and Lee, C.E.(1962). “Resilience characteristics of subgrade soils and their relation to fatigue failures in asphalt pavements.” Proc. 1st Int. Conf. On the Struct. Design of Asphalt Pavements, Ann Arbor, Mich.

22. Ullidtz, P., Harvey.J.T., and Pozzi,J.A. “Layer moduli during HVS testing:comparing loboratory results with backcalculations from FWD and MDD deflections”

23. Van Vuuren, D.J. (1969) “Rapid Determination of CBR with the Portable Dynamic Cone Penetrometer,” The Rhodesign Engineer, No.105.

24. Zhanmin, Z., Claros, G., Lance,M., and Damnjanovic, I. (2004), “Evaluation of the Pavement Structural Condition at Network Level Using Falling Weight Deflectometer (FWD) Data”.

APPENDICES

APPENDIX A

(GRADING TEST RESULTS)

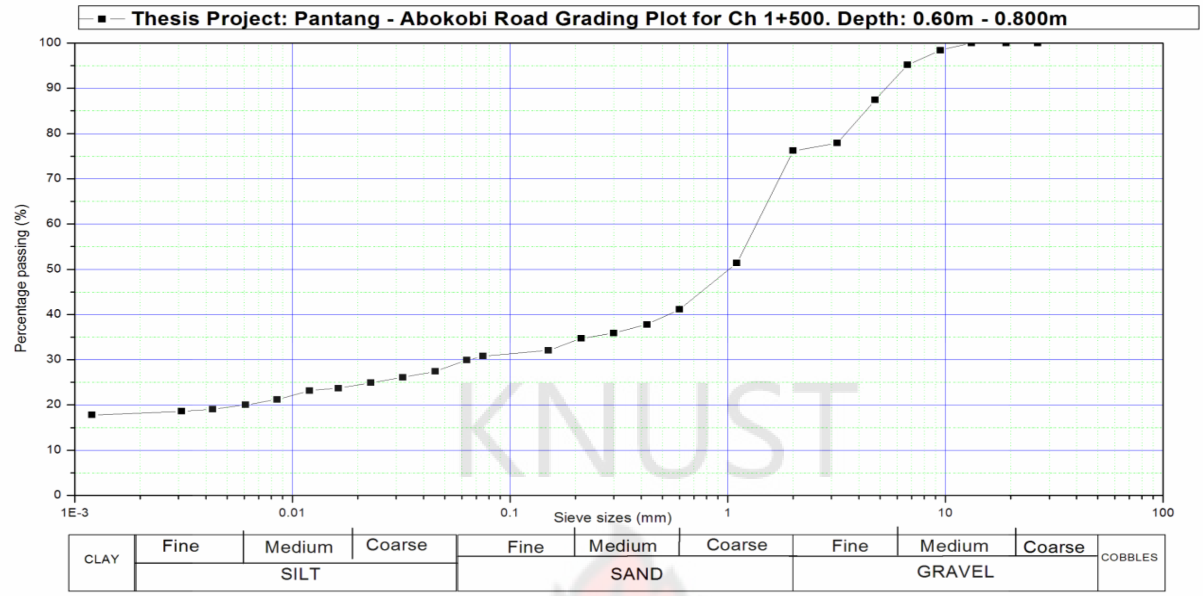

Figure A1: Grading curve for subgrade soil at chainage 0+600

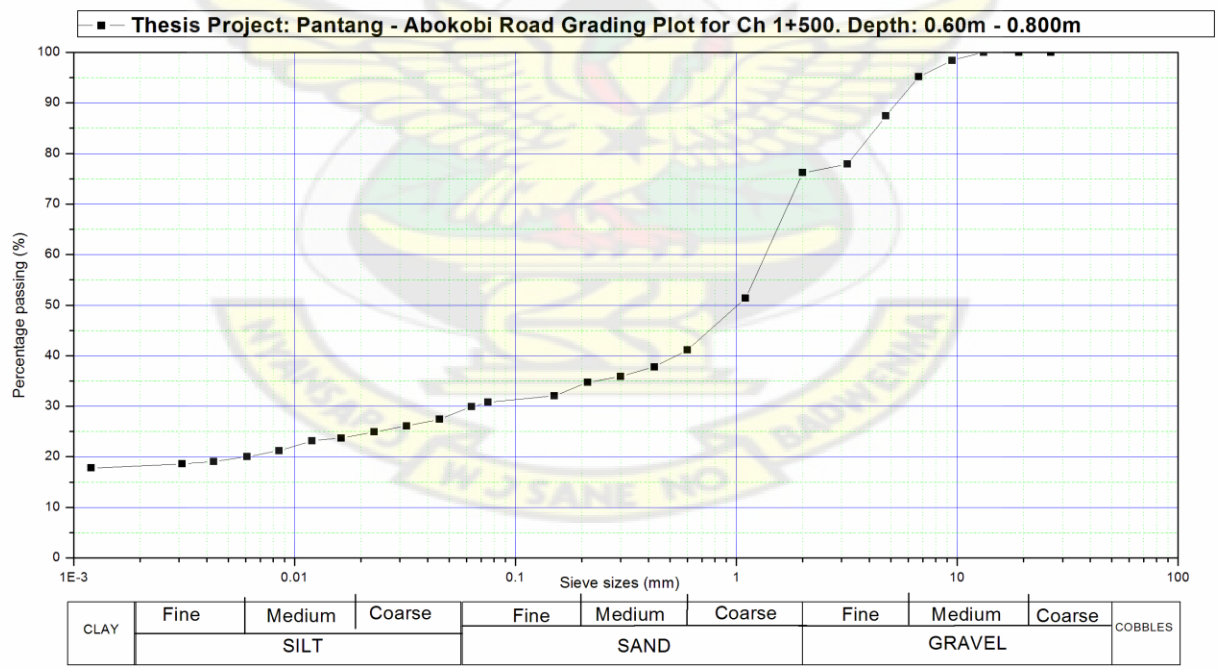

1.1 Figure A2: Grading curve for subgrade soil at chainage 1+500

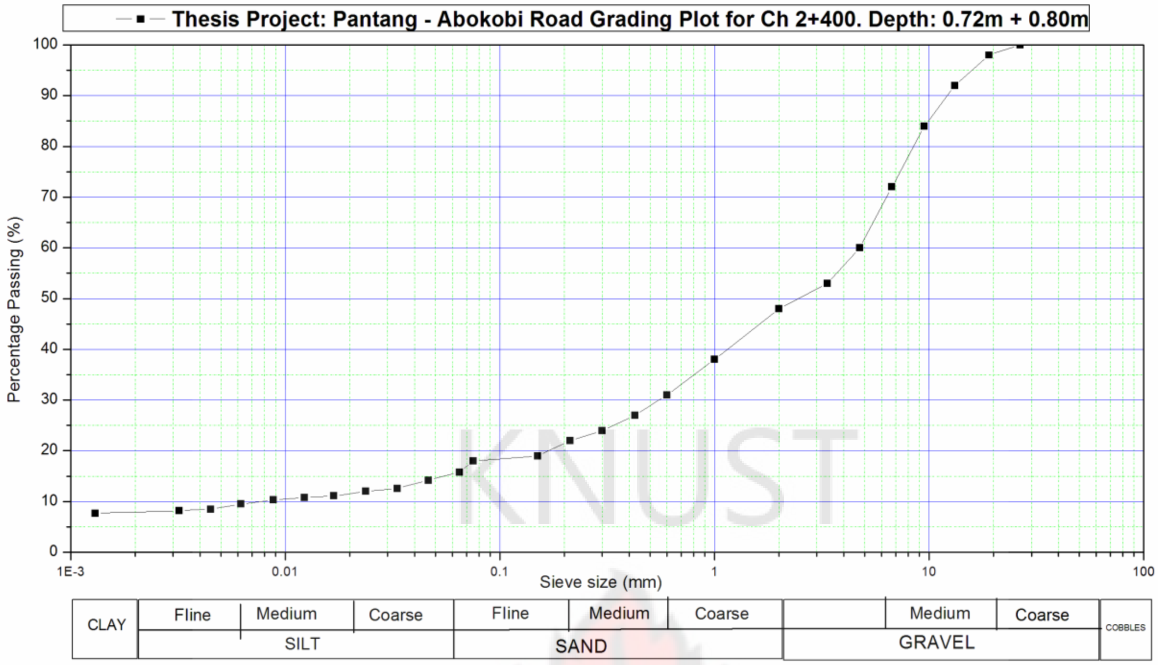

Figure A3: Grading curve for subgrade soil at chainage 2+400

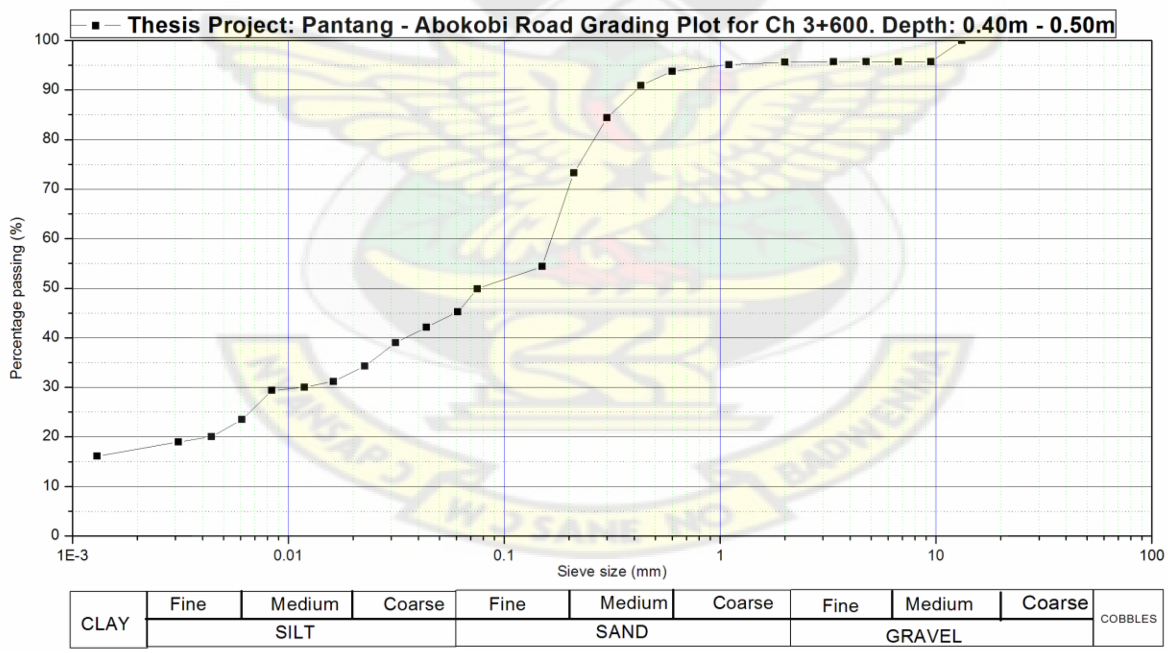

Figure A4: Grading curve for subgrade soil at chainage 3+600

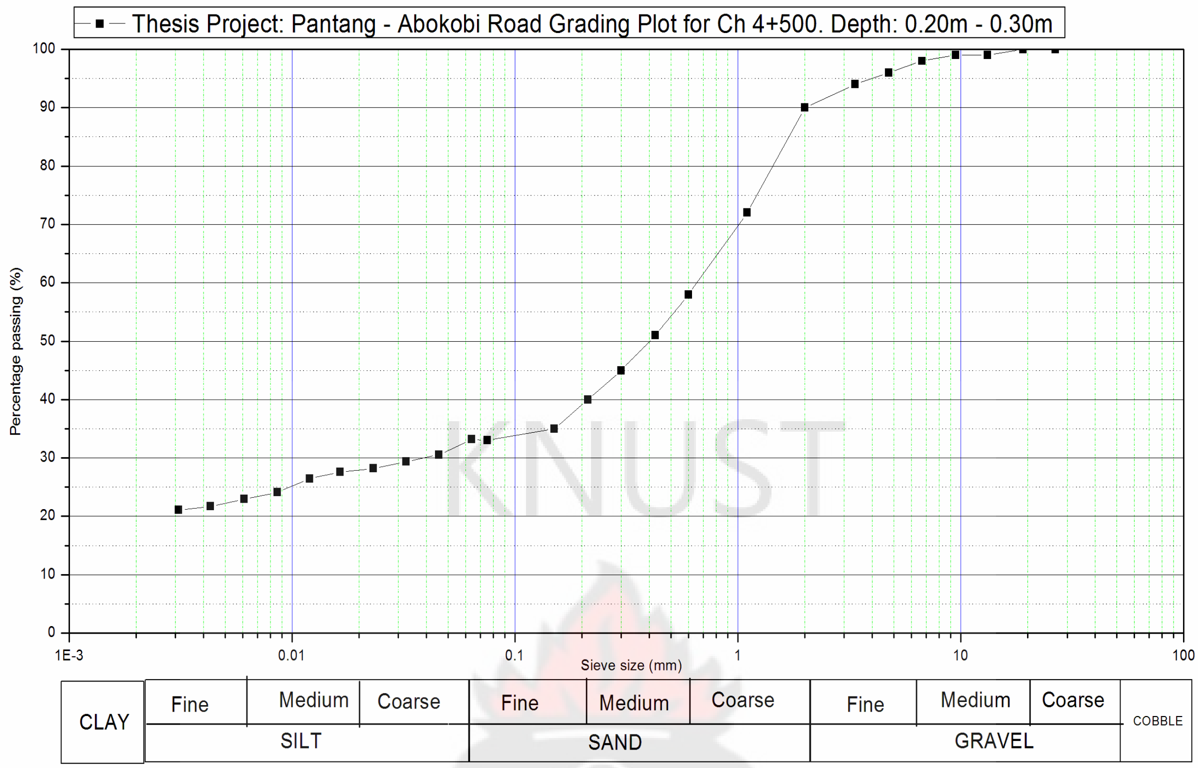

Figure A5: Grading curve for subgrade soil at chainage 4+500

APPENDIX B
(ATTERBERG LIMIT TEST RESULTS)

Table B1: Atterberg limit test for CH 0+600

CIVIL ENGINEERING DEPARTMENT
GEOTECHNICAL ENGINEERING LABORATORY
ATTERBERG LIMIT DETERMINATION

Name of Road:- Pantang- Abokobi

Date :-
20/3/2010

Location:- CH0+600

SAMPLE No./ Depth:
(0.15m-0.30m)

Liquid Limit

CONT. NO	B19	B35	B2	B14	B5X
MASS OF CONT.	3.78	3.76	3.72	3.67	3.72
NO OF BLOWS	44	33	27	17	14
MASS OFWET SAMPLE+CONT	23.89	23.92	22.02	21.1	21.99
MASS OF DRY SAMPLE+CONT	19.45	19.18	17.68	16.72	17.18
MASS OF WATER	4.44	4.74	4.34	4.38	4.81
MASS OF DRY SAMPLE	15.67	15.42	13.96	13.05	13.46
WATER CONTENT %	**28.33**	**30.74**	**31.09**	**33.56**	**35.74**

Plastic Limit		
CONT. NO	A18	K9
MASS OF CONT.	13.69	13.70
MASS OF WET SAMPLE +CONT	12.53	12.54
MASS OF DRY SAMPLE+CONT	3.65	3.65
MASS OF WATER	1.16	1.16
MASS OF DRY SAMPLE	8.88	8.89
WATER CONTENT %	13.1	13.0
AVERAGE WATER CONTENT %	**13.06**	

LL	32.04
PL	13.06
PI	**18.99**

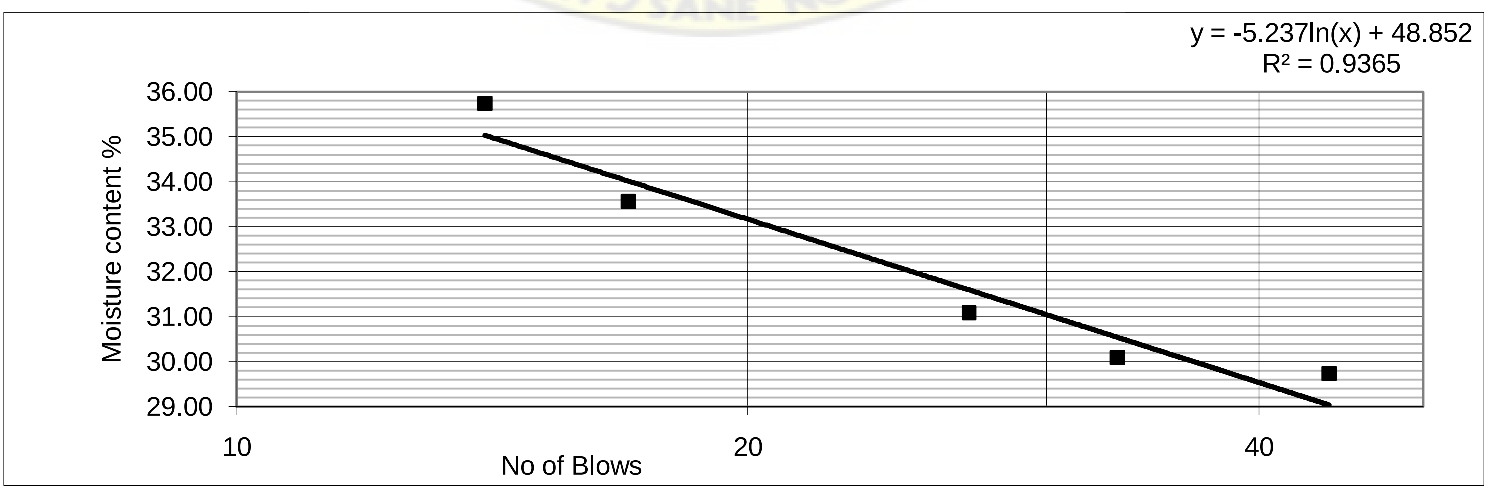

Table B2: Atterberg limit test for CH 0+600

CIVIL ENGINEERING DEPARTMENT
GEOTECHNICAL ENGINEERING LABORATORY
ATTERBERG LIMIT DETERMINATION

Name of Road:- Pantang- Abokobi

Date :-20/3/2010

Location:- CH1+500

SAMPLE No/Depth:
(0.60m - 0.80m)

Liquid Limit

CONT. NO	X15	A23	A15	K2	B6
MASS OF CONT.	3.71	3.71	3.72	3.72	3.67
NO OF BLOWS	39	33	28	19	13
MASS OFWET SAMPLE+CONT	21.12	22.56	23.14	22.47	23.15
MASS OF DRY SAMPLE+CONT	17.97	18.93	19.32	18.68	19.12
MASS OF WATER	3.15	3.63	3.82	3.79	4.03
MASS OF DRY SAMPLE	14.26	15.22	15.6	14.96	15.45
WATER CONTENT %	**22.09**	**23.85**	**24.49**	**25.33**	**26.08**

Plastic limit

CONT. NO	X20	82
MASS OF CONT.	3.64	3.64
MASS OF WET SAMPLE +CONT	16.9	16.13
MASS OF DRY SAMPLE+CONT	15.39	14.78
MASS OF WATER	1.51	1.35
MASS OF DRY SAMPLE	11.75	11.14
WATER CONTENT %	12.85	12.12
AVERAGE WATER CONTENT %	12.48	

LL	24.3
PL	12.5
PI	**11.8**

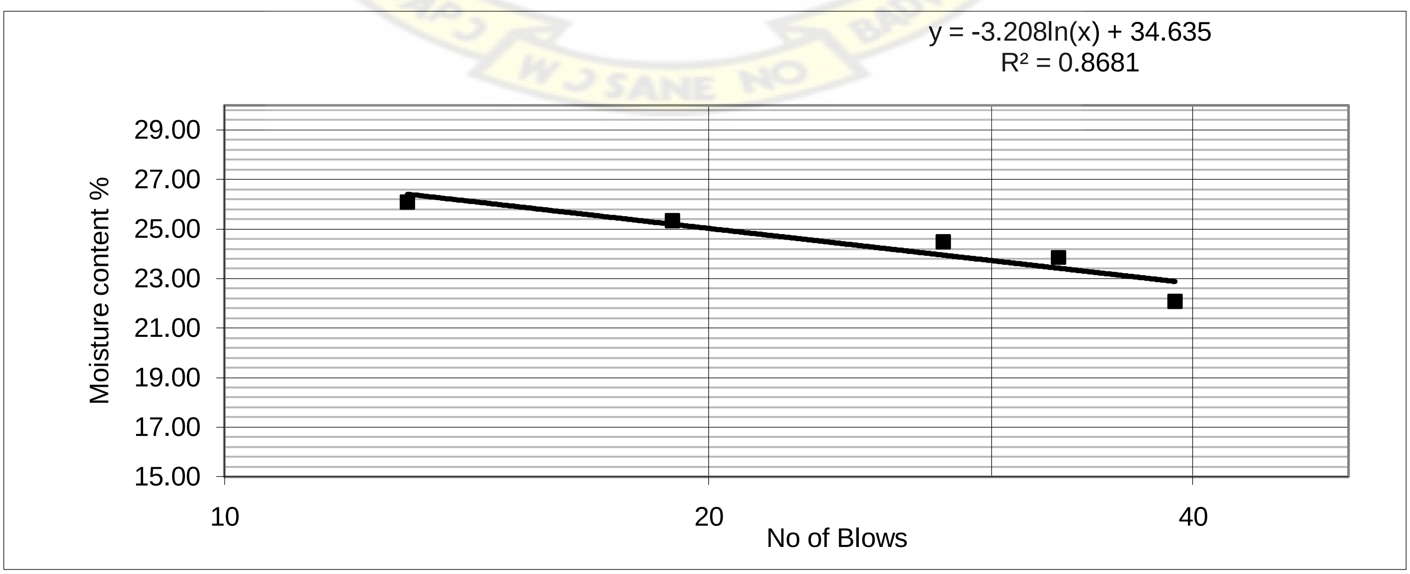

Table B3: Atterberg limit test for CH 0+600

CIVIL ENGINEERING DEPARTMENT
GEOTECHNICAL ENGINEERING LABORATORY
ATTERBERG LIMIT DETERMINATION

Name of Road:- Pantang- Abokobi

Date :- 20/3/2010

Location:- CH2+400

SAMPLE No/Depth: (0.72m - 0.82m)

Liquid Limit

CONT. NO	A7	B44	X13	A24	B11
MASS OF CONT.	3.75	3.69	3.69	3.69	3.92
NO OF BLOWS	49	37	24	17	11
MASS OFWET SAMPLE+CONT	24.28	23.64	24.45	24.31	24.06
MASS OF DRY SAMPLE+CONT	20.72	20.11	20.6	20.24	19.84
MASS OF WATER	3.56	3.53	3.85	4.07	4.22
MASS OF DRY SAMPLE	16.97	16.42	16.91	16.55	15.92
WATER CONTENT %	**20.98**	**21.50**	**22.77**	**24.59**	**26.51**

Plastic limit

CONT. NO	A29	A31
MASS OF CONT.	3.53	3.49
MASS OF WET SAMPLE +CONT	16.87	16.96
MASS OF DRY SAMPLE+CONT	15.38	15.44
MASS OF WATER	1.49	1.52
MASS OF DRY SAMPLE	11.85	11.95
WATER CONTENT %	12.57	12.72
AVERAGE WATER CONTENT %	12.65	

LL	23.1
PL	12.6
PI	**10.5**

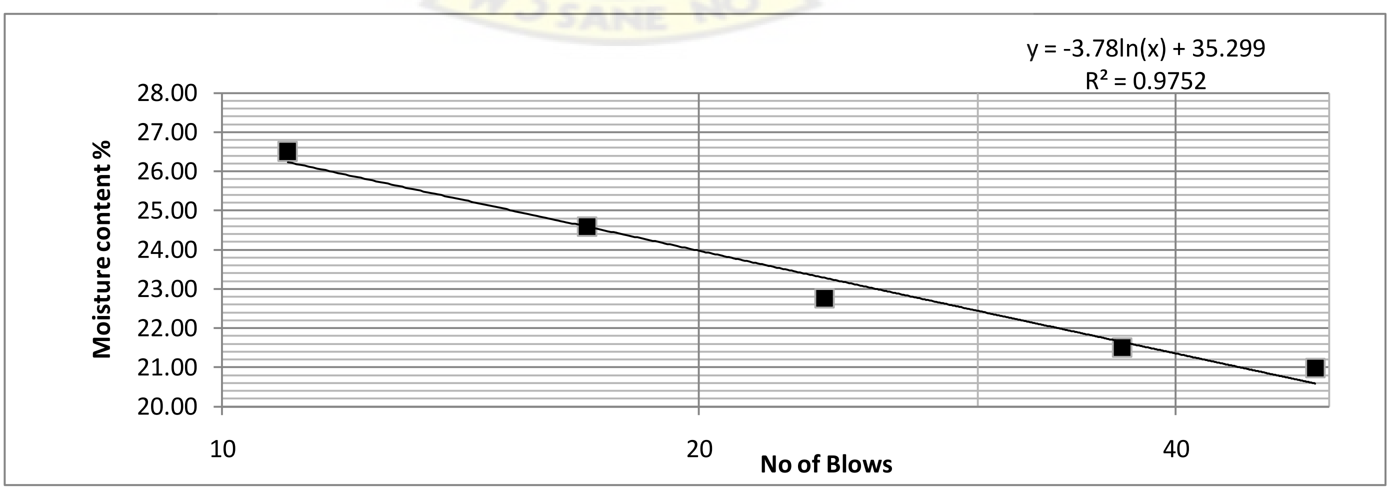

Table B4: Atterberg limit test for CH 3+600

CIVIL ENGINEERING DEPARTMENT
GEOTECHNICAL ENGINEERING LABORATORY

Name of Road:- Pantang- Abokobi

Date :-20/3/2010

Location:- CH3+600

SAMPLE No/Depth:
(0.46m-0.50m)

Liquid Limit

CONT. NO	C23	B37	A19	B40	A27
MASS OF CONT.	3.77	3.72	3.73	3.71	3.73
NO OF BLOWS	48	39	28	20	16
MASS OFWET SAMPLE+CONT	30.12	29.21	31.35	30.82	31.89
MASS OF DRY SAMPLE+CONT	23.23	22.12	22.98	22.16	22.71
MASS OF WATER	6.89	7.09	8.37	8.66	9.18
MASS OF DRY SAMPLE	19.46	18.4	19.25	18.45	18.98
WATER CONTENT %	**35.41**	**38.53**	**43.48**	**46.94**	**48.37**

Plastic limit

CONT. NO	A6	A2
MASS OF CONT.	3.57	3.6
MASS OF WET SAMPLE +CONT	25.96	24.87
MASS OF DRY SAMPLE+CONT	21.43	21.16
MASS OF WATER	4.53	3.71
MASS OF DRY SAMPLE	17.86	17.56
WATER CONTENT %	25.36	21.13
AVERAGE WATER CONTENT %	23.25	

LL	43.9
PL	23.2
PI	**20.6**

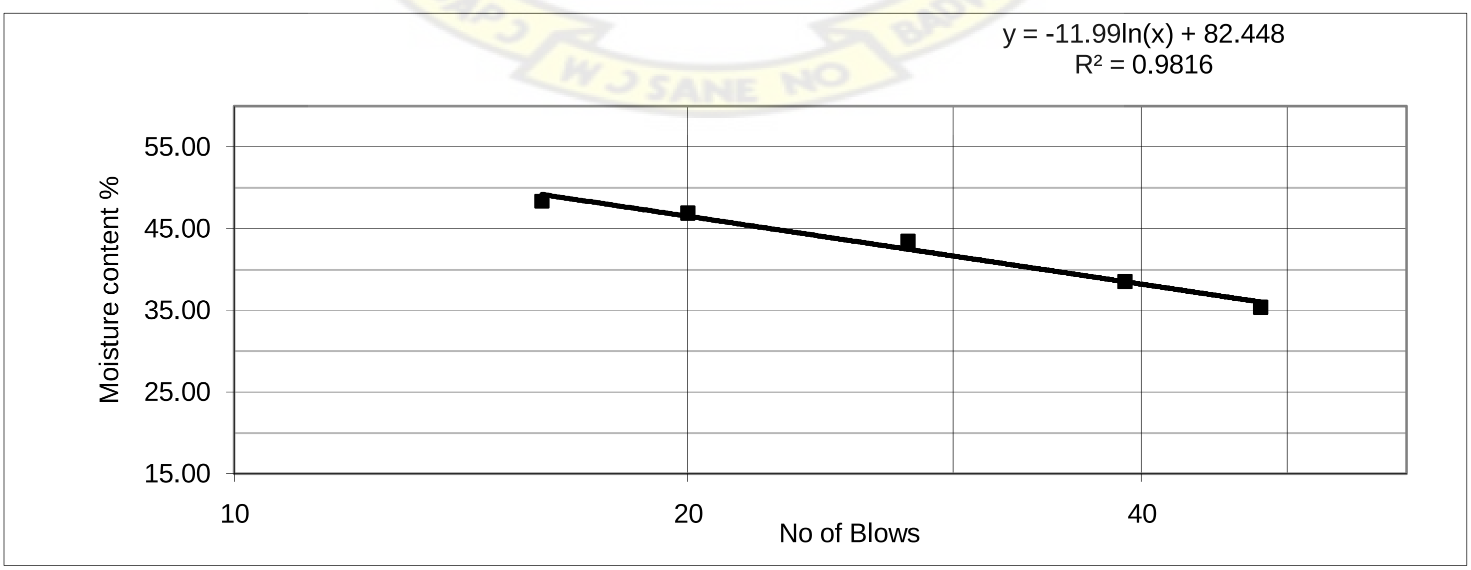

Table B5: Atterberg limit test for CH 4+500

CIVIL ENGINEERING DEPARTMENT
GEOTECHNICAL ENGINEERING LABORATORY

Name of Road:- Pantang- Abokobi

Date :-20/3/2010

Location:- CH4+500

SAMPLE No/Depth:
(0.20m-0.30m)

Liquid Limit

CONT. NO	B19	B35	B2	B14	B5X
MASS OF CONT.	3.78	3.76	3.72	3.67	3.72
NO OF BLOWS	43	34	26	18	14
MASS OFWET SAMPLE+CONT	24.11	23.82	22.02	21.1	21.99
MASS OF DRY SAMPLE+CONT	19.45	19.18	17.68	16.72	17.18
MASS OF WATER	4.66	4.64	4.34	4.38	4.81
MASS OF DRY SAMPLE	15.67	15.42	13.96	13.05	13.46
WATER CONTENT %	**29.74**	**30.09**	**31.09**	**33.56**	**35.74**

Plastic limit

CONT. NO	A18	K9
MASS OF CONT.	3.65	3.67
MASS OF WET SAMPLE +CONT	19.21	19.14
MASS OF DRY SAMPLE+CONT	16.98	16.9
MASS OF WATER	2.23	2.24
MASS OF DRY SAMPLE	13.33	13.23
WATER CONTENT %	16.73	16.93
AVERAGE WATER CONTENT %	16.83	

LL	32.0
PL	16.8
PI	**15.2**

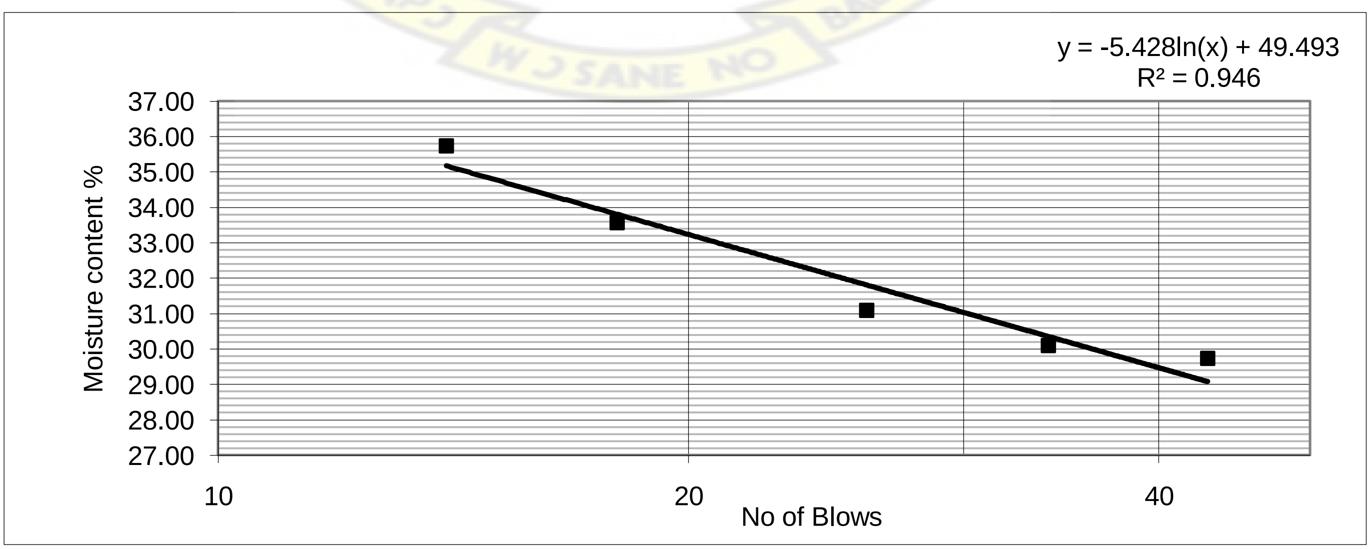

APPENDIX C

(TRIAL PIT LOGS)

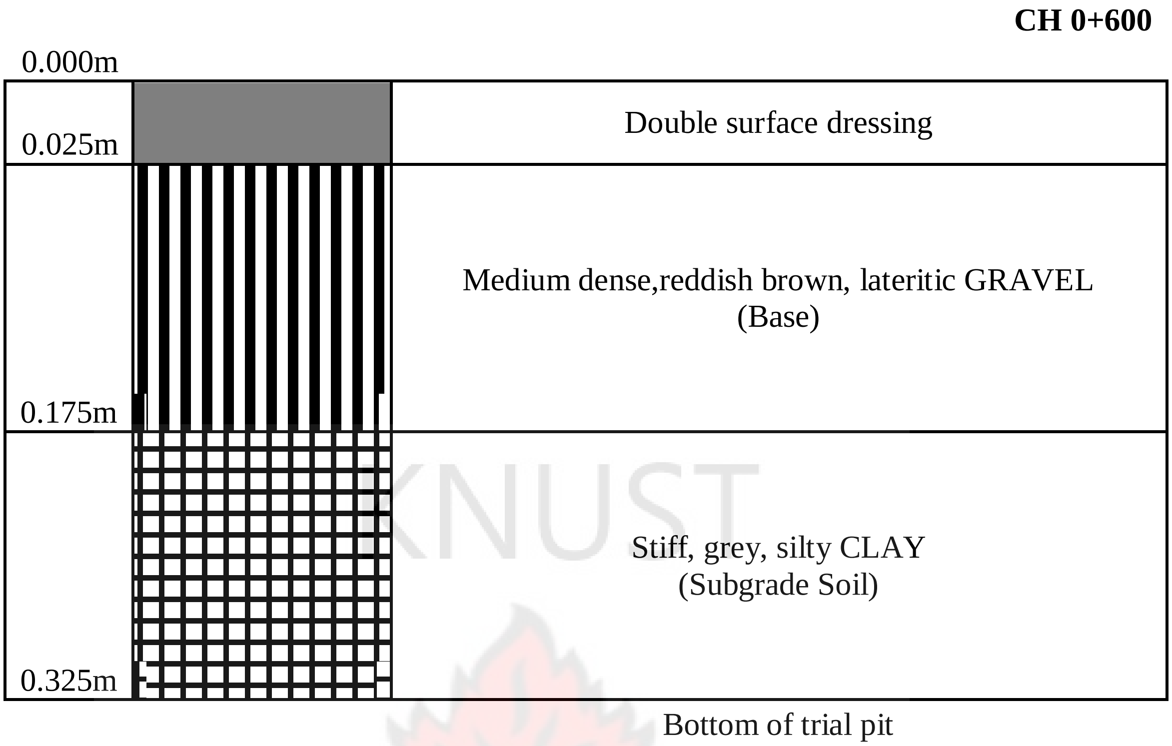

Figure C1: Trial pit log for ch 0+600

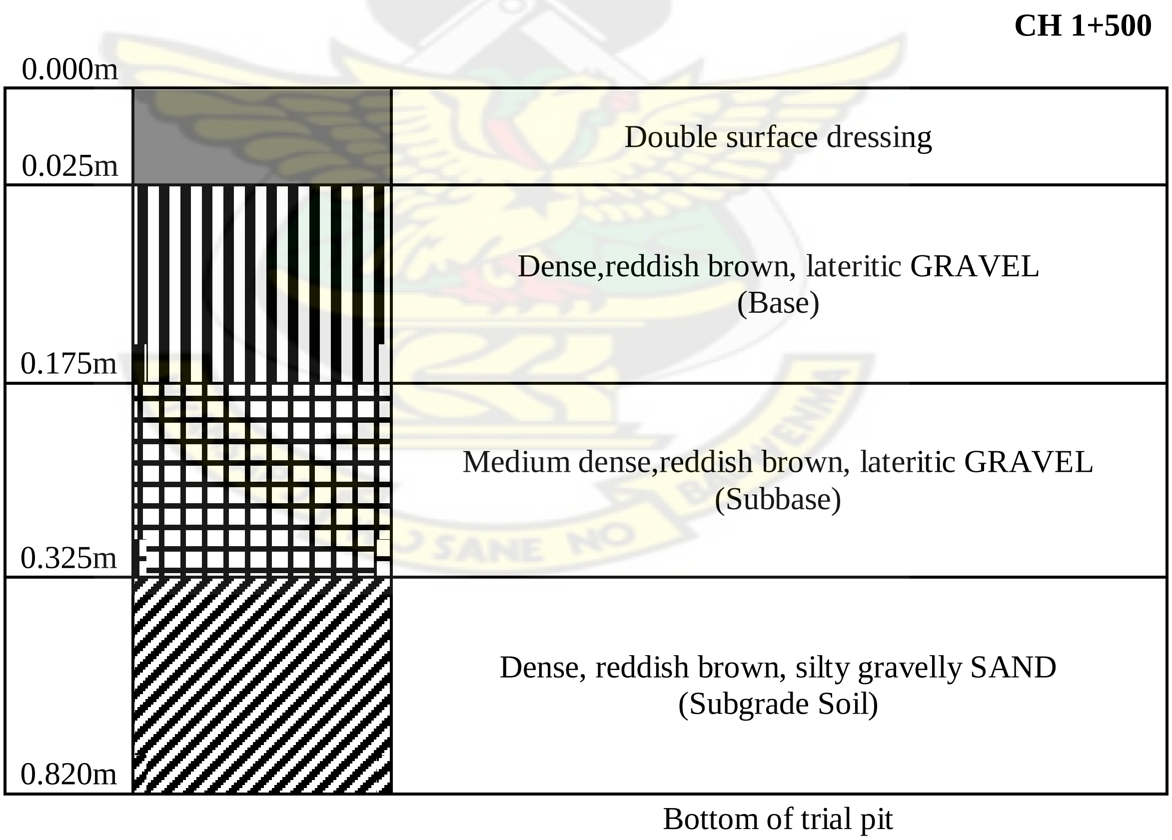

Figure C2: Trial pit log for ch 1+500

CH 2+400

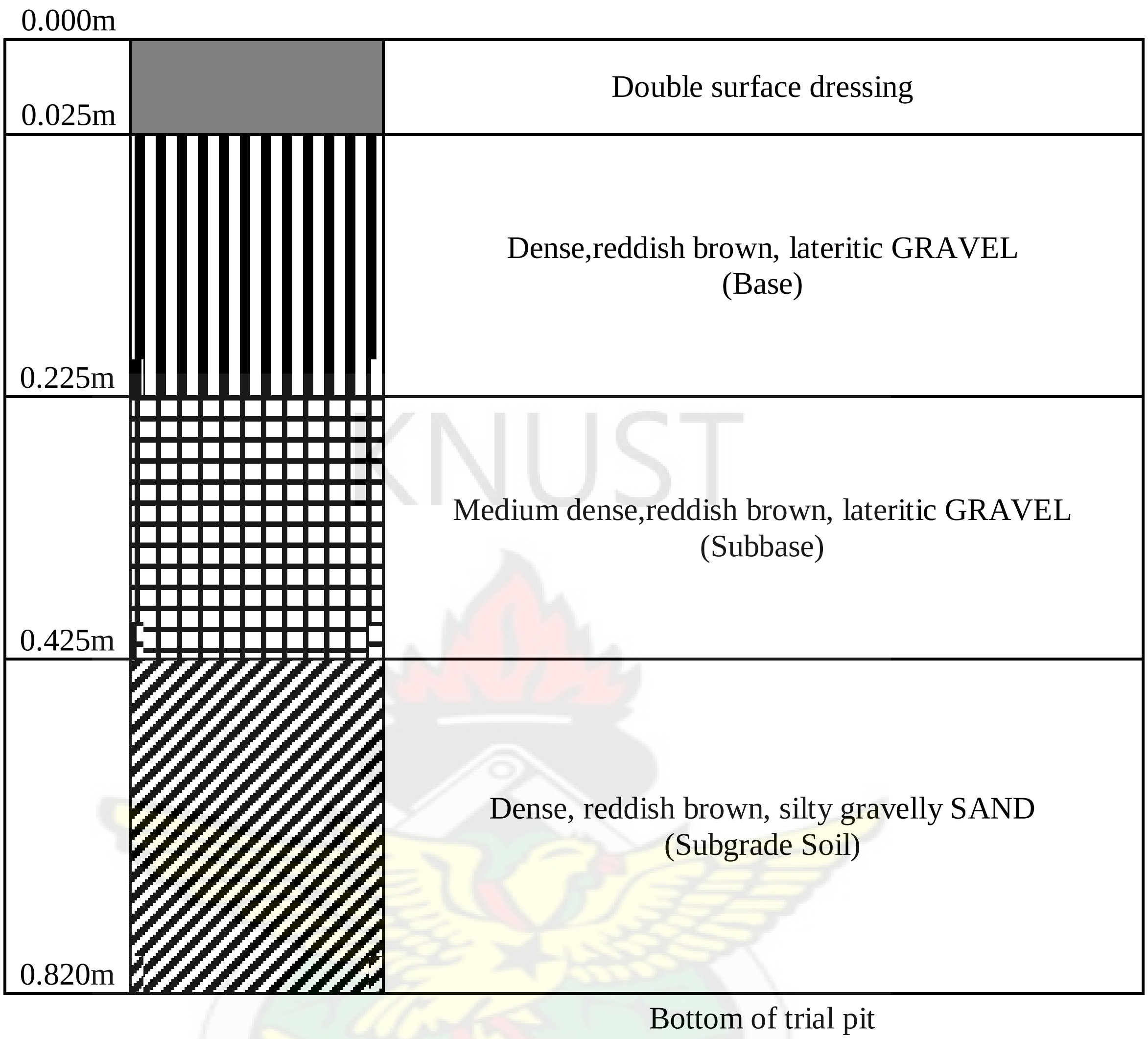

Figure C3: Trial pit log for ch 2+400

CH 3+600

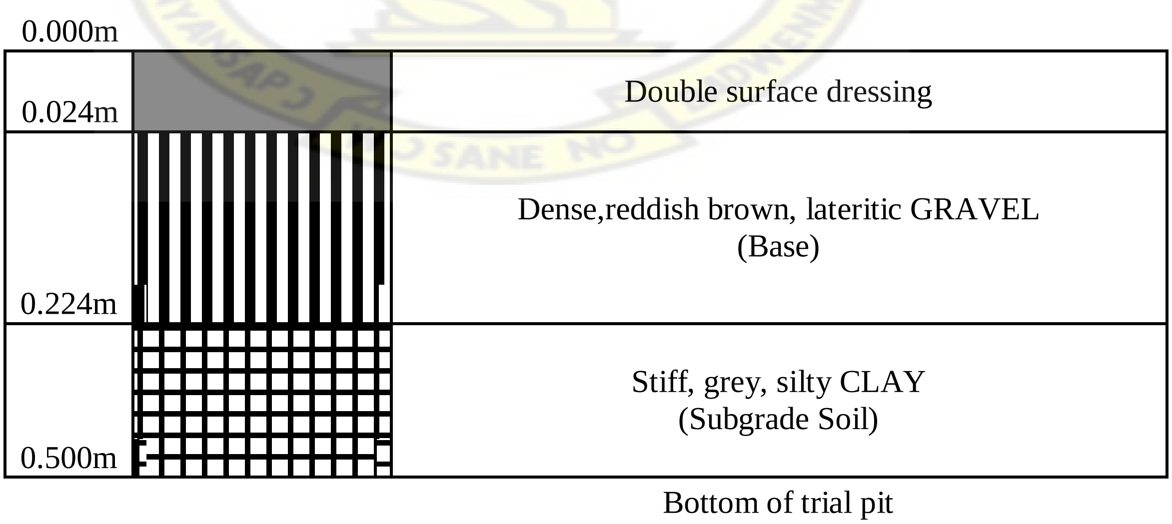

Figure C4: Trial pit log for ch 3+600

CH 4+500

Depth	Description
0.000m – 0.024m	Double surface dressing
0.024m – 0.224m	Dense,reddish brown, lateritic GRAVEL (Base)
0.224m – 0.300m	Stiff, grey, silty CLAY (Subgrade Soil)

Bottom of trial pit

Figure C5: Trial pit log for ch 4+500

APPENDIX D

(FWD SENSORS OUTPUT)

Table D1 FWD sensor output

Station ID	Drop ID	Stress (MPa)	Force kN	Deflections x 10^{-3} mm						
				D1	D2	D3	D4	D5	D6	D7
1	1	1084.00	76.62	613.10	467.40	305.90	201.60	152.10	88.80	53.70
1	2	1088.00	76.91	613.00	472.50	304.70	201.70	150.90	89.30	53.00
2	3	1090.00	77.03	914.70	620.00	424.30	264.10	173.60	80.30	30.80
2	4	1090.00	77.05	888.10	612.70	422.40	265.20	175.60	80.40	30.60
3	5	1079.00	76.23	732.90	482.50	299.60	174.60	120.30	71.80	33.10
3	6	1088.00	76.89	717.30	472.80	294.10	171.80	119.10	70.30	32.60
4	7	1093.00	77.22	559.30	299.50	204.20	138.30	110.90	81.20	52.40
4	8	1094.00	77.35	906.60	297.90	203.80	139.00	113.10	82.40	52.60
5	9	1083.00	76.57	501.90	341.20	198.60	101.00	76.10	45.00	24.40
5	10	1081.00	76.43	498.50	332.30	196.50	101.90	75.50	45.30	24.30
6	11	1069.00	75.55	1041.70	525.30	337.30	192.00	114.30	53.00	26.40
6	12	1072.00	75.74	974.50	511.30	331.70	189.20	111.40	53.00	27.00
7	13	1076.00	76.02	526.40	388.50	256.50	154.60	117.20	64.10	34.90
7	14	1075.00	75.97	513.70	384.40	256.40	156.30	111.30	63.10	36.20
8	15	1056.00	74.64	1179.40	761.90	520.10	311.50	197.70	99.30	42.50
8	16	1052.00	74.33	1154.10	740.30	505.20	310.30	200.20	101.00	38.80
9	17	1085.00	76.72	385.80	202.60	122.70	81.60	57.50	37.70	22.60
9	18	1087.00	76.80	376.60	199.70	121.70	81.60	58.30	38.40	22.90
10	19	1092.00	77.15	717.40	474.10	320.40	189.20	126.30	79.10	44.10
10	20	1028.00	72.65	694.30	466.70	312.20	188.70	129.30	82.80	44.60
11	21	1022.00	72.24	1037.10	756.90	528.20	361.80	269.90	162.50	73.80
11	22	1025.00	72.42	1002.40	740.90	518.50	352.80	274.70	165.70	75.30
12	23	1061.00	75.00	737.10	492.20	325.40	216.70	160.90	107.20	70.40
12	24	1066.00	75.34	730.50	485.40	327.50	215.60	161.60	108.10	67.50
13	25	1052.00	74.36	796.20	404.80	262.60	151.80	108.30	69.80	48.60
13	26	1054.00	74.47	651.40	394.40	266.40	152.30	109.30	69.80	49.20
14	27	1001.00	70.78	1314.70	898.40	596.20	374.60	258.10	156.70	76.10
14	28	997.00	70.46	1278.60	875.70	587.20	373.60	259.10	158.60	77.90
15	29	1061.00	75.00	890.50	624.80	447.20	314.50	229.70	151.20	82.80
15	30	664.00	46.92	603.20	414.50	286.30	192.70	132.80	85.10	40.40
16	31	650.00	45.97	715.60	446.80	270.20	155.90	128.90	70.20	32.80
16	32	656.00	46.33	706.70	443.90	270.60	156.30	131.70	71.40	35.80
17	33	1074.00	75.90	654.40	363.90	230.90	158.20	126.90	79.50	39.10
17	34	1075.00	75.99	629.40	355.60	230.40	155.40	124.20	80.50	39.00
18	35	1022.00	72.21	1460.00	852.00	538.00	342.30	230.10	130.60	61.50

Table D2 FWD sensor output

Station ID	Drop ID	Stress (MPa)	Force kN	Deflections x 10^{-3} mm						
				D1	D2	D3	D4	D5	D6	D7
18	36	1020.00	72.06	1641.40	833.40	533.50	331.20	225.80	129.00	60.70
19	37	1085.00	76.68	708.90	405.40	294.60	218.00	172.70	100.50	50.40
19	38	1084.00	76.61	692.80	402.70	294.70	219.60	172.80	100.50	47.10
20	39	1085.00	76.69	577.60	388.20	267.80	174.80	148.60	86.50	48.60
20	40	1077.00	76.11	568.50	378.70	263.00	174.30	148.80	85.10	46.60
21	41	1094.00	77.33	450.20	277.00	163.00	103.40	89.90	68.80	40.60
21	42	1085.00	76.72	447.00	273.30	161.90	101.90	88.70	68.50	42.30
22	43	1053.00	74.43	1407.70	670.00	295.70	183.30	133.90	68.40	36.20
22	44	1054.00	74.52	723.10	544.00	278.50	181.80	136.00	70.10	36.60
23	45	1128.00	79.72	539.30	375.30	244.20	144.40	96.20	65.60	36.00
23	46	1128.00	79.70	534.00	375.10	242.40	144.40	96.80	65.70	38.00
24	47	1082.00	76.47	727.60	479.20	300.30	174.20	121.60	74.80	38.40
24	48	1085.00	76.72	716.70	477.20	299.30	174.80	121.50	75.10	38.70
25	49	1060.00	74.89	702.60	484.90	350.20	246.50	188.50	123.30	59.10
25	50	1050.00	74.22	704.00	489.80	352.40	247.30	188.90	124.30	60.40
26	51	1083.00	76.54	819.40	550.90	386.90	262.80	179.70	103.80	48.20
26	52	1081.00	76.41	811.30	549.80	388.20	266.70	183.30	105.70	49.00
27	53	1080.00	76.31	779.70	513.80	334.80	237.00	192.80	113.50	59.00
27	54	1080.00	76.33	768.70	512.40	332.40	243.70	194.30	112.30	57.20
28	55	1029.00	72.74	1409.60	990.30	623.40	351.10	217.20	104.00	48.20
28	56	1028.00	72.66	1455.70	975.00	619.90	349.30	216.10	103.70	48.20
29	57	1086.00	76.76	604.60	379.00	230.00	149.90	108.40	54.20	25.60
29	58	1085.00	76.69	600.60	373.20	230.70	156.00	109.10	57.00	25.30
30	59	1028.00	72.66	836.80	551.90	395.90	281.80	221.90	142.30	72.40
30	60	1035.00	73.16	805.80	537.90	390.20	279.90	222.10	144.90	69.30
31	61	1032.00	72.93	939.00	645.70	507.70	346.90	253.10	146.20	74.00
31	62	1030.00	72.79	937.60	641.60	506.60	346.70	252.90	147.70	74.20
32	63	1028.00	72.66	1041.70	772.50	469.10	284.40	198.00	128.30	81.20
32	64	1027.00	72.59	1014.00	756.90	465.40	283.60	200.60	133.10	81.70
33	65	1074.00	75.88	933.40	700.30	525.80	363.10	265.90	160.40	85.60
33	66	1073.00	75.87	920.80	697.40	522.50	364.80	270.00	161.80	86.60
34	67	1085.00	76.68	987.30	613.40	447.80	318.00	234.80	140.70	57.40
34	68	1089.00	76.94	961.30	599.90	444.00	316.70	234.90	141.40	57.00
35	69	1073.00	75.81	827.40	540.30	323.40	190.30	127.60	78.70	44.60
35	70	1076.00	76.08	777.50	519.80	315.00	190.90	128.00	78.40	45.80

Table D3 FWD sensor output

Station ID	Drop ID	Stress (MPa)	Force kN	Deflections x 10^{-3} mm						
				D1	D2	D3	D4	D5	D6	D7
36	71	1060.00	74.95	1145.20	750.00	500.40	320.40	228.90	148.00	79.80
36	72	1058.00	74.81	1105.50	730.90	493.20	317.20	229.40	147.90	79.70
37	73	1021.00	72.17	1547.80	918.50	624.80	423.20	315.30	193.50	101.70
37	74	1021.00	72.13	1365.80	902.90	624.50	429.60	321.10	197.10	104.40
38	75	1014.00	71.70	1184.00	793.60	555.70	317.90	226.60	148.30	86.50
38	76	1016.00	71.80	1180.40	775.00	526.40	317.30	231.20	149.40	85.20
39	77	1052.00	74.35	981.70	658.50	466.40	338.00	276.90	204.30	129.20
39	78	1057.00	74.70	960.80	647.20	458.30	335.50	272.50	204.40	131.50
40	79	1068.00	75.46	700.10	480.20	322.30	221.70	162.50	96.40	46.70
40	80	1068.00	75.48	691.40	466.00	319.90	222.30	163.50	96.80	46.50
41	81	1053.00	74.40	1045.80	621.80	407.40	261.50	189.70	118.10	63.30
41	82	645.00	45.56	726.20	400.00	253.90	153.00	109.10	64.10	33.40
42	83	629.00	44.48	907.50	580.60	372.30	169.40	94.70	65.00	35.90
42	84	633.00	44.73	902.90	587.10	377.70	171.60	96.80	65.00	35.80
43	85	1044.00	73.80	717.50	564.80	363.20	237.90	184.50	123.30	53.90
43	86	1046.00	73.94	712.30	553.70	362.00	238.10	186.00	124.10	54.80
44	87	1062.00	75.09	638.30	377.00	246.20	160.60	118.30	64.80	27.00
44	88	1066.00	75.37	628.10	372.00	246.10	160.40	117.80	64.10	26.60
45	89	1058.00	74.77	1147.90	611.50	374.70	275.30	208.00	122.10	65.20
45	90	1063.00	75.10	915.70	604.40	366.40	270.90	206.70	121.70	64.80
46	91	1064.00	75.20	1046.30	554.30	381.20	295.10	238.40	131.40	58.70
46	92	1062.00	75.07	899.80	548.70	380.50	297.30	240.10	131.40	60.10
47	93	1088.00	76.87	530.90	313.90	215.10	139.50	104.10	65.90	38.50
47	94	1090.00	77.05	530.20	310.50	212.40	137.50	104.20	64.80	39.40
48	95	1085.00	76.72	973.80	710.40	486.70	295.80	201.60	105.00	38.40
48	96	1088.00	76.91	959.00	703.50	485.70	296.70	205.70	110.10	38.40
49	97	1058.00	74.77	808.80	422.00	266.90	188.20	148.60	96.60	54.60
49	98	1061.00	74.98	793.50	426.60	265.60	187.90	145.70	96.60	53.00
50	99	1107.00	78.21	783.10	474.10	307.70	194.50	147.30	78.50	44.70
50	100	1111.00	78.53	776.00	468.10	304.80	194.10	147.20	79.40	45.20
51	101	655.00	46.30	452.00	241.10	156.50	89.70	65.50	30.50	7.40
51	102	657.00	46.44	443.10	237.40	152.60	85.60	63.20	29.60	8.90
52	103	1097.00	77.53	610.00	335.20	189.10	150.70	123.20	58.10	18.60
52	104	1099.00	77.67	597.90	327.30	187.70	149.30	124.20	59.00	19.20
53	105	1063.00	75.12	628.60	352.80	224.20	120.70	98.90	69.80	21.30

APPENDIX E

(PLOTS AND NUMERICAL VALUES OF DCP TESTS)

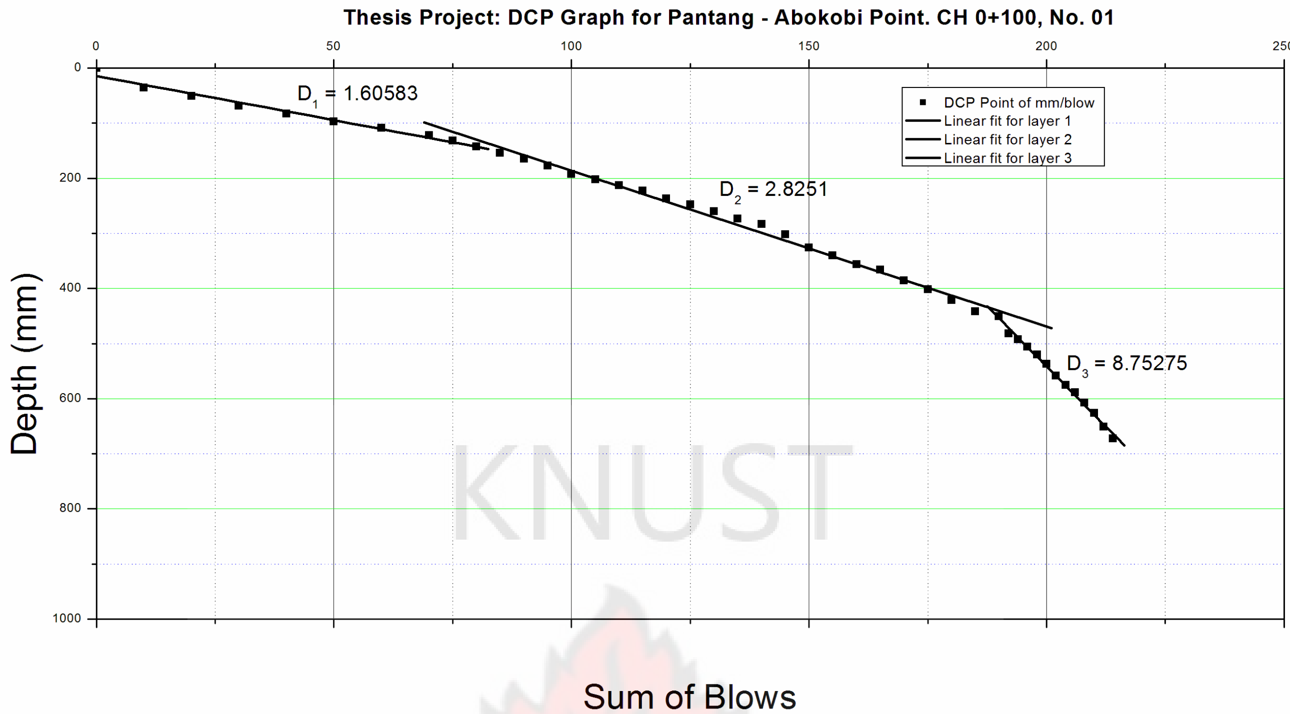

Figure E1: DCP Graph for Chainage 0+100

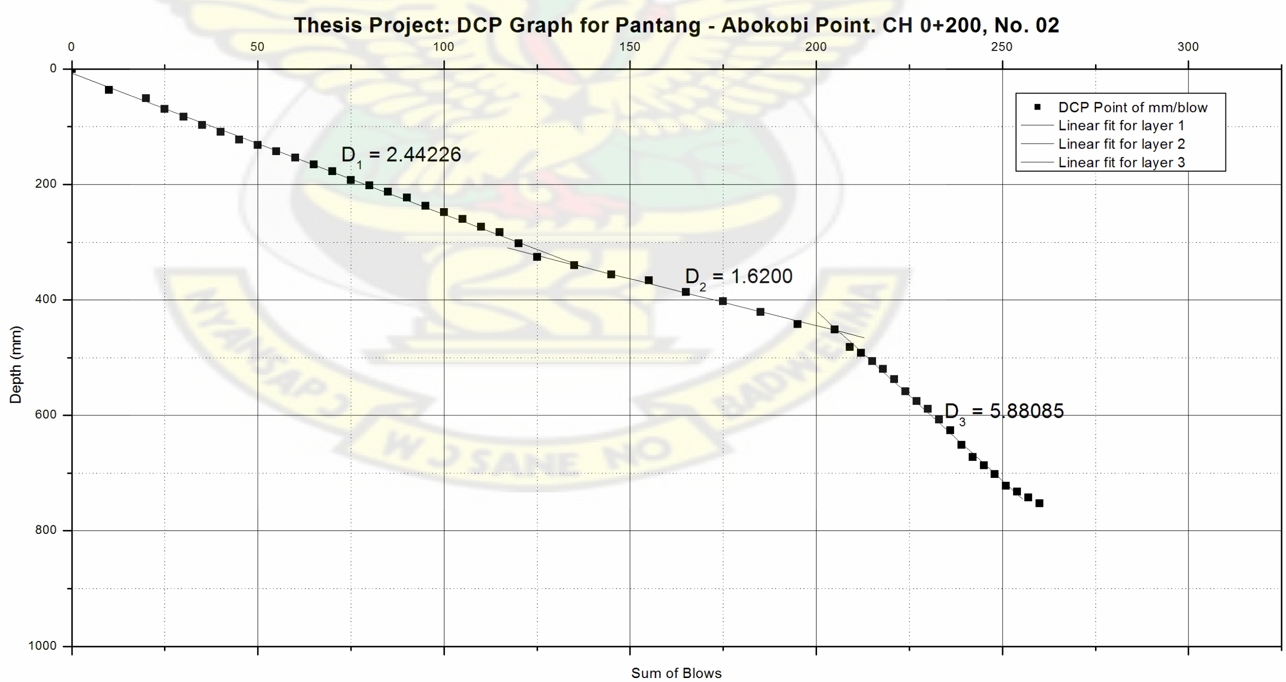

Figure E2: DCP Graph for Chainage 0+200

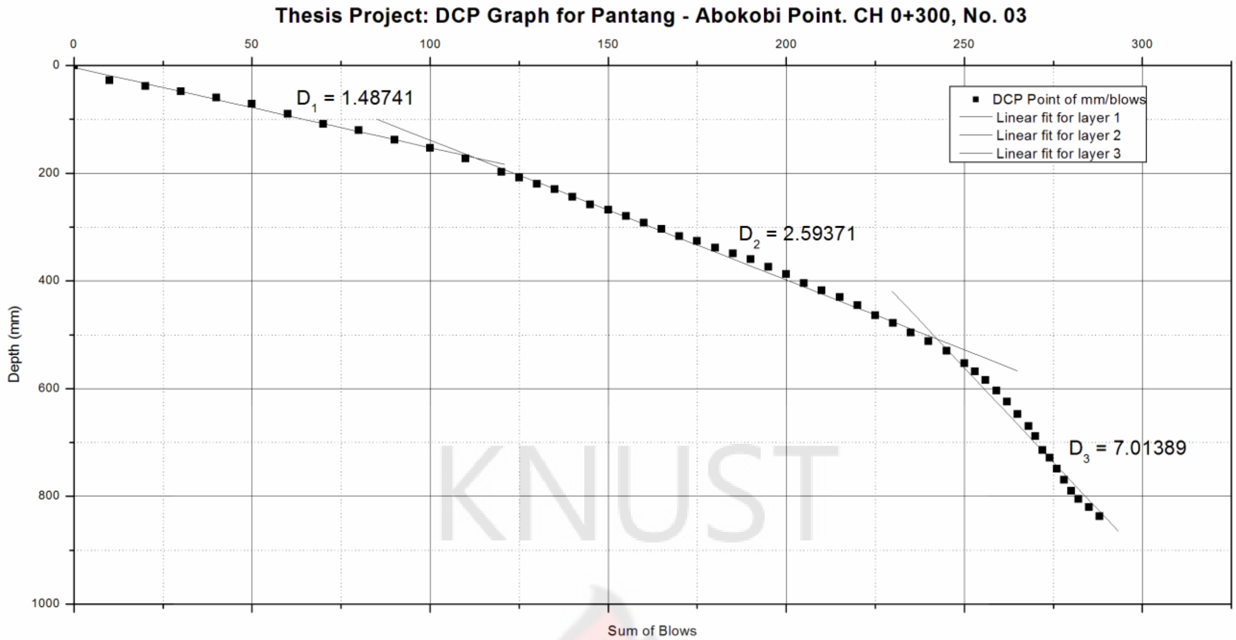

Figure E3: DCP Graph for Chainage 0+300

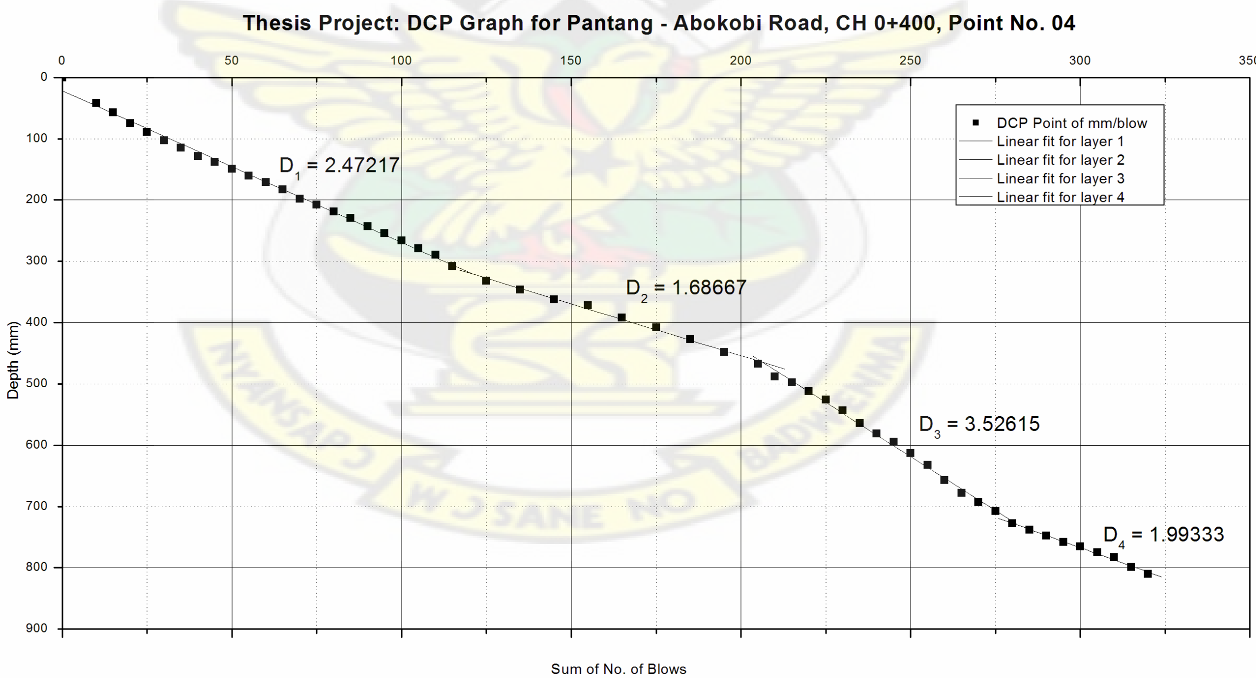

Figure E4: DCP Graph for Chainage 0+400

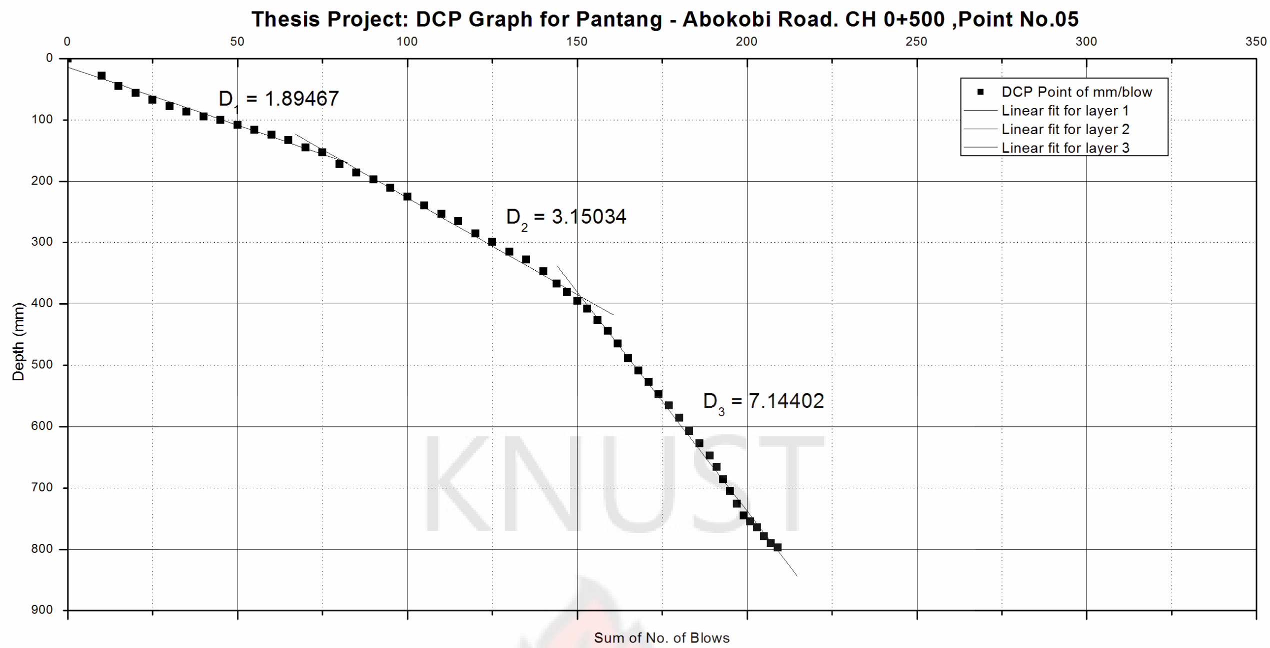

Figure E5: DCP Graph for Chainage 0+500

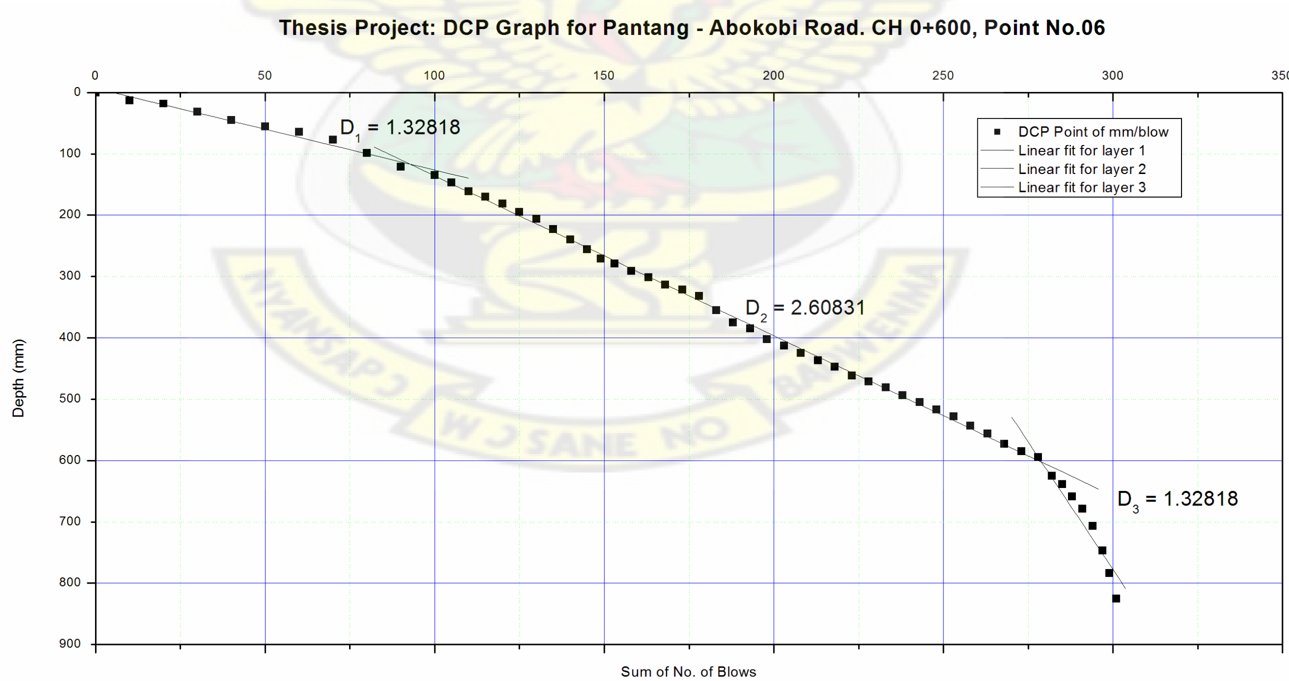

Figure E6 : DCP Graph for Chainage 0+600

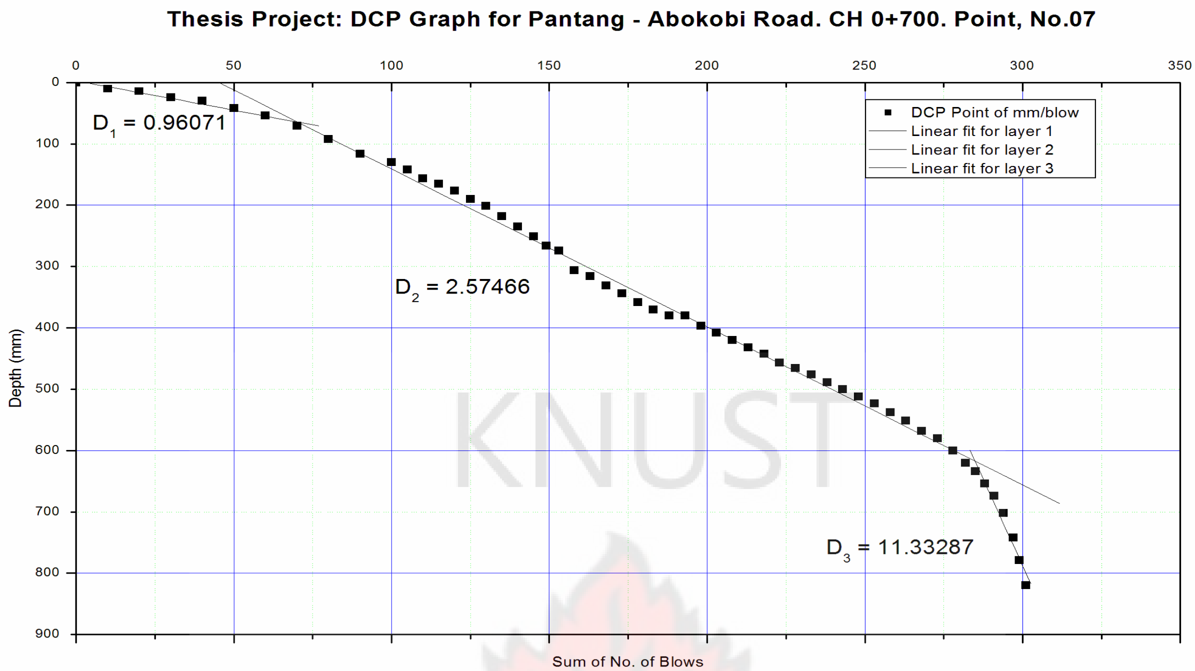

Figure E7 : DCP Graph for Chainage 0+700

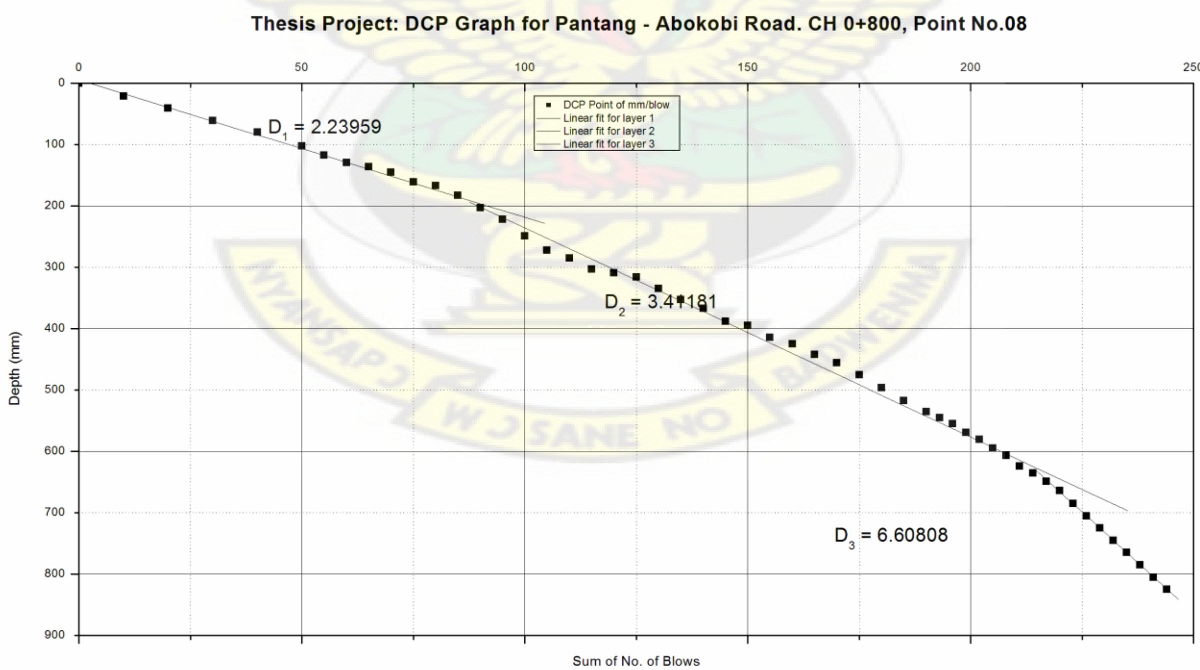

Figure E8: DCP Graph for Chainage 0+800

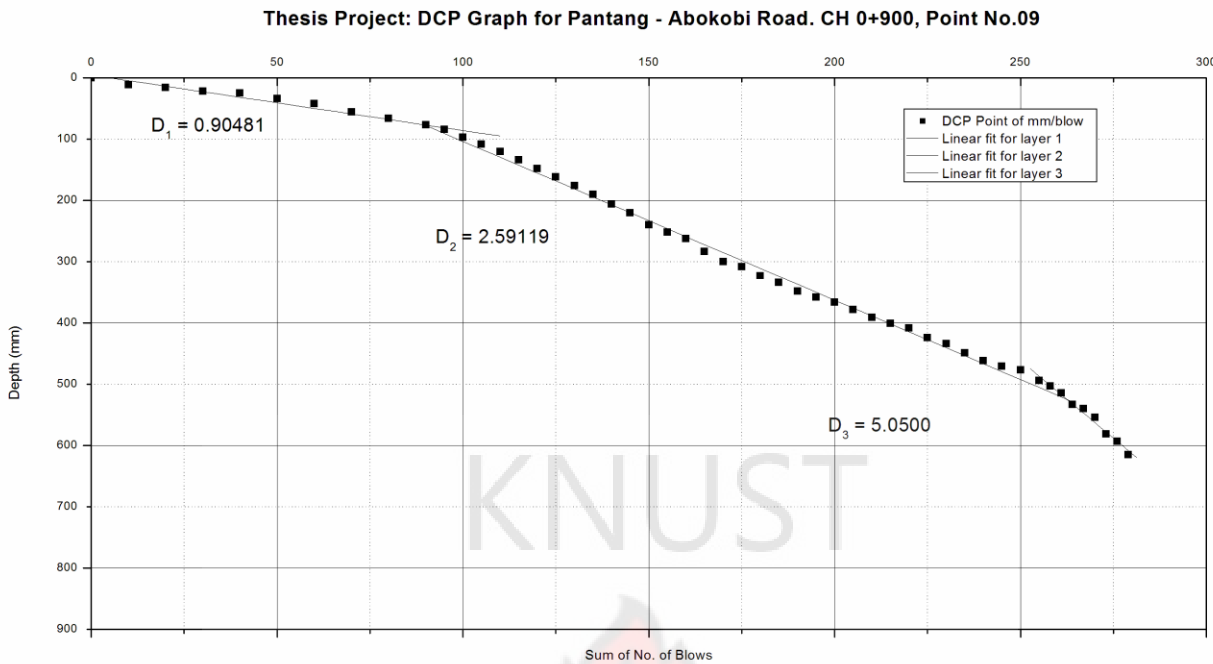

Figure E9: DCP Graph for Chainage 0+900

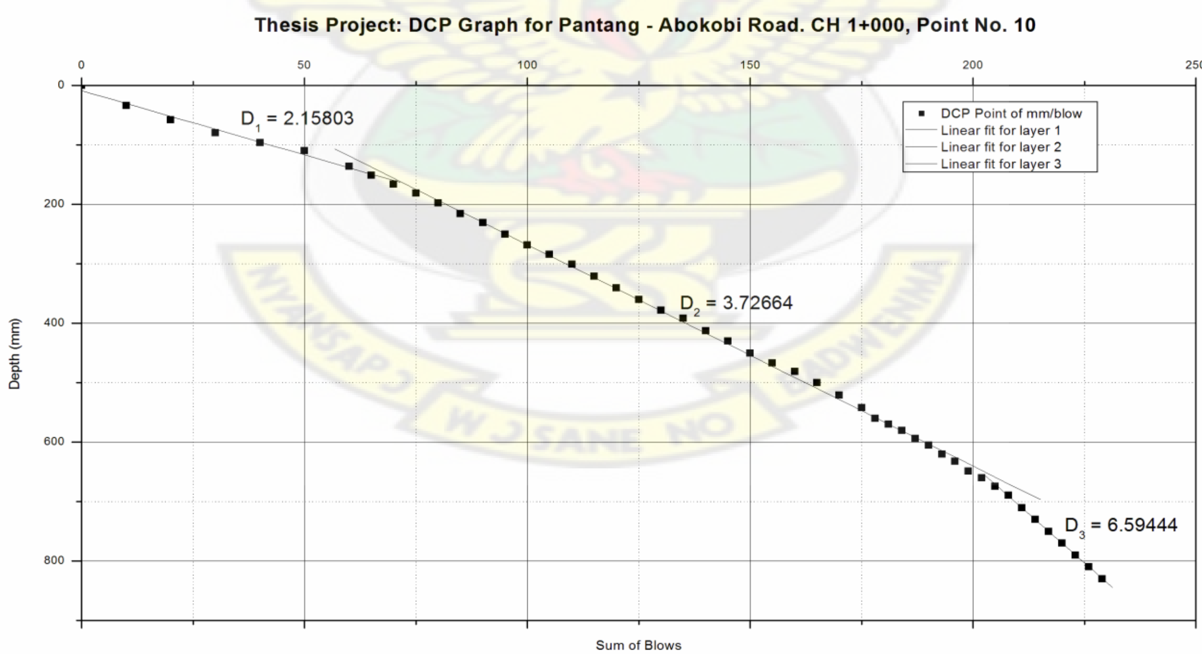

Figure E10: DCP Graph for Chainage 1+000

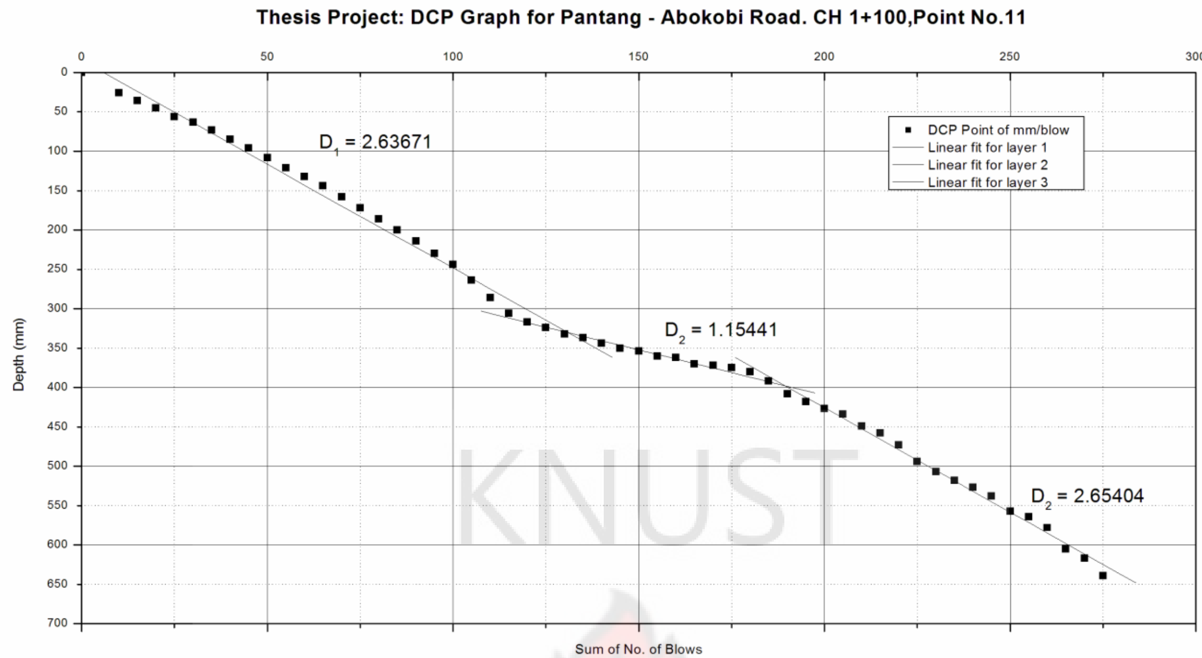

Figure E11: DCP Graph for Chainage 1+100

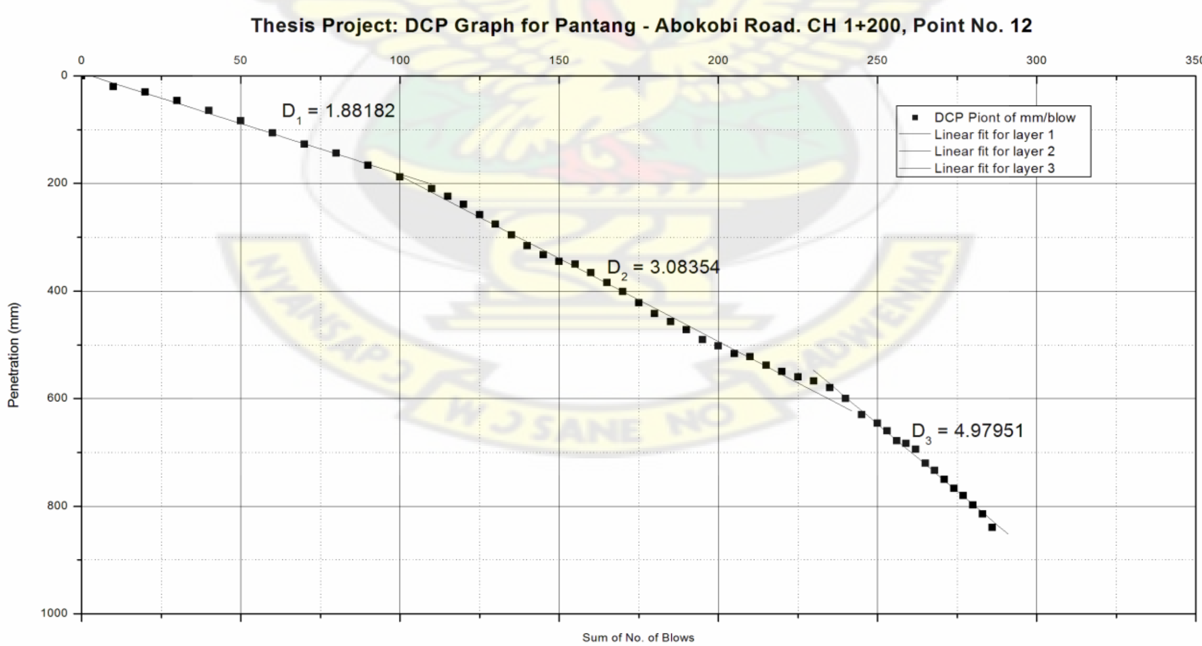

Figure E12: DCP Graph for Chainage 1+200

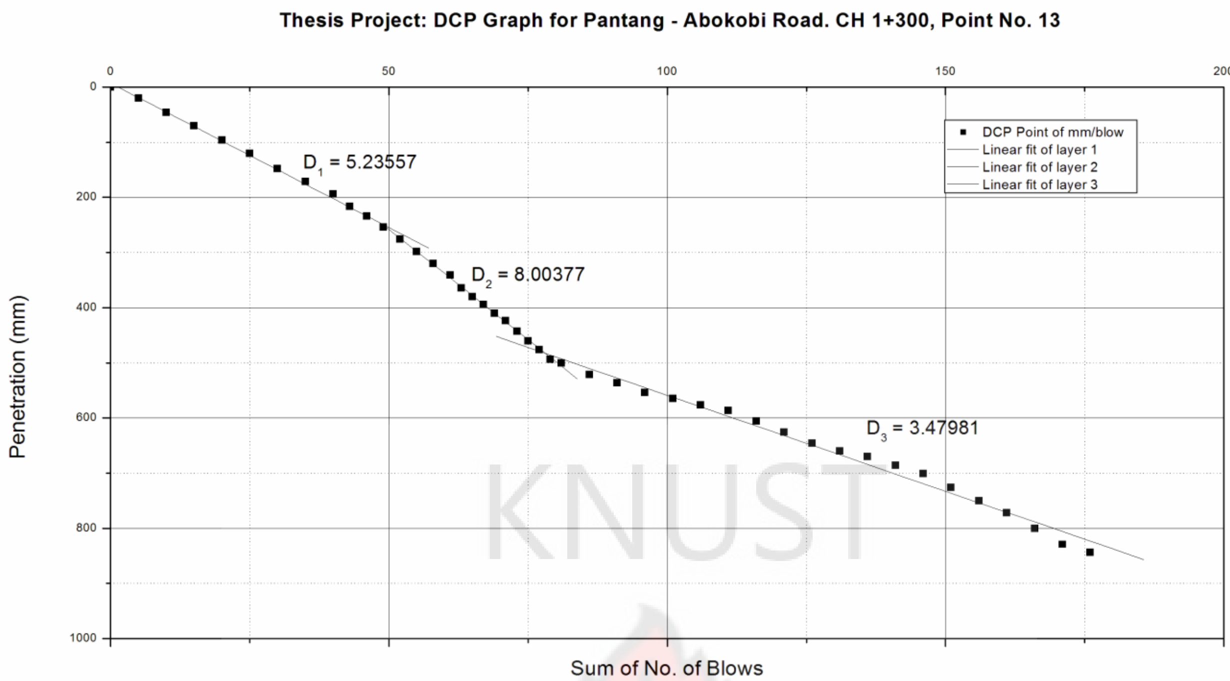

Figure E13: DCP Graph for Chainage 1+300

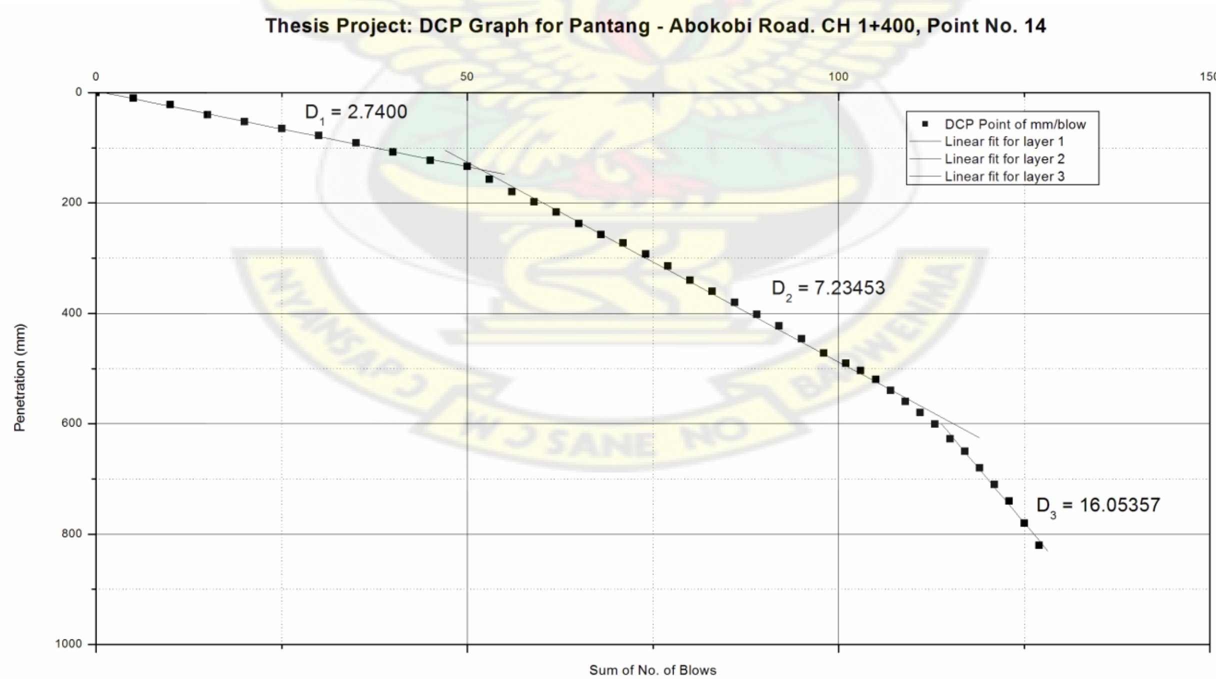

Figure E14: DCP Graph for Chainage 1+400

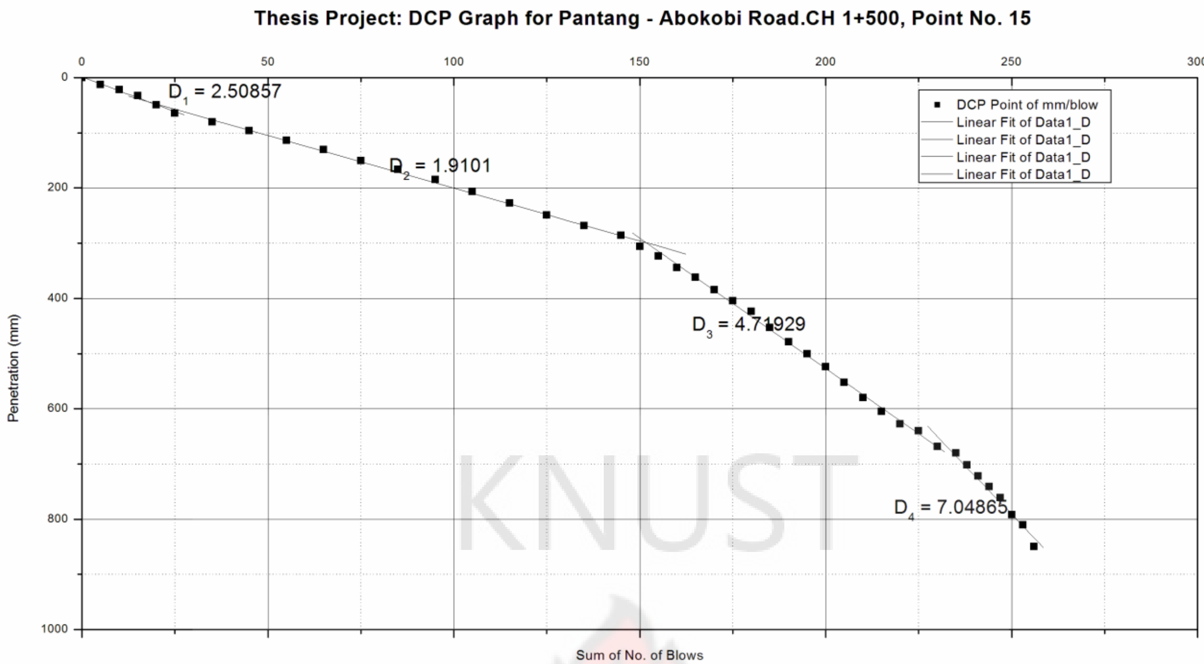

Figure E15: DCP Graph for Chainage 1+500

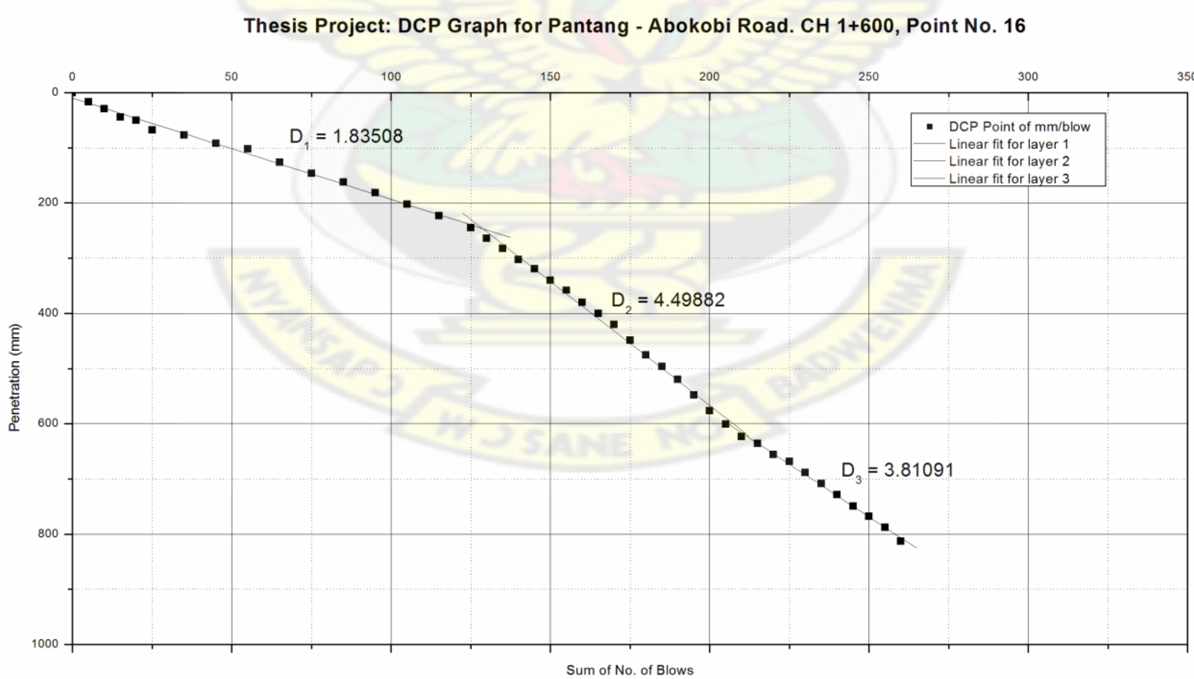

Figure E16: DCP Graph for Chainage 1+600

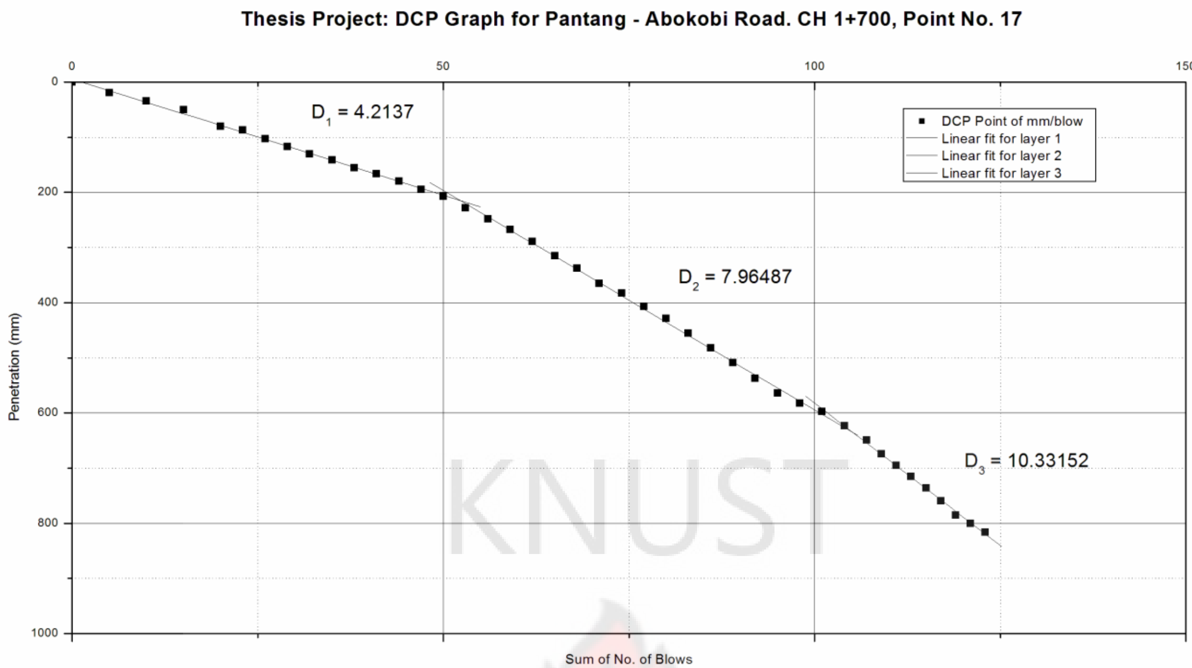

Figure E17: DCP Graph for Chainage 1+700

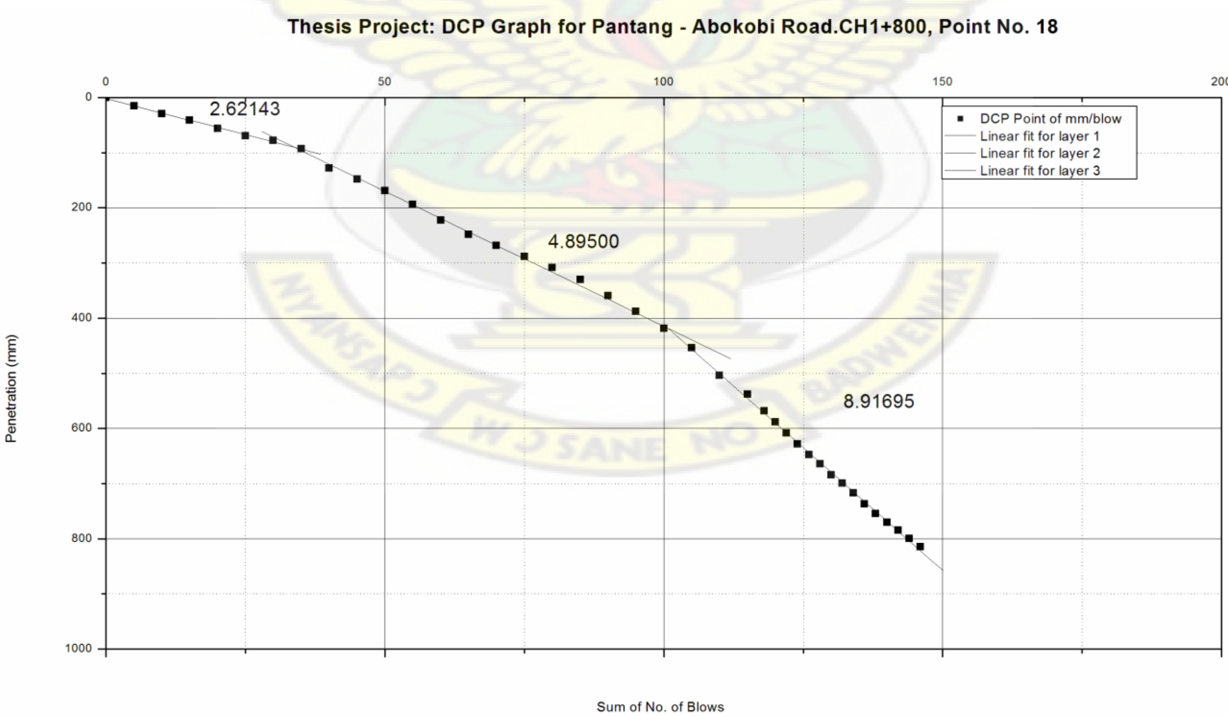

Figure 18: DCP Graph for Chainage 1+800

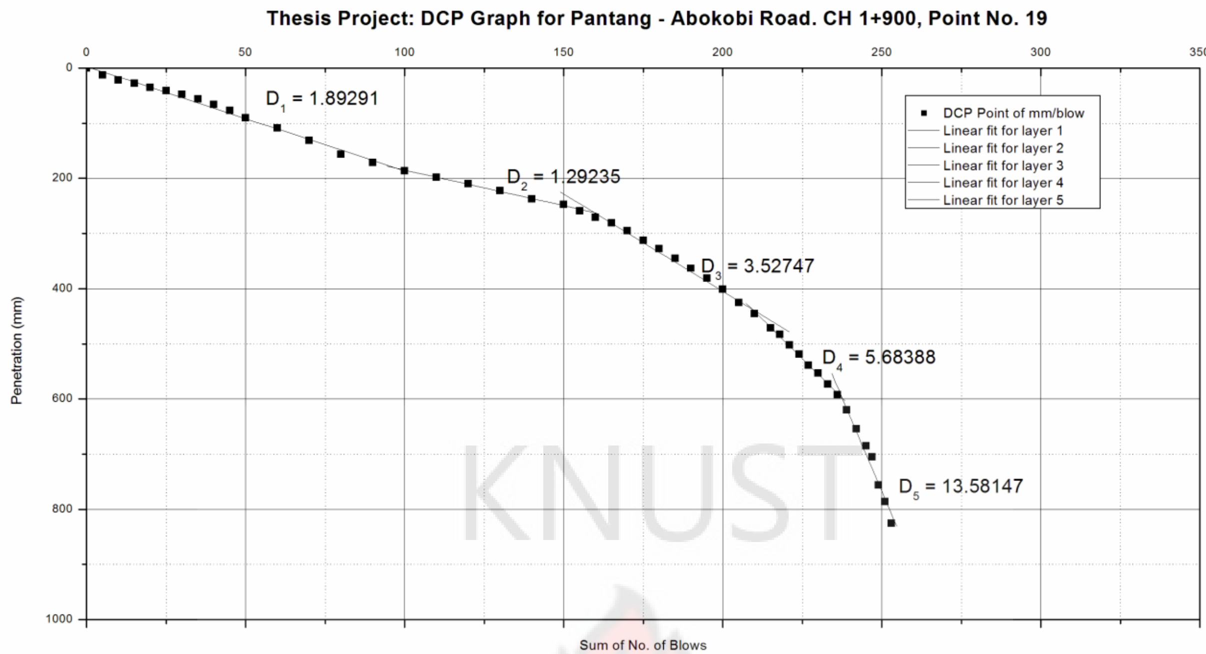

Figure E19: DCP Graph for Chainage 1+900

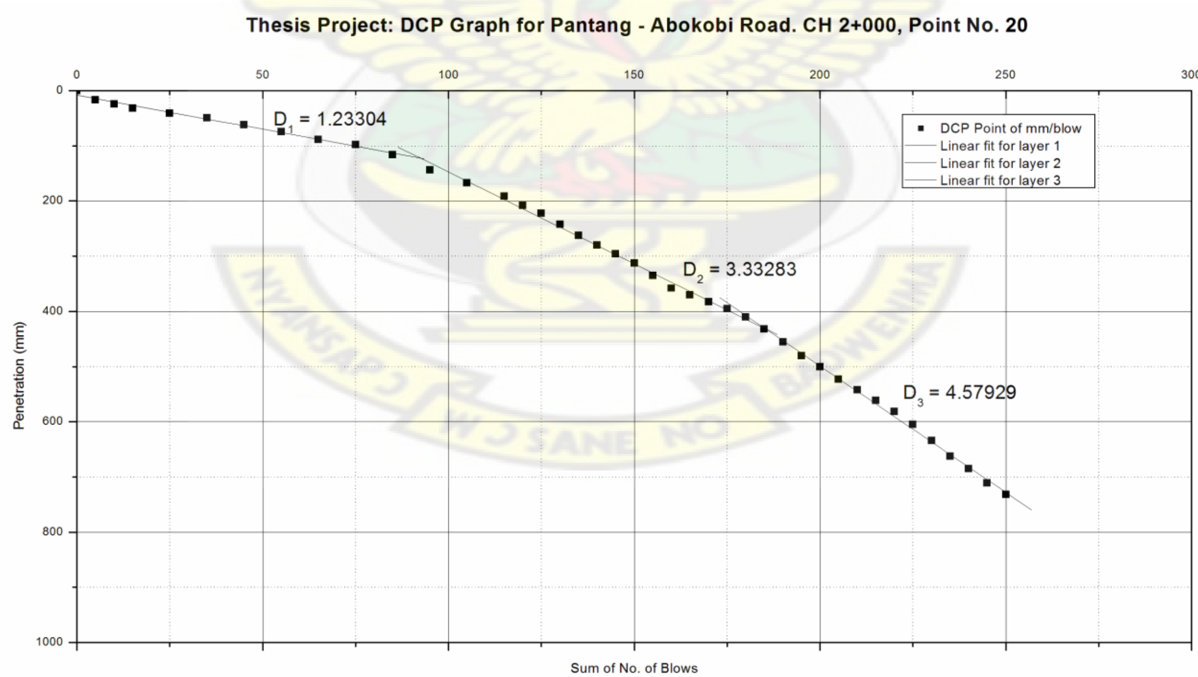

Figure E20: DCP Graph for Chainage 2+000

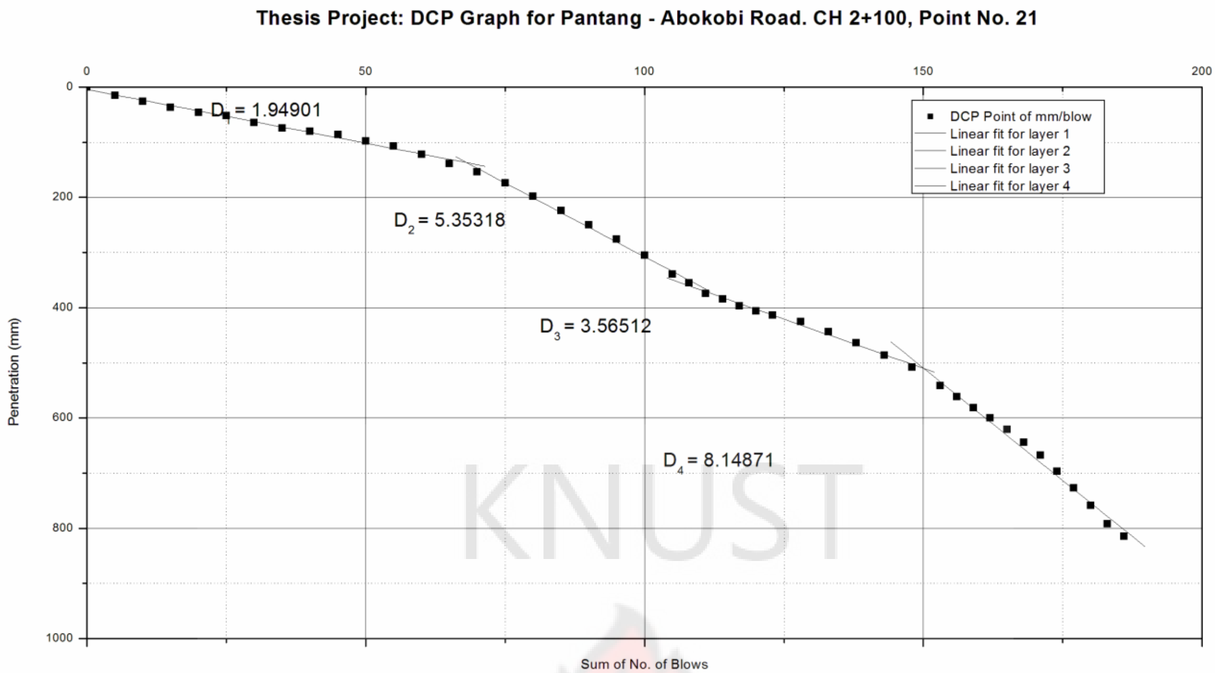

Figure E21: DCP Graph for Chainage 2+100

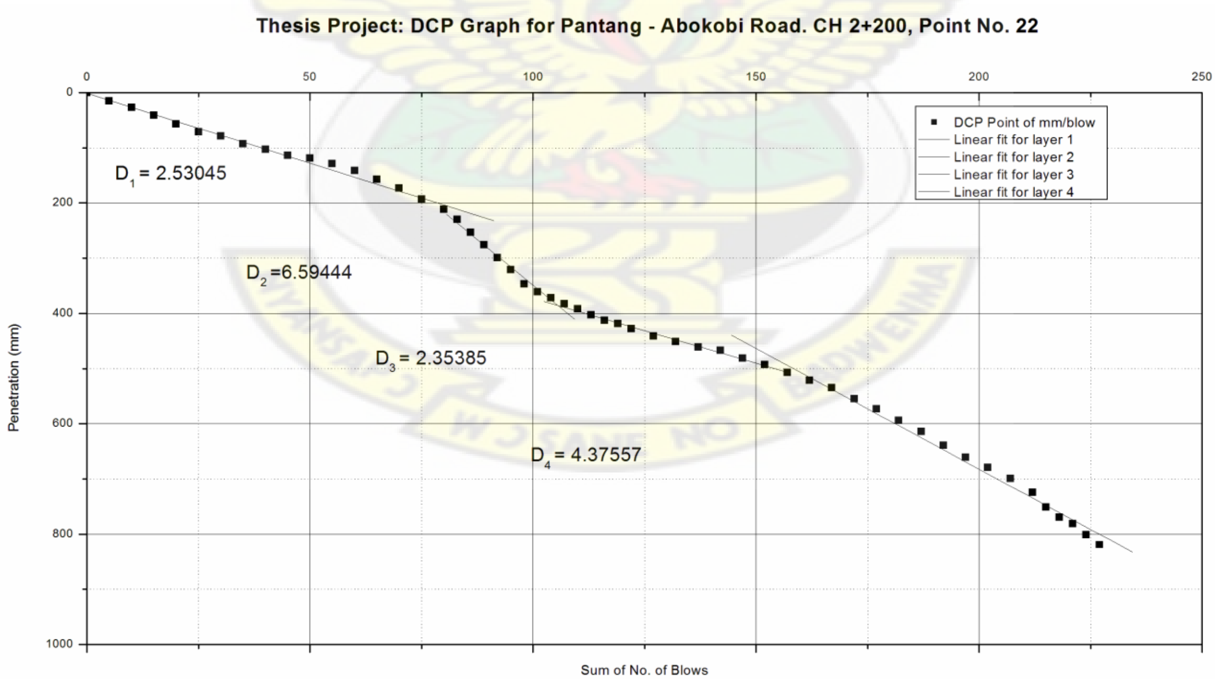

Figure E22: DCP Graph for Chainage 2+200

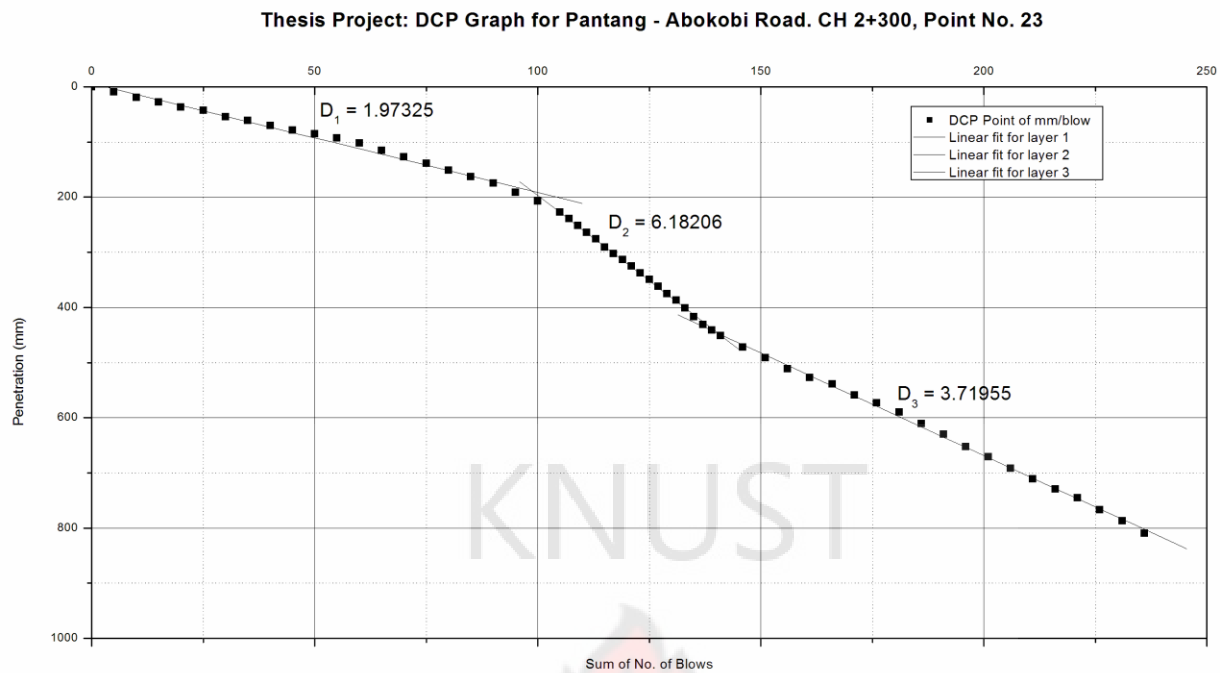

Figure E23: DCP Graph for Chainage 2+300

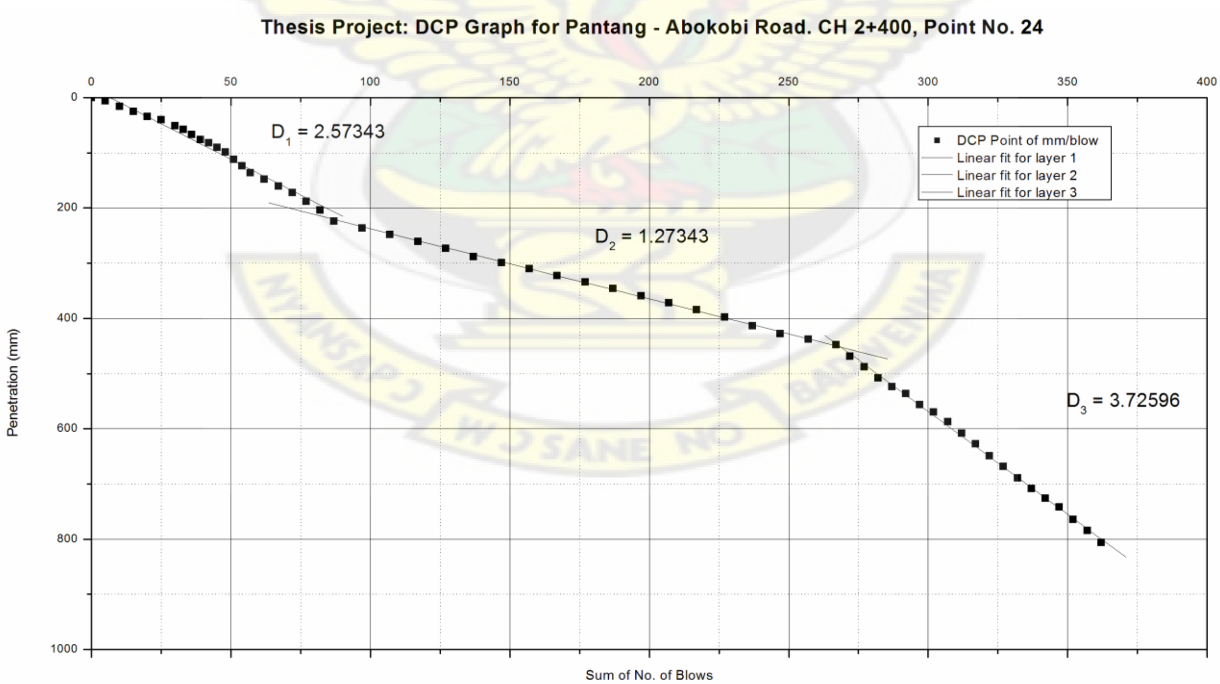

Figure E24: DCP Graph for Chainage 2+400

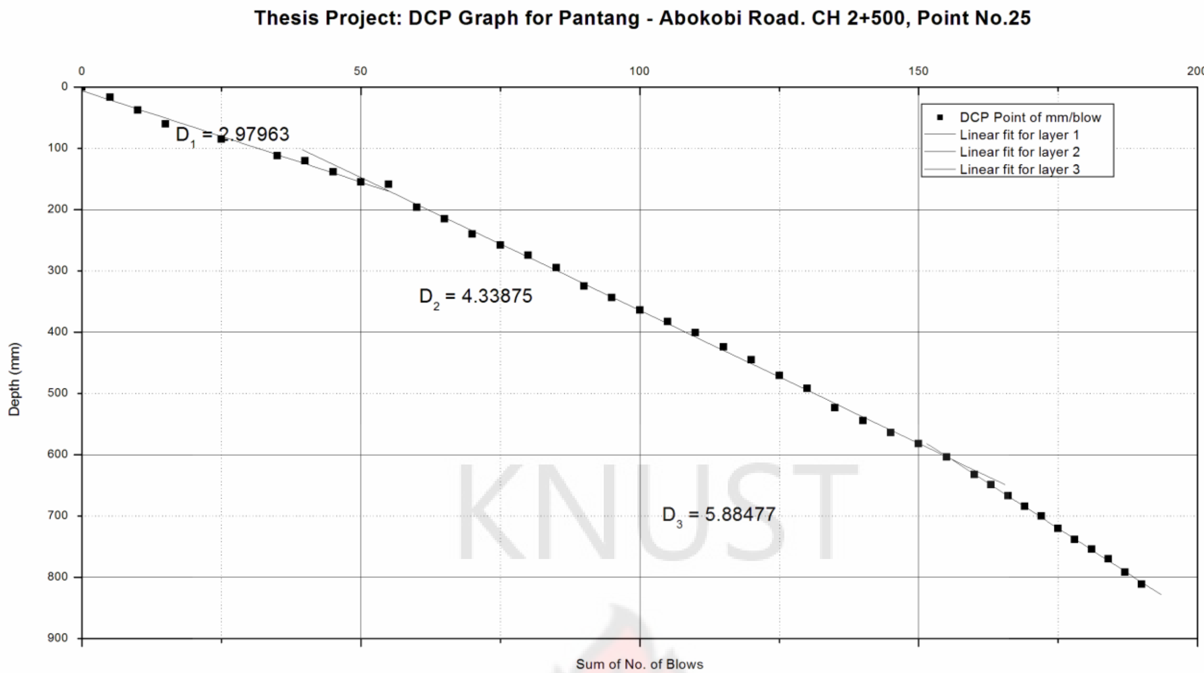

Figure E25: DCP Graph for Chainage 2+500

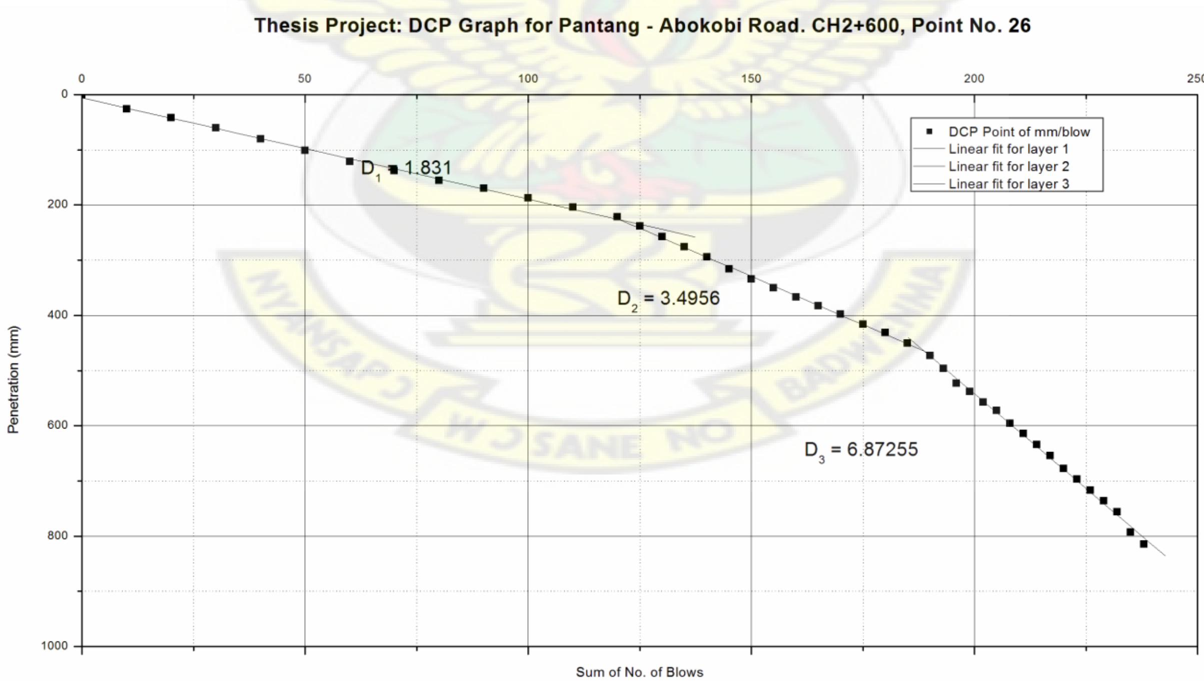

Figure E26: DCP Graph for Chainage 2+600

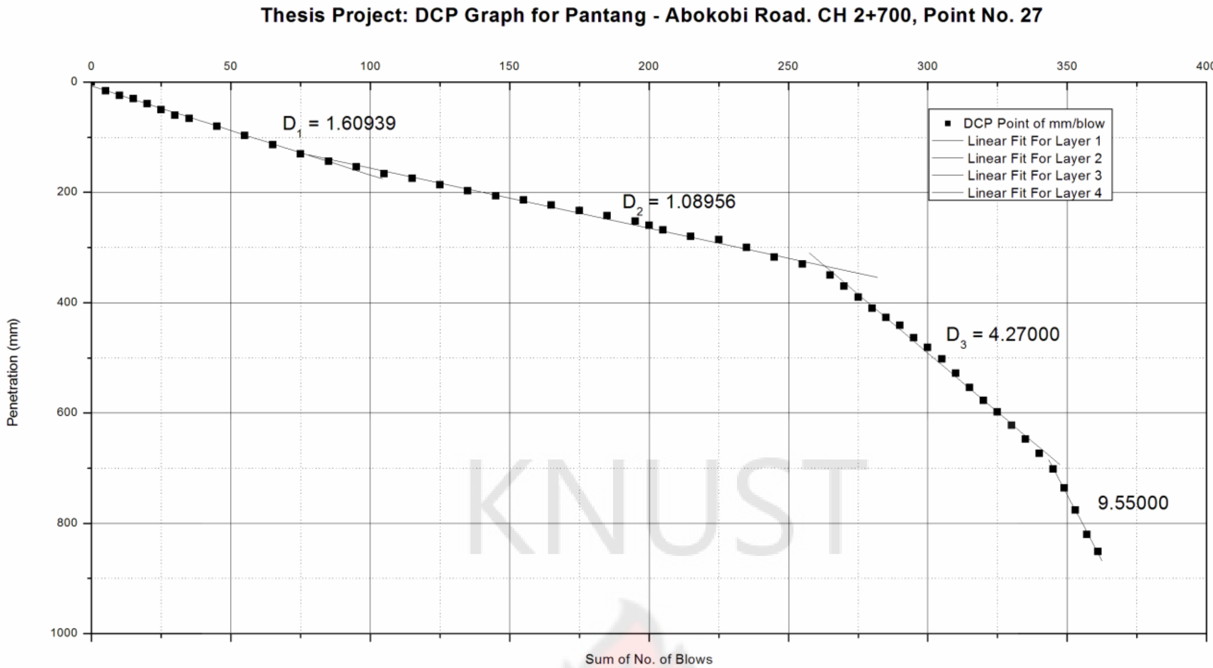

Figure E27: DCP Graph for Chainage 2+700

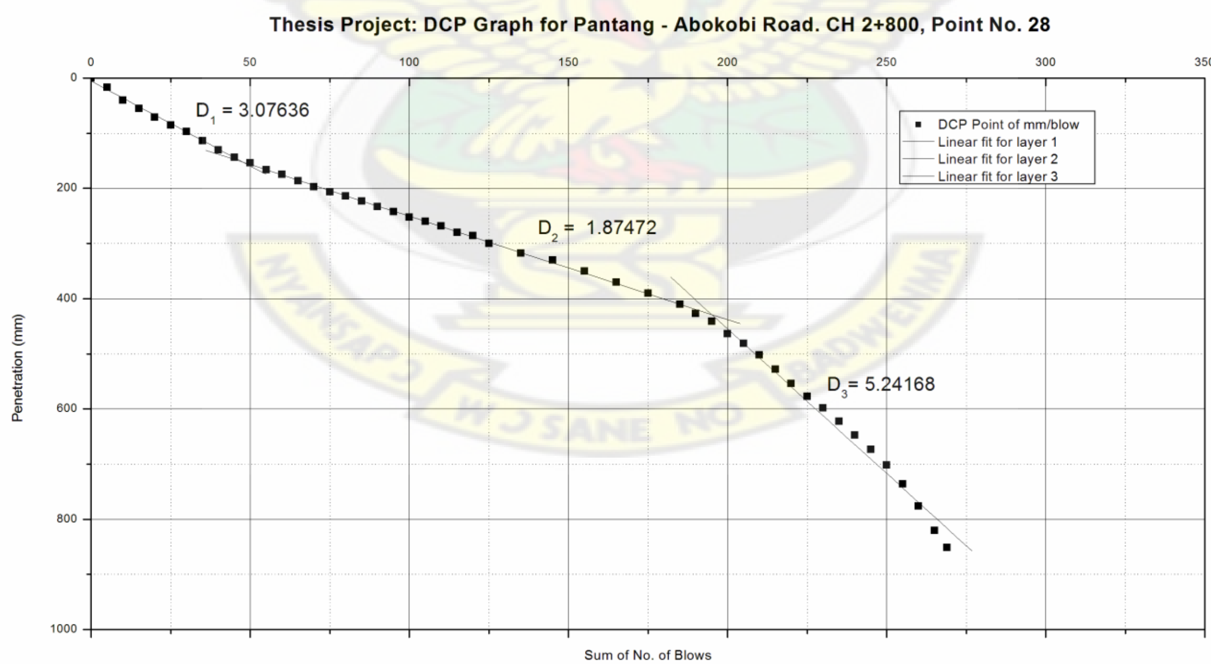

Figure E28: DCP Graph for Chainage 2+800

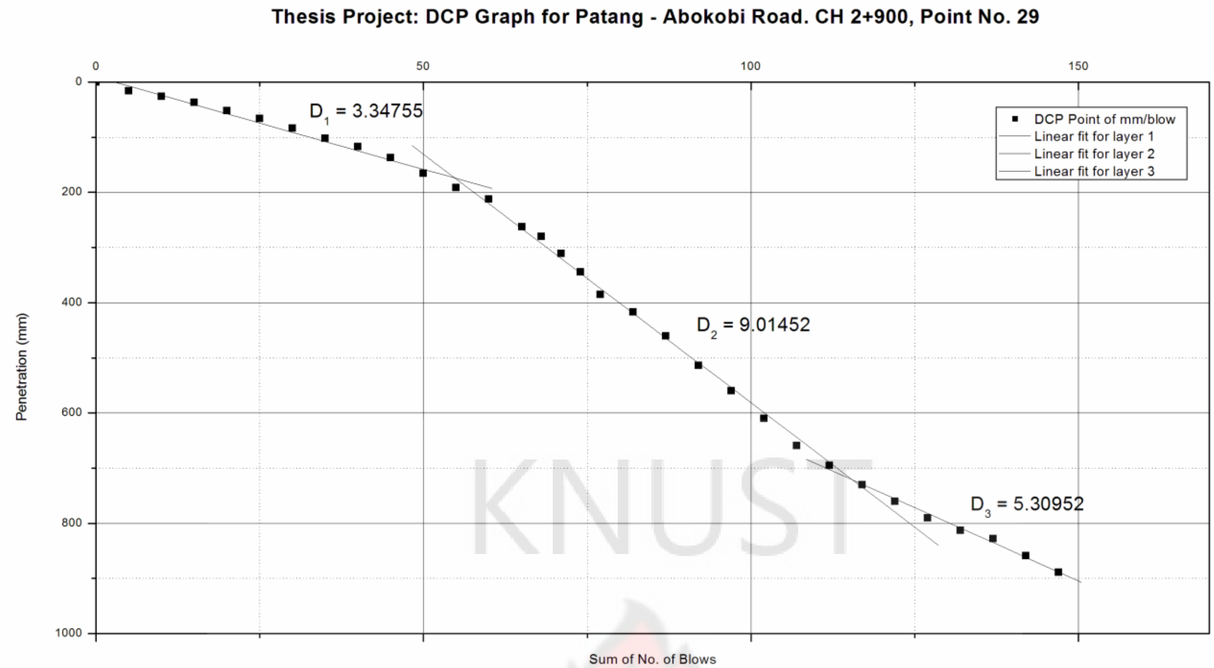

Figure E29: DCP Graph for Chainage 2+900

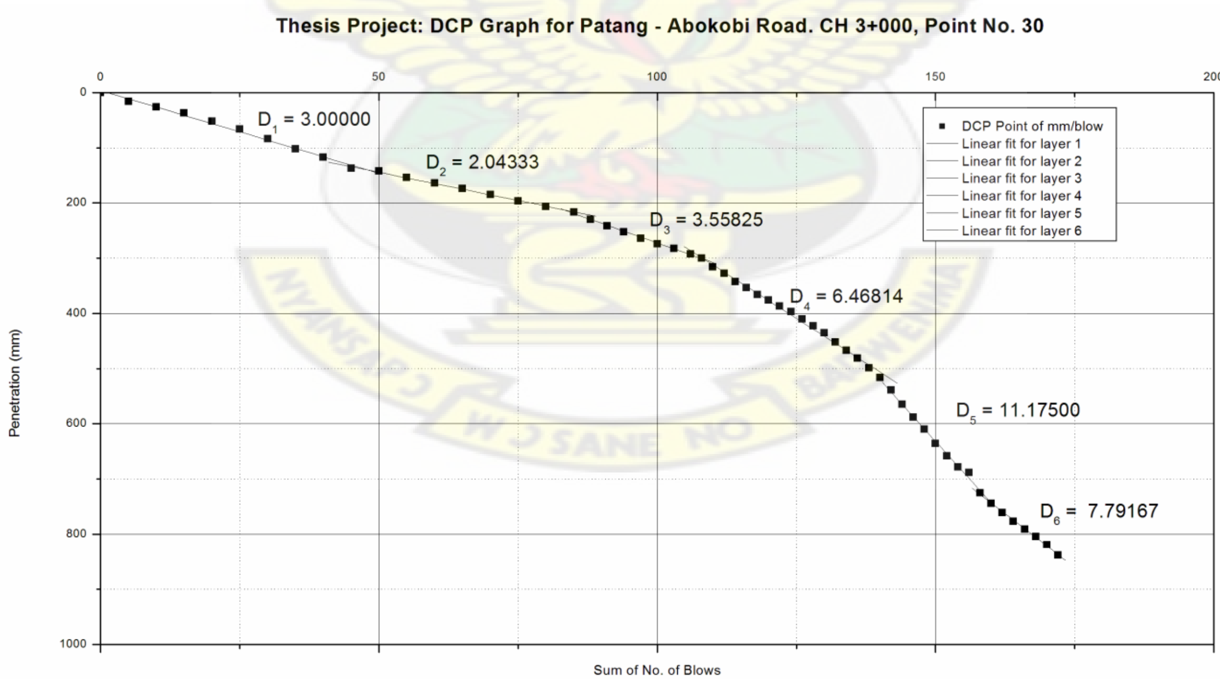

Figure E30: DCP Graph for Chainage 3+000

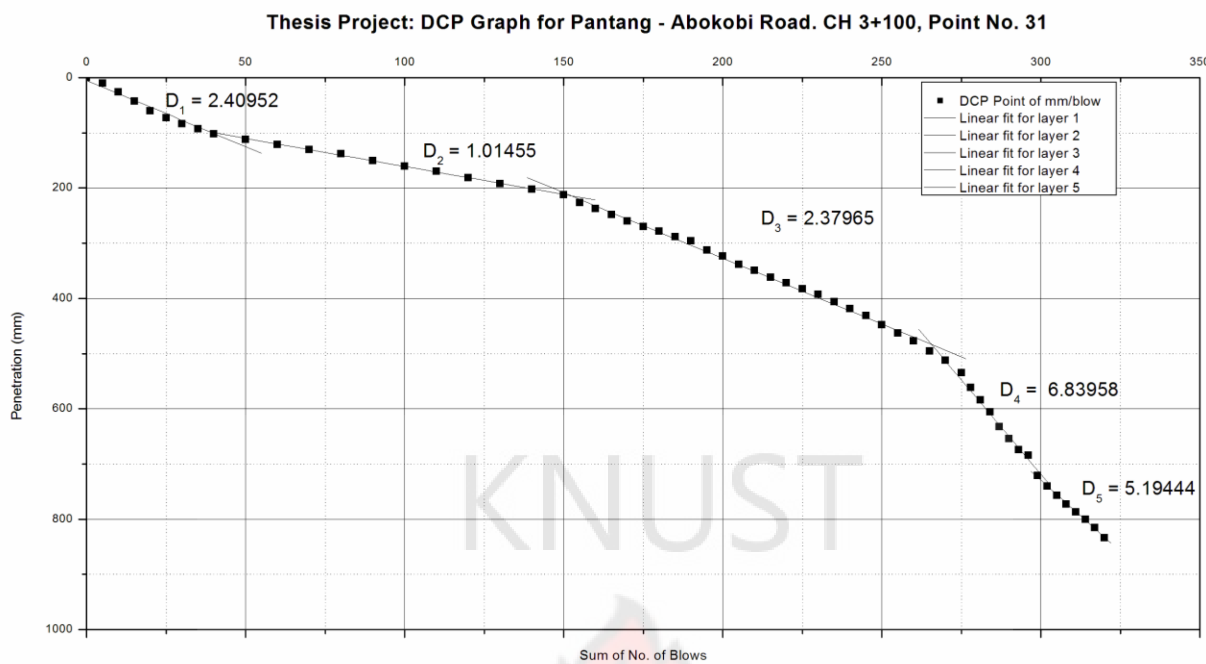

Figure E31: DCP Graph for Chainage 3+100

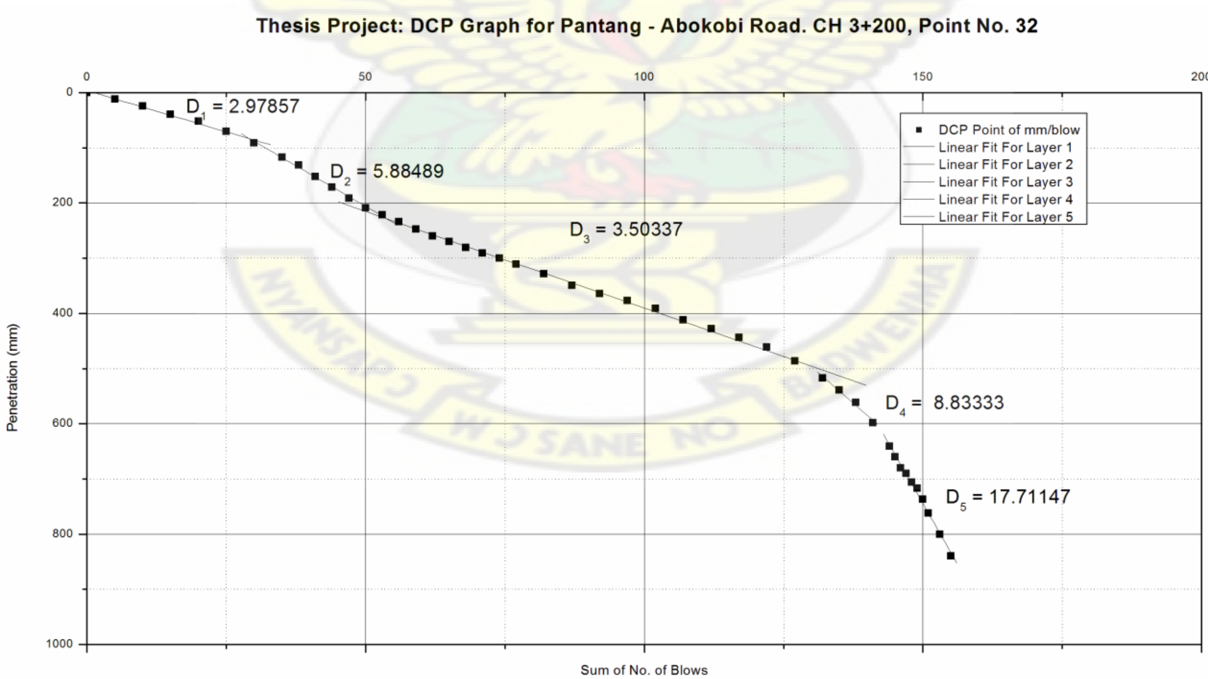

Figure E32: DCP Graph for Chainage 3+200

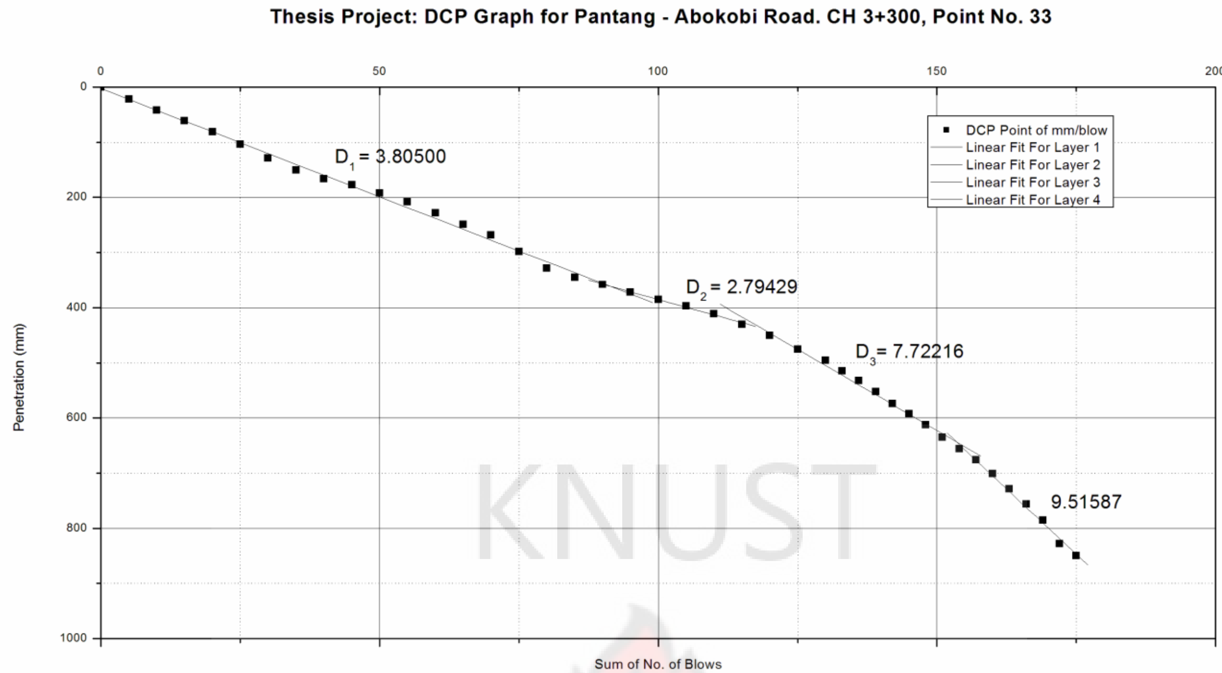

Figure E33: DCP Graph for Chainage 3+300

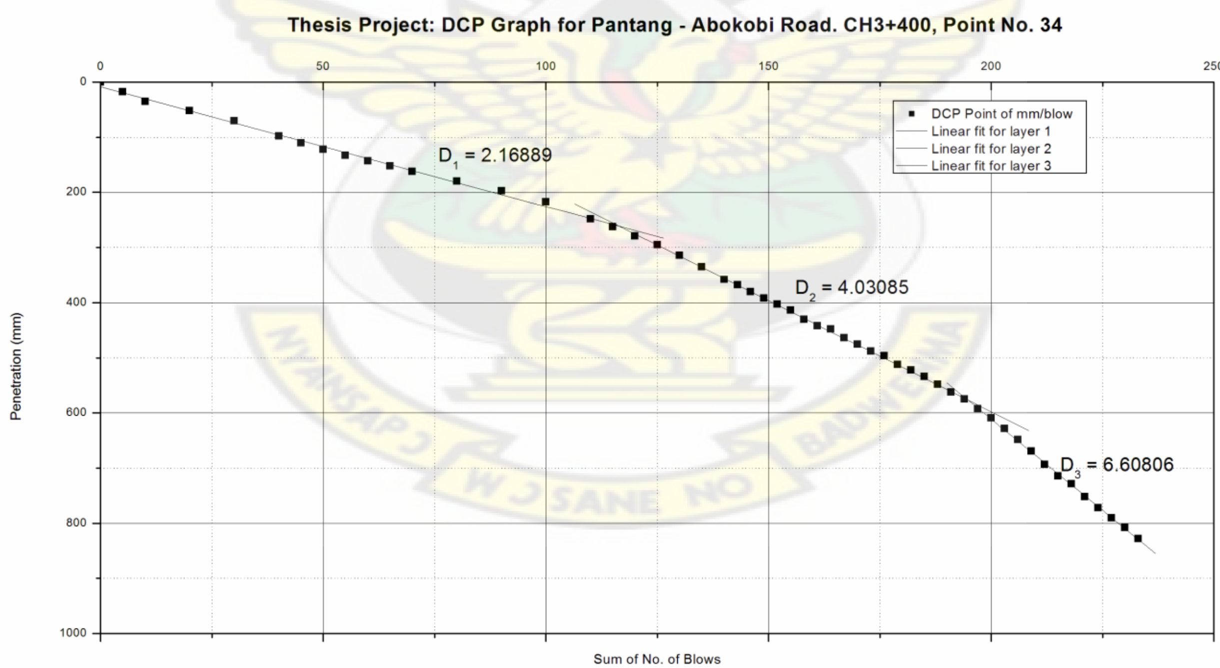

Figure E34: DCP Graph for Chainage 3+400

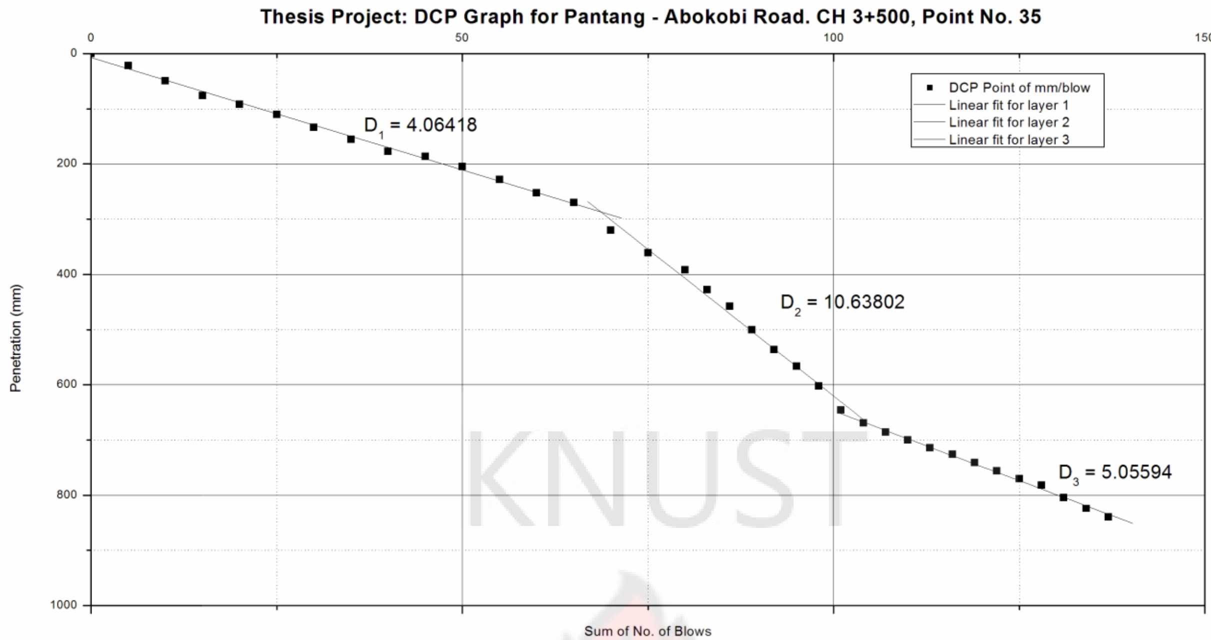

Figure E35: DCP Graph for Chainage 3+500

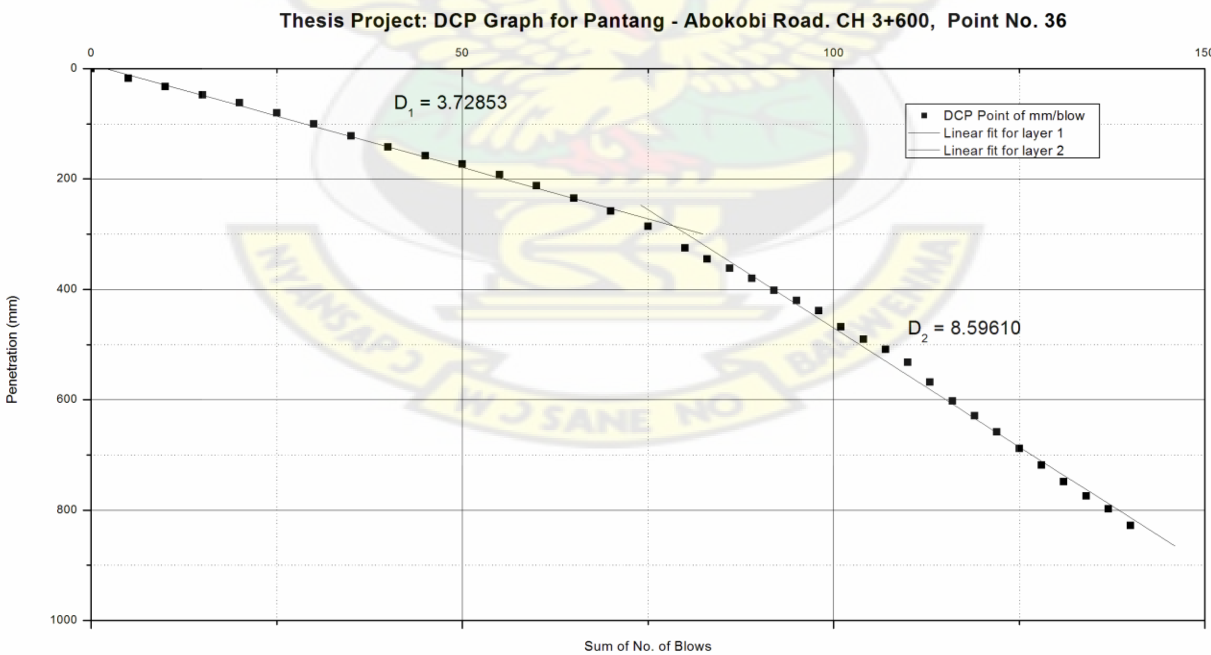

Figure E36: DCP Graph for Chainage 3+600

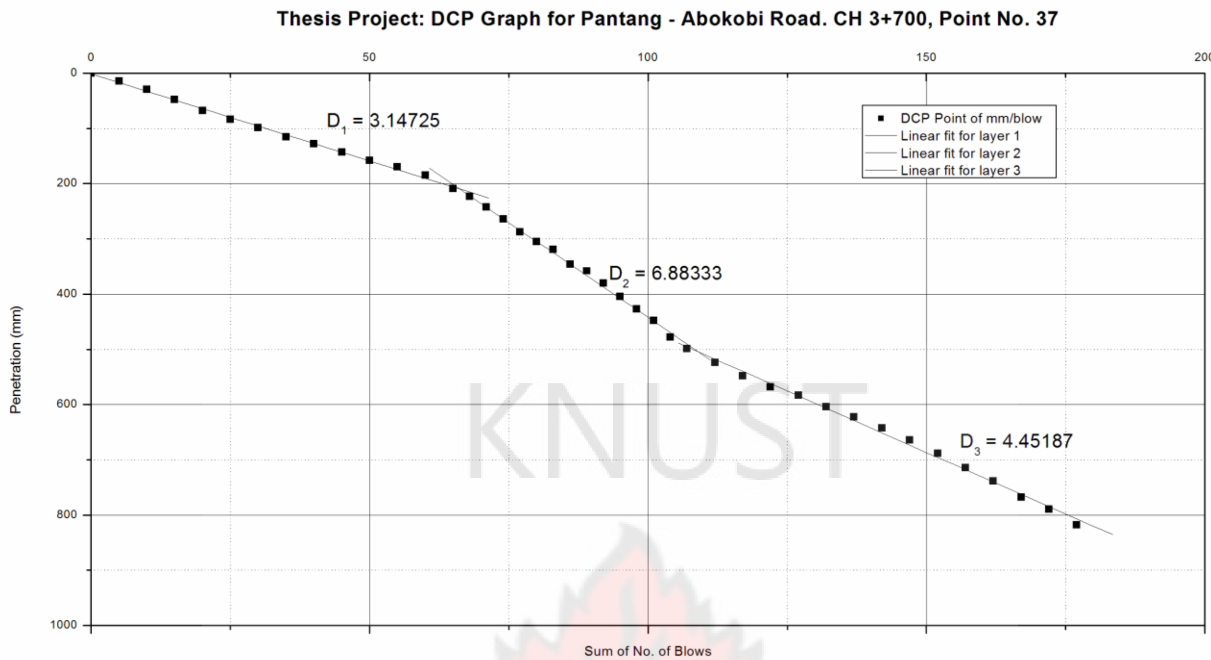

Figure E37: DCP Graph for Chainage 3+700

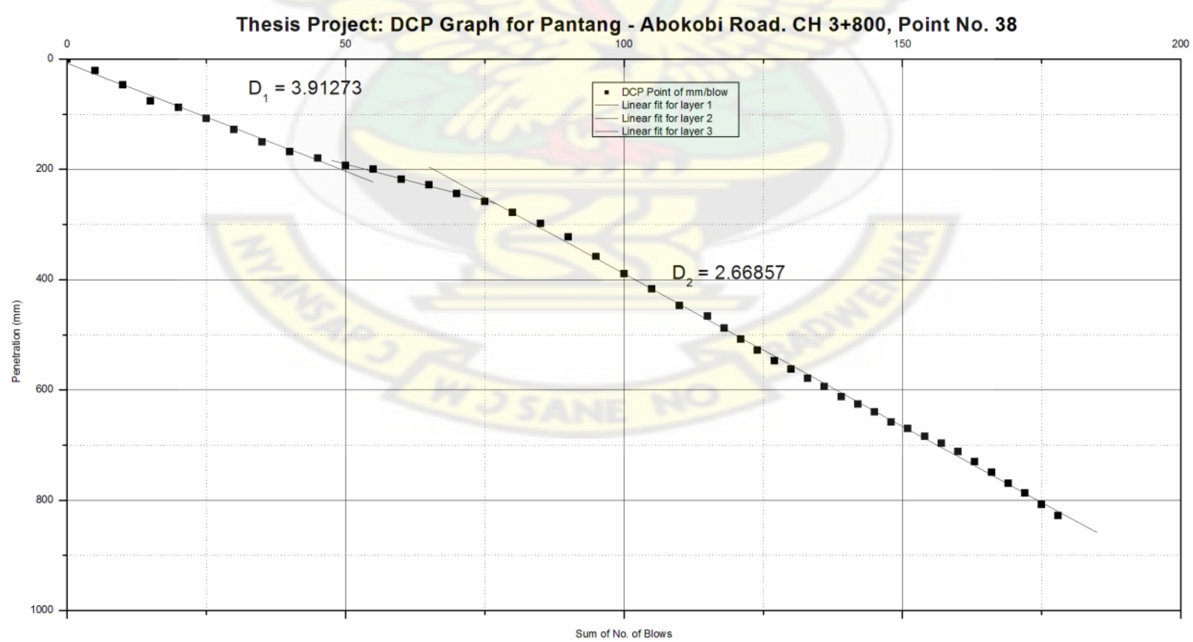

Figure E38: DCP Graph for Chainage 3+800

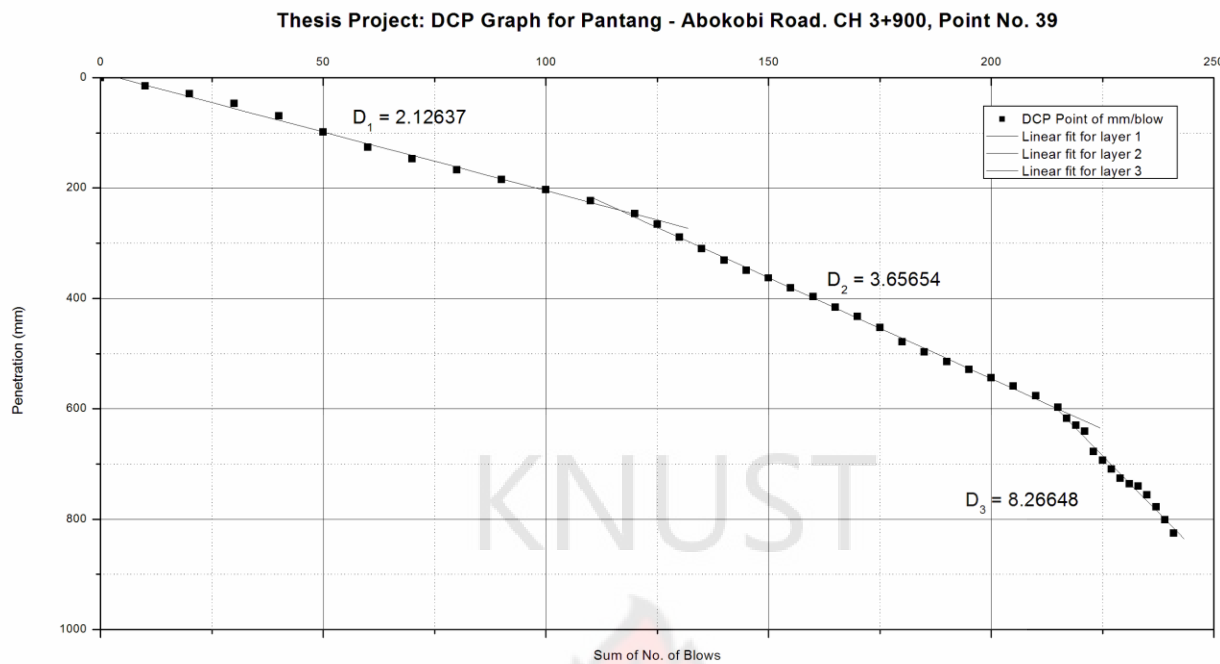

Figure E39: DCP Graph for Chainage 3+900

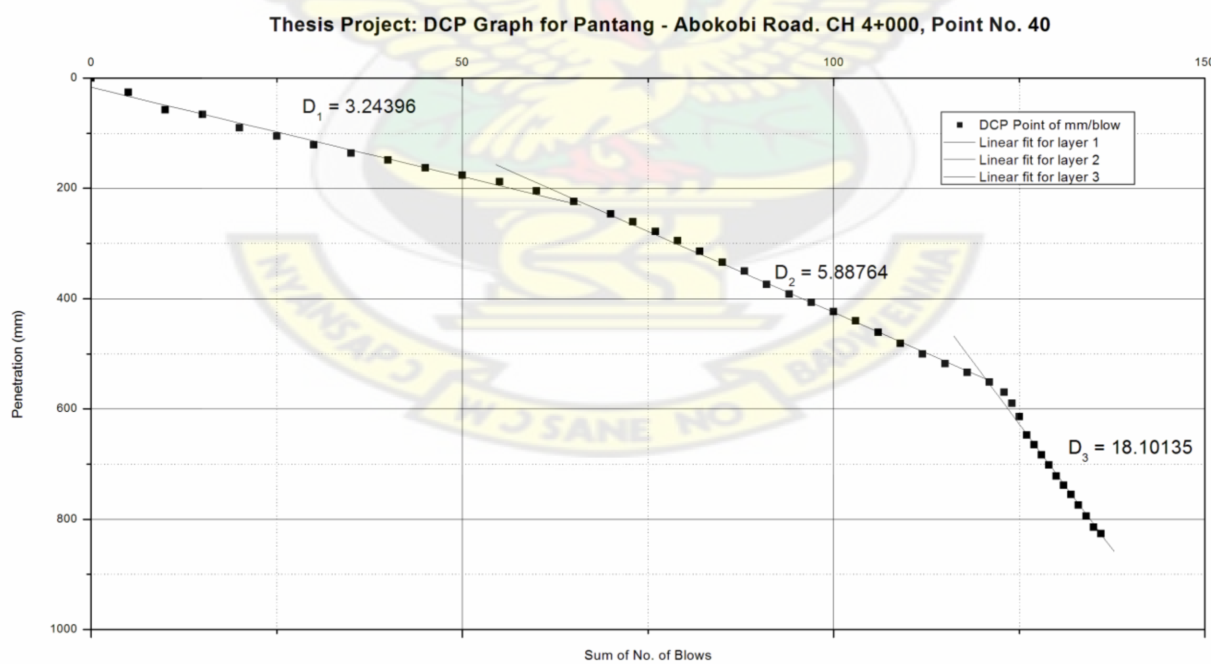

Figure E40: DCP Graph for Chainage 4+000

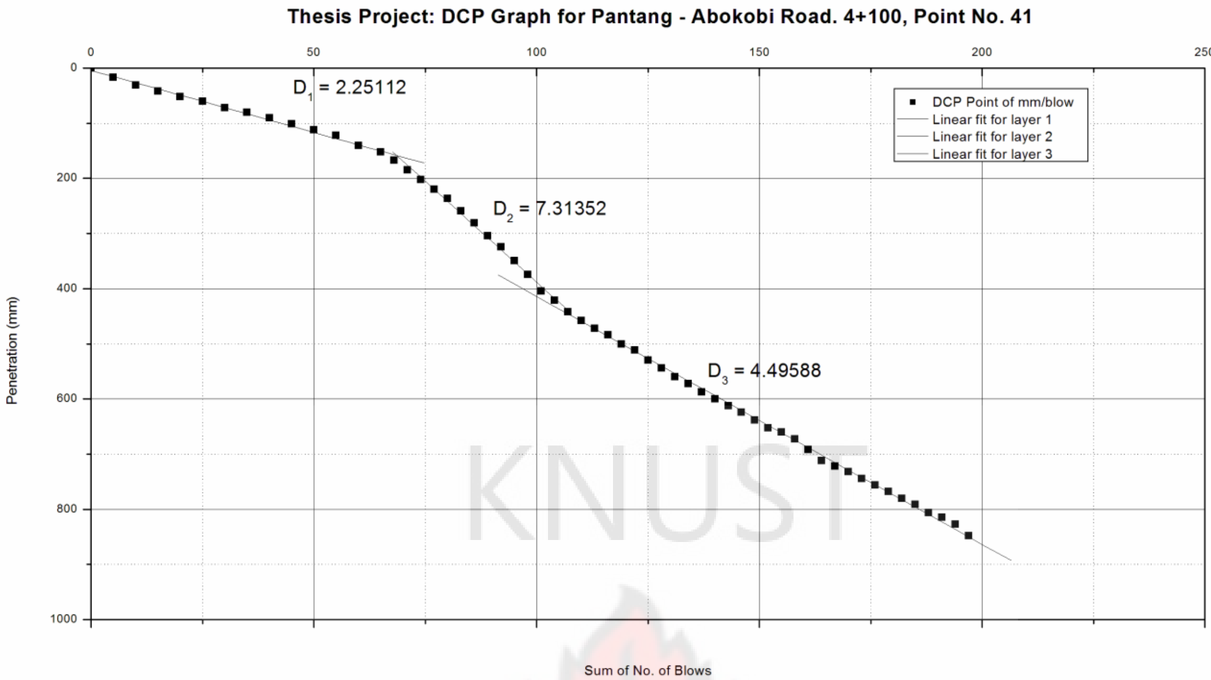

Figure E41: DCP Graph for Chainage 4+100

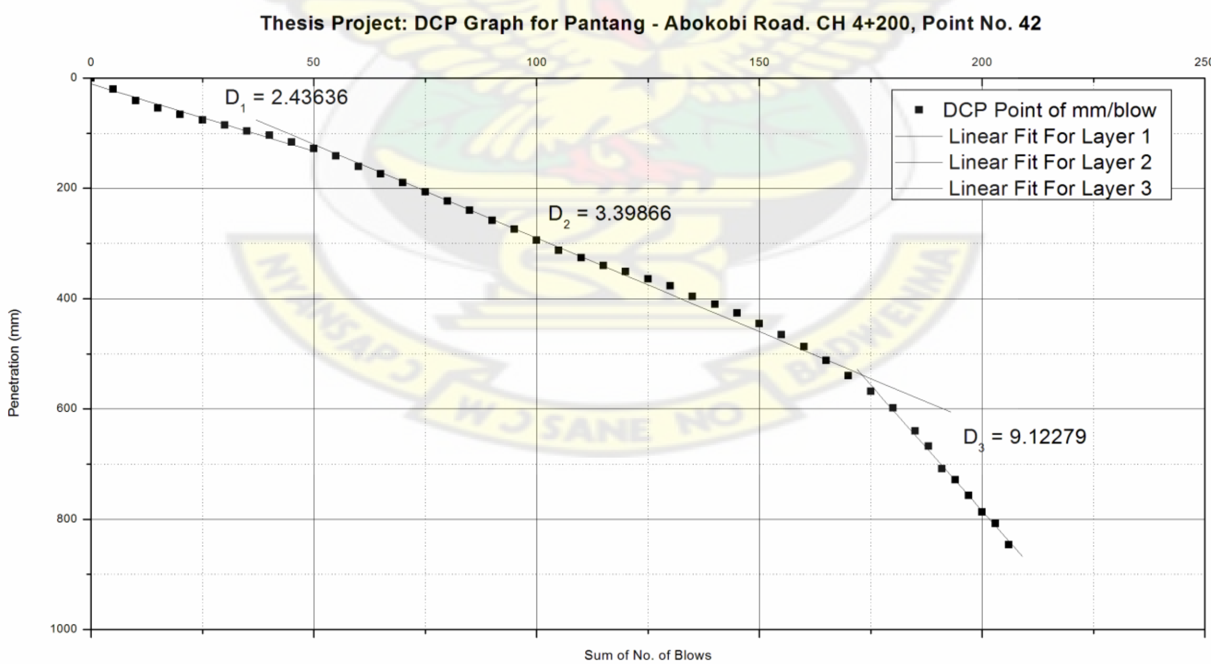

Figure E42: DCP Graph for Chainage 4+200

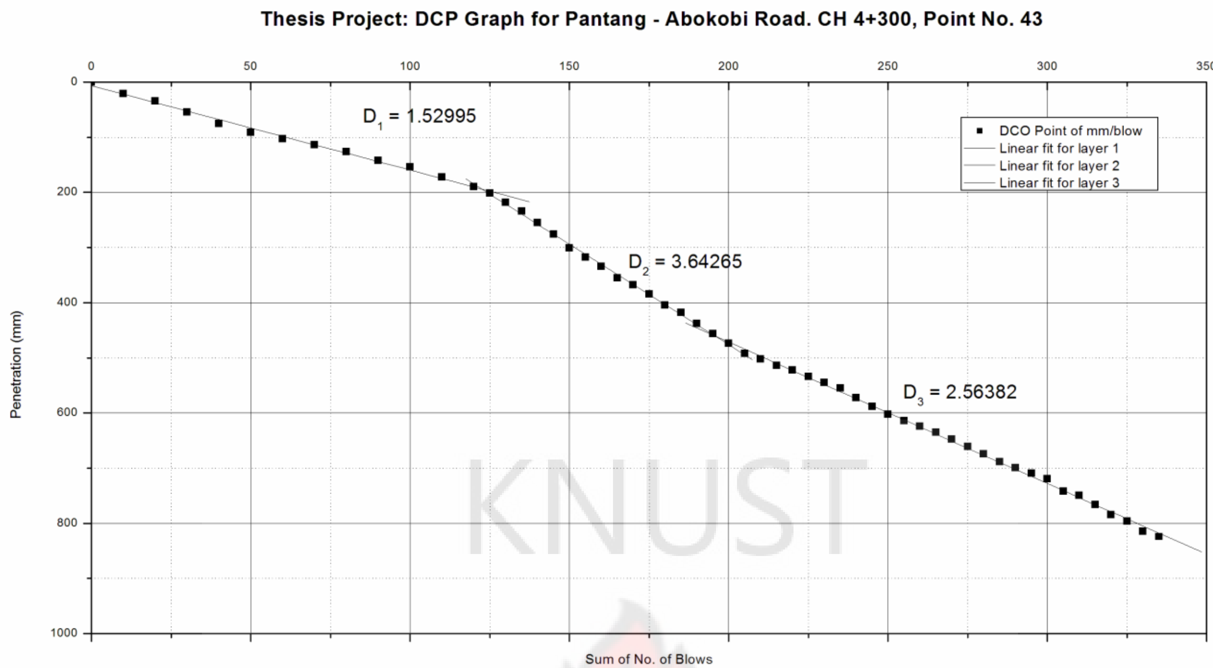

Figure E43: DCP Graph for Chainage 4+300

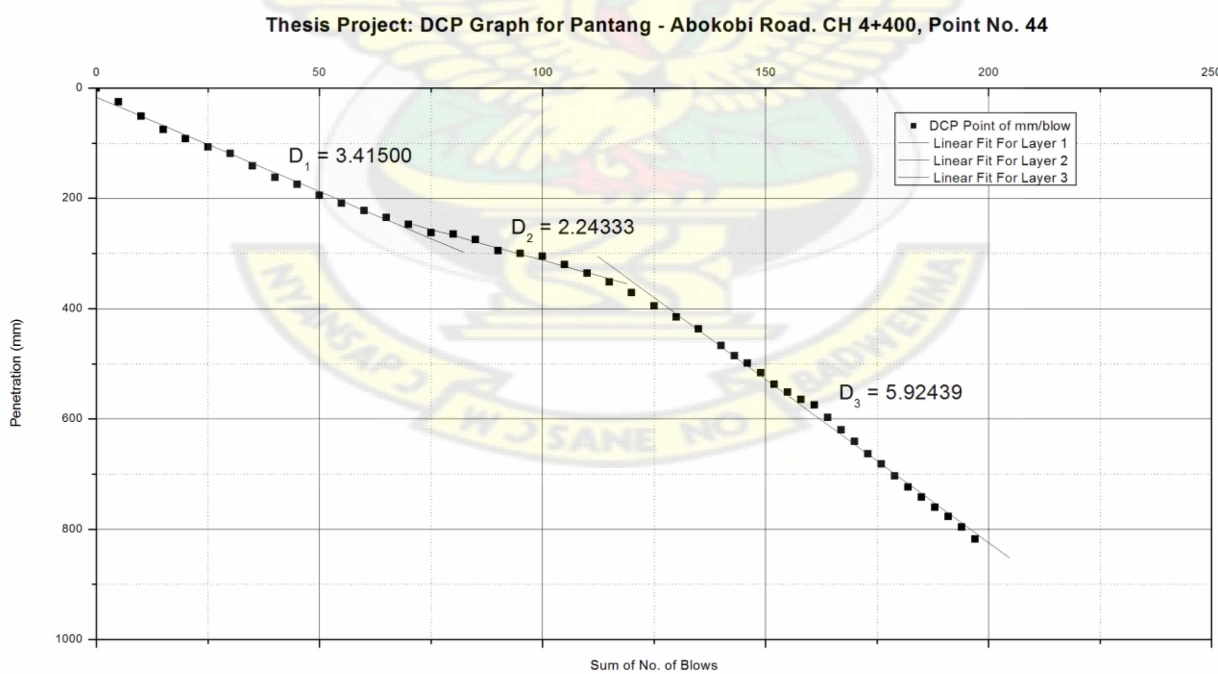

Figure E44: DCP Graph for Chainage 4+400

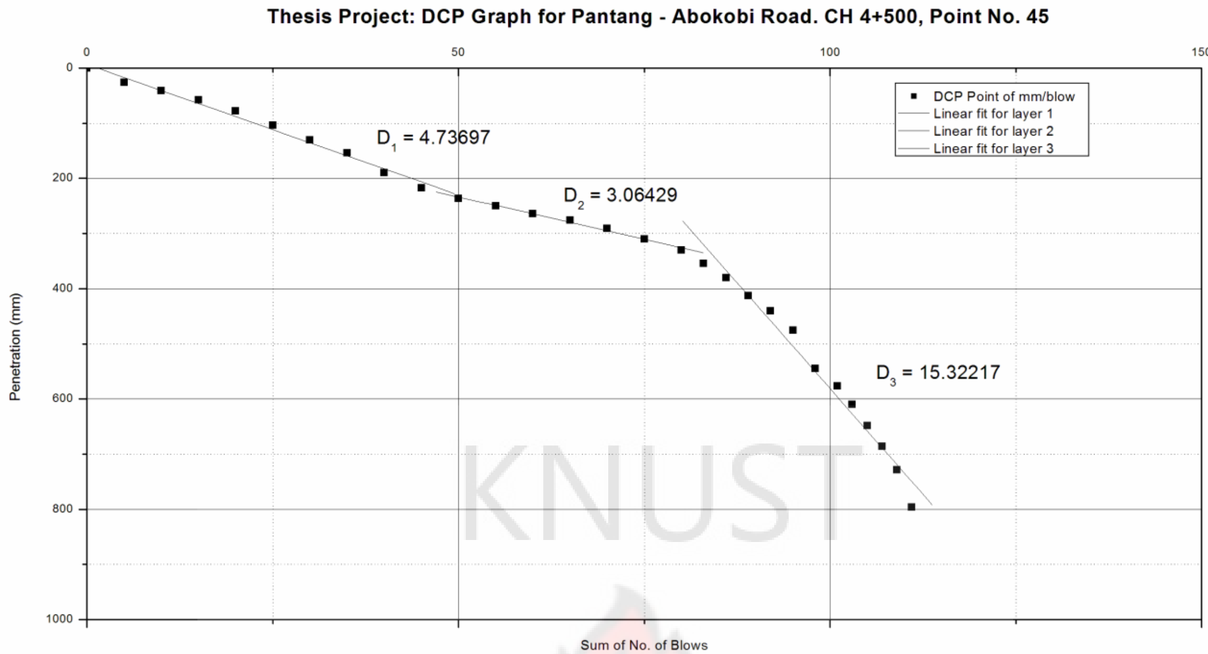

Figure E45: DCP Graph for Chainage 4+500

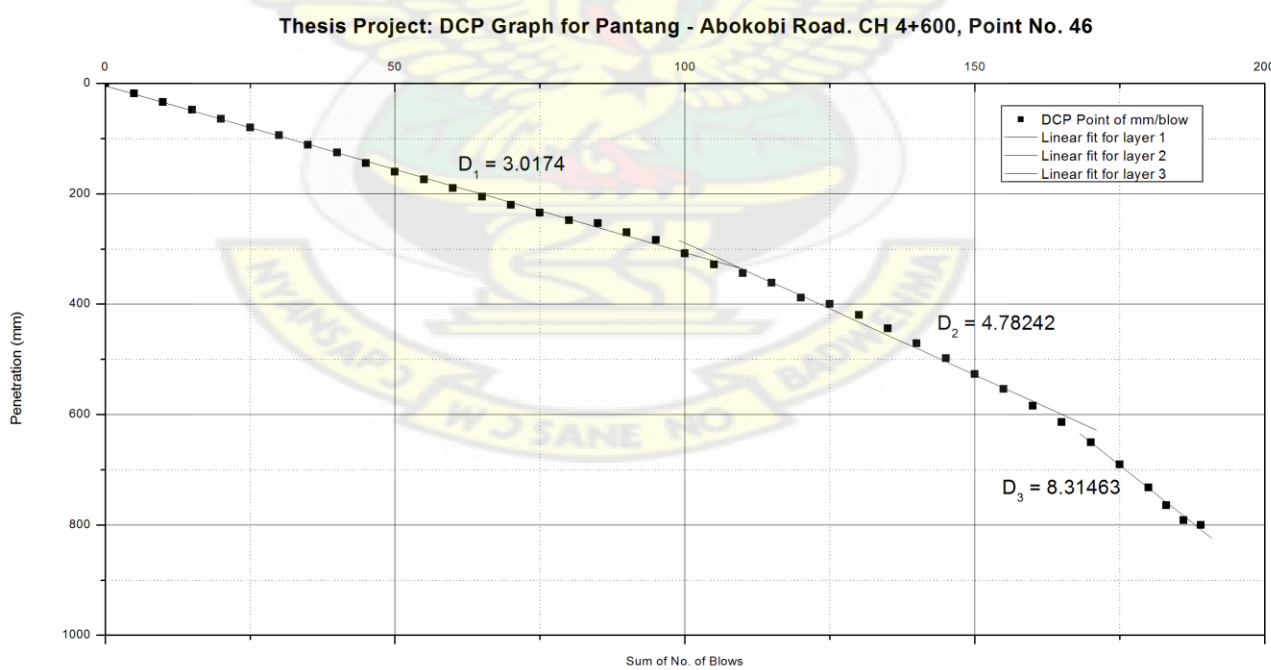

Figure E46: DCP Graph for Chainage 4+600

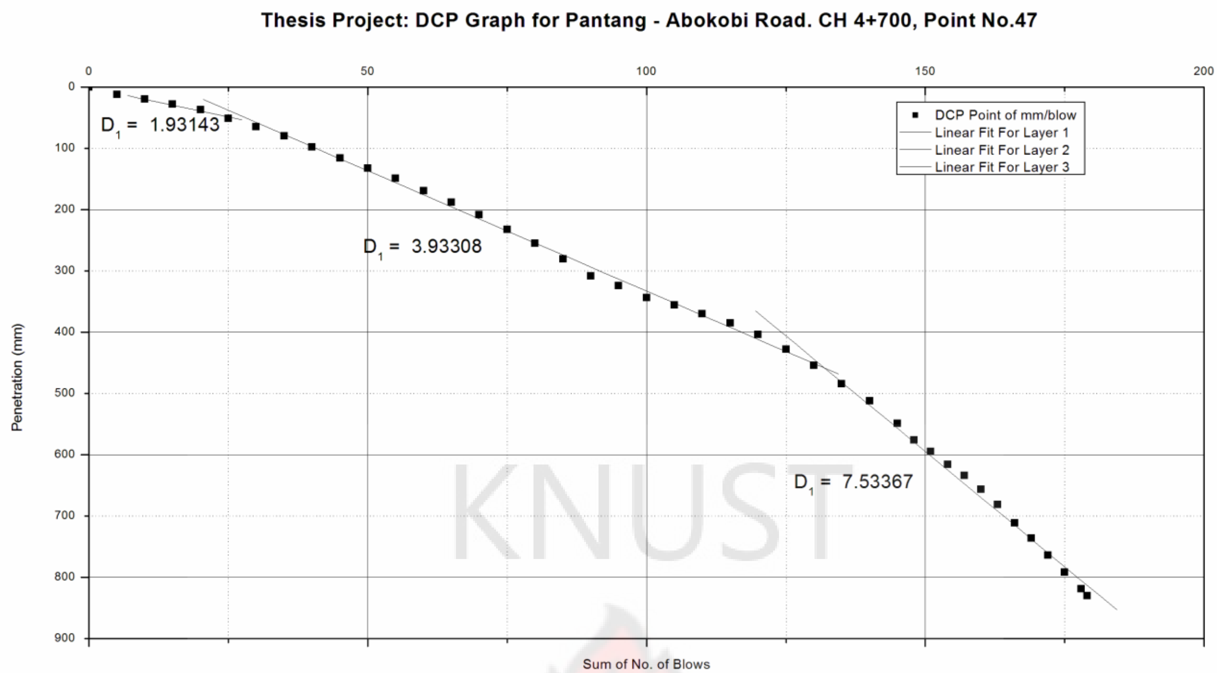

Figure E47: DCP Graph for Chainage 4+700

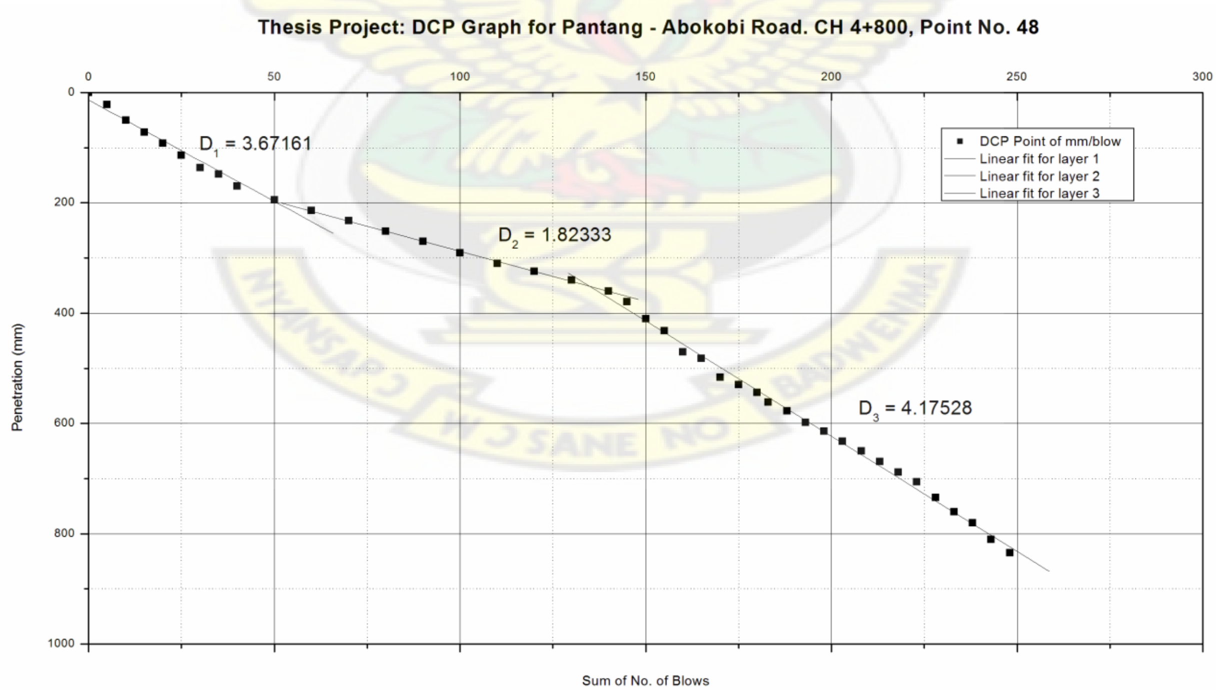

Figure E48: DCP Graph for Chainage 4+800

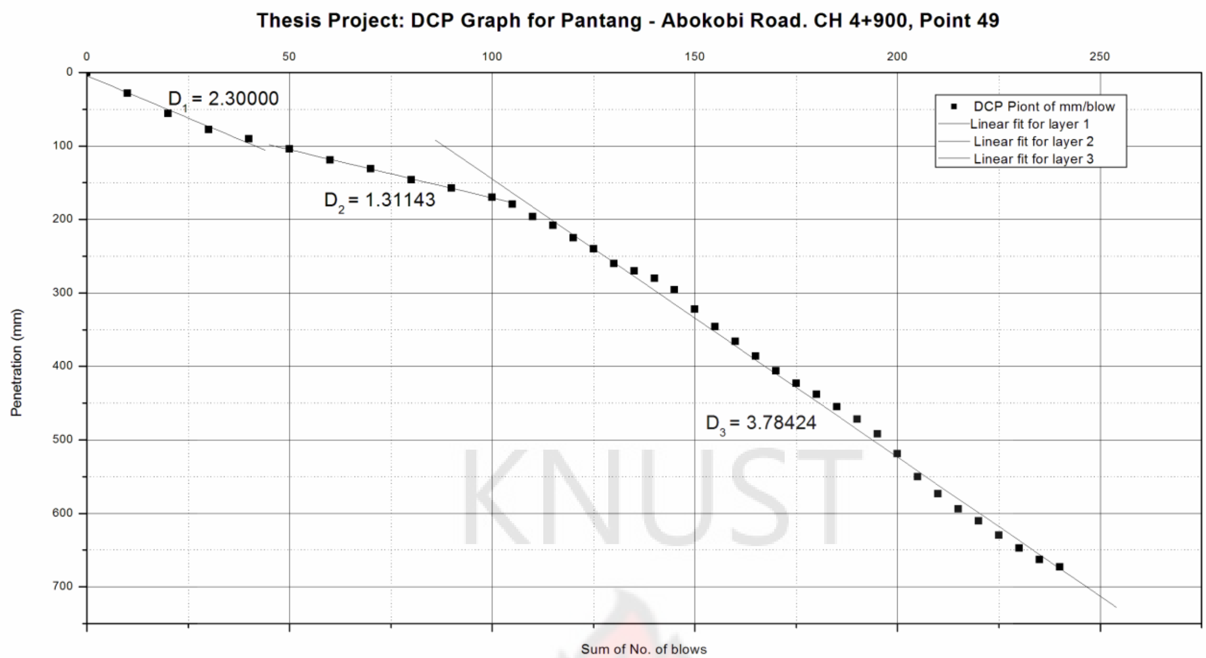

Figure E49: DCP Graph for Chainage 4+900

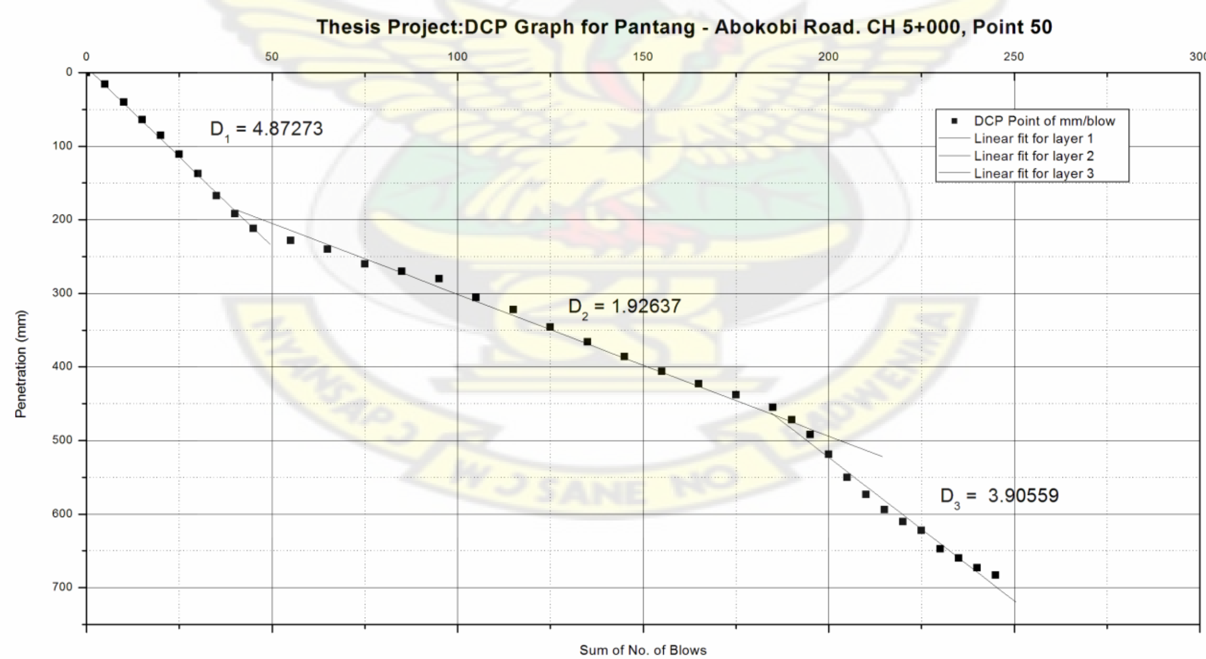

Figure E50: DCP Graph for Chainage 5+000

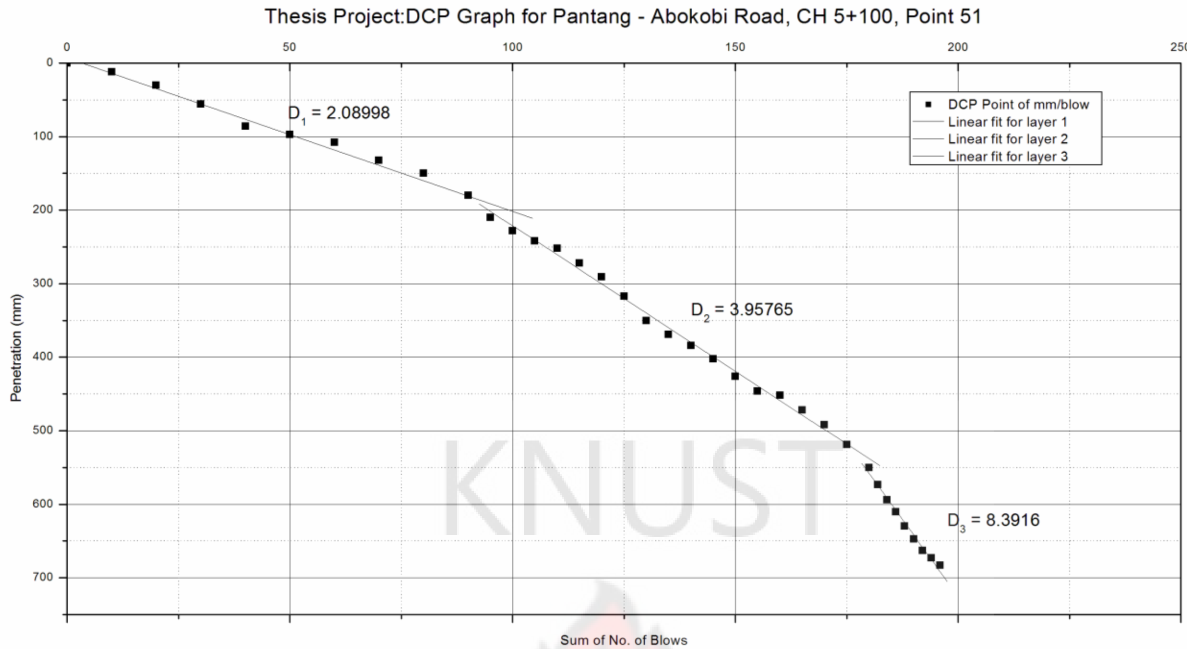

Figure E51: DCP Graph for Chainage 5+100

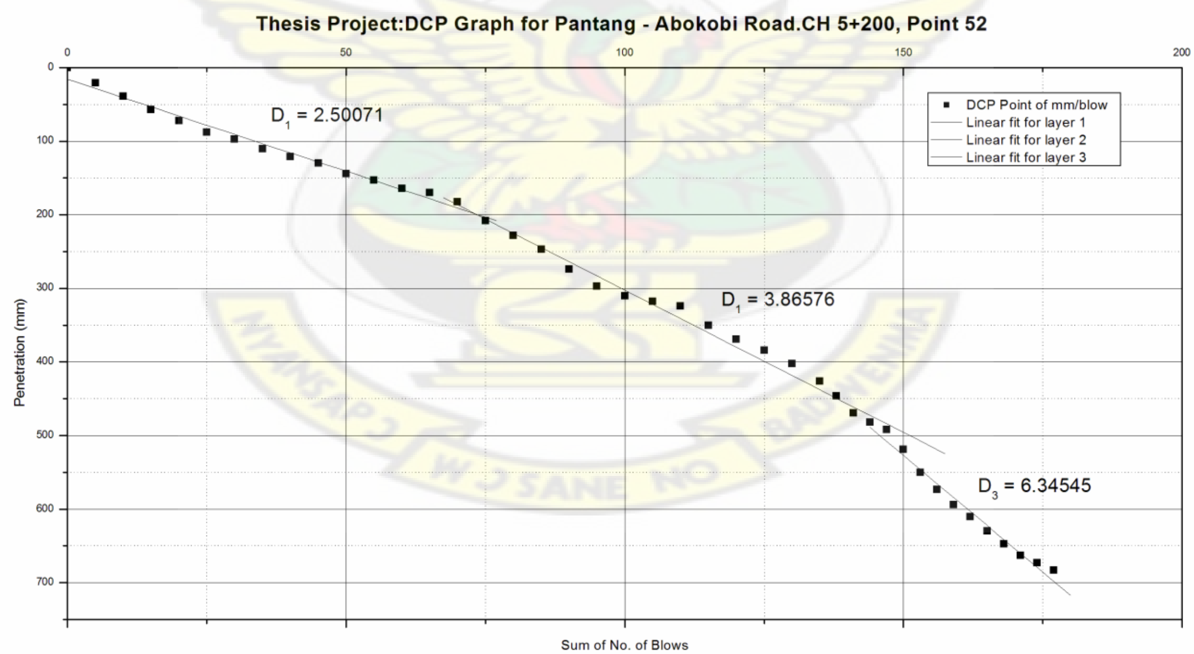

Figure E52: DCP Graph for Chainage 5+200

Table E2: Values of DCP blows against the penetration readings (mm)

CH: 0+100

A	B	C	D
Blows	Sum of Blows	Penetration (mm)	Corrected Penetration (mm)
0	0	54	0
10	10	90	36
10	20	105	51
10	30	123	69
10	40	137	83
10	50	151	97
10	60	163	109
10	70	176	122
5	75	186	132
5	80	197	143
5	85	208	154
5	90	219	165
5	95	231	177
5	100	246	192
5	105	256	202
5	110	267	213
5	115	277	223
5	120	291	237
5	125	302	248
5	130	314	260
5	135	327	273
5	140	337	283
5	145	356	302
5	150	380	326
5	155	394	340
5	160	410	356
5	165	420	366
5	170	440	386
5	175	456	402
5	180	475	421
5	185	496	442
5	190	505	451
2	192	536	482
2	194	546	492
2	196	560	506
2	198	574	520
2	200	591	537
2	202	612	558
2	204	629	575
2	206	643	589
2	208	661	607
2	210	680	626
2	212	705	651
2	214	726	672

Table E3: Values of DCP blows against the penetration readings (mm)

A	B	C	D
CH:0+200	--	--	--
Blows	Sum of Blows	Penetration (mm)	Corrected Penetration (mm)
0	0	54	0
10	10	90	36
10	20	105	51
5	25	123	69
5	30	137	83
5	35	151	97
5	40	163	109
5	45	176	122
5	50	186	132
5	55	197	143
5	60	208	154
5	65	219	165
5	70	231	177
5	75	246	192
5	80	256	202
5	85	267	213
5	90	277	223
5	95	291	237
5	100	302	248
5	105	314	260
5	110	327	273
5	115	337	283
5	120	356	302
5	125	380	326
10	135	394	340
10	145	410	356
10	155	420	366
10	165	440	386
10	175	456	402
10	185	475	421
10	195	496	442
10	205	505	451
4	209	536	482
3	212	546	492
3	215	560	506
3	218	574	520
3	221	591	537
3	224	612	558
3	227	629	575
3	230	643	589
3	233	661	607
3	236	680	626
3	239	705	651
3	242	726	672
3	245	741	687
3	248	756	702
3	251	776	722
3	254	786	732
3	257	796	742
3	260	806	752

Table E4: Values of DCP blows against the penetration readings (mm)

A	B	C	D
CH:0+300--	--	--	--
Blows	Sum of Blows	Penetration (mm)	Corrected Penetration (mm)
0	0	42	0
10	10	70	28
10	20	80	38
10	30	90	48
10	40	102	60
10	50	113	71
10	60	132	90
10	70	151	109
10	80	162	120
10	90	180	138
10	100	195	153
10	110	215	173
10	120	240	198
5	125	250	208
5	130	262	220
5	135	272	230
5	140	286	244
5	145	300	258
5	150	310	268
5	155	322	280
5	160	334	292
5	165	346	304
5	170	359	317
5	175	368	326
5	180	380	338
5	185	391	349
5	190	402	360
5	195	416	374
5	200	429	387
5	205	446	404
5	210	460	418
5	215	472	430
5	220	487	445
5	225	506	464
5	230	520	478
5	235	538	496
5	240	554	512
5	245	572	530
5	250	595	553
3	253	610	568
3	256	626	584
3	259	646	604
3	262	666	624
3	265	689	647
3	268	712	670
2	270	730	688
2	272	756	714
2	274	770	728
2	276	791	749
2	278	811	769
2	280	832	790
2	282	847	805
3	285	862	820
3	288	879	837

Table E5: Values of DCP blows against the penetration readings (mm)

A	B	C	D
CH:0+400--	--	--	--
No. Of Blows	Sum of No. Of Blows	Penetration (mm)	Corrected Penetration (mm)
0	0	48	0
10	10	90	42
5	15	105	57
5	20	123	75
5	25	137	89
5	30	151	103
5	35	163	115
5	40	176	128
5	45	186	138
5	50	197	149
5	55	208	160
5	60	219	171
5	65	231	183
5	70	246	198
5	75	256	208
5	80	267	219
5	85	277	229
5	90	291	243
5	95	302	254
5	100	314	266
5	105	327	279
5	110	337	289
5	115	356	308
10	125	380	332
10	135	394	346
10	145	410	362
10	155	420	372
10	165	440	392
10	175	456	408
10	185	475	427
10	195	496	448
10	205	515	467
5	210	536	488
5	215	546	498
5	220	560	512
5	225	574	526
5	230	591	543
5	235	612	564
5	240	629	581
5	245	643	595
5	250	661	613
5	255	680	632
5	260	705	657
5	265	726	678
5	270	741	693
5	275	756	708
5	280	776	728
5	285	786	738
5	290	796	748
5	295	806	758
5	300	813	765
5	305	823	775
5	310	831	783
5	315	847	799
5	320	858	810

Table E6: Values of DCP blows against the penetration readings (mm)

A	B	C	D
CH:0+500		--	--
No. Of Blows	Sum of No. Of Blows	Penetration (mm)	Corrected Penetration (mm)
0	0	65	0
10	10	93	28
5	15	110	45
5	20	121	56
5	25	132	67
5	30	143	78
5	35	152	87
5	40	160	95
5	45	165	100
5	50	173	108
5	55	181	116
5	60	189	124
5	65	198	133
5	70	210	145
5	75	220	155
5	80	237	172
5	85	251	186
5	90	262	197
5	95	276	211
5	100	290	225
5	105	305	240
5	110	318	253
5	115	330	265
5	120	350	285
5	125	364	299
5	130	380	315
5	135	393	328
5	140	412	347
4	144	432	367
3	147	446	381
3	150	460	395
3	153	473	408
3	156	491	426
3	159	509	444
3	162	530	465
3	165	554	489
3	168	574	509
3	171	592	527
3	174	612	547
3	177	631	566
3	180	651	586
3	183	672	607
3	186	692	627
3	189	712	647
2	191	731	666
2	193	751	686
2	195	770	705
2	197	791	726
2	199	810	745
2	201	820	755
2	203	829	764
2	205	844	779
2	207	855	790
2	209	862	797

Table E7: Values of DCP blows against the penetration readings (mm)

A	B	C	D
CH 0+600	--	--	--
No. Of Blows	Sum of No. Of Blows	Penetration (mm)	Corrected Penetration (mm)
0	0	65	0
10	10	78	13
10	20	83	18
10	30	96	31
5	35	110	45
5	40	120	55
5	45	129	64
5	50	142	77
5	55	164	99
5	60	186	121
5	65	200	135
5	70	212	147
5	75	226	161
5	80	235	170
5	85	246	181
5	90	260	195
5	95	271	206
5	100	288	223
5	105	305	240
5	110	321	256
5	115	336	271
5	120	344	279
5	125	356	291
5	130	366	301
5	135	378	313
5	140	386	321
5	145	397	332
5	150	420	355
5	155	440	375
5	160	450	385
5	165	467	402
5	170	478	413
5	175	490	425
5	180	502	437
5	185	512	447
5	190	527	462
5	195	536	471
5	200	546	481
5	205	559	494
5	210	570	505
5	215	582	517
5	220	593	528
5	225	608	543
5	230	621	556
5	235	638	573
5	240	650	585
5	245	660	595
4	249	690	625
3	252	704	639
3	255	724	659
3	258	744	679
3	261	772	707
3	264	812	747
2	266	849	784
2	268	890	825

Table E8: Values of DCP blows against the penetration readings (mm)

A	B	C	D
CH:0+700	--	--	--
No. Of Blows	Sum of No. Of Blows	Penetration (mm)	Corrected Penetration (mm)
0	0	70	0
10	10	80	10
10	20	84	14
10	30	94	24
10	40	100	30
10	50	112	42
10	60	124	54
10	70	141	71
10	80	162	92
10	90	186	116
10	100	200	130
5	105	212	142
5	110	226	156
5	115	235	165
5	120	246	176
5	125	260	190
5	130	271	201
5	135	288	218
5	140	305	235
5	145	321	251
4	149	336	266
4	153	344	274
5	158	376	306
5	163	386	316
5	168	401	331
5	173	414	344
5	178	428	358
5	183	440	370
5	188	450	380
5	193	450	380
5	198	467	397
5	203	478	408
5	208	490	420
5	213	502	432
5	218	512	442
5	223	527	457
5	228	536	466
5	233	546	476
5	238	559	489
5	243	570	500
5	248	582	512
5	253	593	523
5	258	608	538
5	263	621	551
5	268	638	568
5	273	650	580
5	278	670	600
4	282	690	620
3	285	704	634
3	288	724	654
3	291	744	674
3	294	772	702
3	297	812	742
2	299	849	779
2	301	890	820

Table E9: Values of DCP blows against the penetration readings (mm)

A	B	C	D
CH:0+800			
No. Of Blows	Sum of No. Of Blows	Penetration (mm)	Corrected Penetration (mm)
0	0	65	0
10	10	86	21
10	20	106	41
10	30	126	61
10	40	145	80
10	50	167	102
5	55	182	117
5	60	194	129
5	65	201	136
5	70	210	145
5	75	226	161
5	80	232	167
5	85	248	183
5	90	268	203
5	95	287	222
5	100	314	249
5	105	337	272
5	110	350	285
5	115	368	303
5	120	374	309
5	125	381	316
5	130	400	335
5	135	418	353
5	140	432	367
5	145	453	388
5	150	460	395
5	155	479	414
5	160	490	425
5	165	507	442
5	170	521	456
5	175	540	475
5	180	561	496
5	185	582	517
5	190	600	535
3	193	610	545
3	196	620	555
3	199	634	569
3	202	645	580
3	205	660	595
3	208	672	607
3	211	689	624
3	214	700	635
3	217	714	649
3	220	729	664
3	223	750	685
3	226	770	705
3	229	790	725
3	232	810	745
3	235	830	765
3	238	850	785
3	241	870	805
3	244	890	825

Table E10: Values of DCP blows against the penetration readings (mm)

A	B	C	D
CH:0+900	--	--	--
No. Of Blows	Sum of No. Of Blows	Penetration (mm)	Corrected Penetration (mm)
0	0	64	0
10	10	75	11
10	20	80	16
10	30	86	22
10	40	89	25
10	50	98	34
10	60	106	42
10	70	120	56
10	80	130	66
10	90	141	77
5	95	148	84
5	100	161	97
5	105	172	108
5	110	184	120
5	115	198	134
5	120	212	148
5	125	226	162
5	130	240	176
5	135	254	190
5	140	270	206
5	145	284	220
5	150	304	240
5	155	316	252
5	160	326	262
5	165	347	283
5	170	364	300
5	175	372	308
5	180	387	323
5	185	398	334
5	190	412	348
5	195	422	358
5	200	430	366
5	205	442	378
5	210	455	391
5	215	465	401
5	220	472	408
5	225	488	424
5	230	498	434
5	235	513	449
5	240	526	462
5	245	535	471
5	250	541	477
5	255	558	494
3	258	567	503
3	261	578	514
3	264	597	533
3	267	604	540
3	270	618	554
3	273	645	581
3	276	657	593
3	279	679	615

Table E11: Values of DCP blows against the penetration readings (mm)

A	B	C	D
CH: 1+000	--	--	--
No. Of Blows	Sum of No. of Blows	Penetration (mm)	Corrected Penetration (mm)
0	0	40	0
10	10	74	34
10	20	98	58
10	30	120	80
10	40	136	96
10	50	150	110
10	60	176	136
5	65	191	151
5	70	206	166
5	75	221	181
5	80	238	198
5	85	256	216
5	90	271	231
5	95	290	250
5	100	308	268
5	105	324	284
5	110	341	301
5	115	361	321
5	120	381	341
5	125	400	360
5	130	418	378
5	135	432	392
5	140	453	413
5	145	470	430
5	150	490	450
5	155	507	467
5	160	521	481
5	165	540	500
5	170	561	521
5	175	582	542
3	178	600	560
3	181	610	570
3	184	620	580
3	187	634	594
3	190	645	605
3	193	660	620
3	196	672	632
3	199	689	649
3	202	700	660
3	205	714	674
3	208	729	689
3	211	750	710
3	214	770	730
3	217	790	750
3	220	810	770
3	223	830	790
3	226	850	810
3	229	870	830

Table E12: Values of DCP blows against the penetration readings (mm)

A	B	C	D
CH:1+100	--	--	--
No. Of Blows	Sum of No. Of Blows	Penetration (mm)	Corrected Penetration (mm)
0	0	40	0
10	10	66	26
5	15	76	36
5	20	85	45
5	25	96	56
5	30	103	63
5	35	113	73
5	40	125	85
5	45	136	96
5	50	148	108
5	55	161	121
5	60	172	132
5	65	184	144
5	70	198	158
5	75	212	172
5	80	226	186
5	85	240	200
5	90	254	214
5	95	270	230
5	100	284	244
5	105	304	264
5	110	326	286
5	115	346	306
5	120	357	317
5	125	364	324
5	130	372	332
5	135	377	337
5	140	384	344
5	145	390	350
5	150	394	354
5	155	400	360
5	160	402	362
5	165	410	370
5	170	412	372
5	175	415	375
5	180	420	380
5	185	432	392
5	190	448	408
5	195	458	418
5	200	467	427
5	205	474	434
5	210	489	449
5	215	498	458
5	220	513	473
5	225	534	494
5	230	547	507
5	235	558	518
5	240	567	527
5	245	578	538
5	250	597	557
5	255	604	564
5	260	618	578
5	265	645	605
5	270	657	617
5	275	679	639

Table E13: Values of DCP blows against the penetration readings (mm)

A	B	C	D
CH:1+200	--	--	--
No. Of Blows	Sum of No. Of Blows	Penetration (mm)	Corrected Penetration (mm)
0	0	40	0
10	10	60	20
10	20	70	30
10	30	86	46
10	40	104	64
10	50	124	84
10	60	146	106
10	70	167	127
10	80	184	144
10	90	206	166
10	100	228	188
10	110	250	210
5	115	264	224
5	120	279	239
5	125	298	258
5	130	316	276
5	135	336	296
5	140	356	316
5	145	372	332
5	150	385	345
5	155	390	350
5	160	406	366
5	165	424	384
5	170	441	401
5	175	462	422
5	180	482	442
5	185	497	457
5	190	512	472
5	195	530	490
5	200	542	502
5	205	556	516
5	210	562	522
5	215	578	538
5	220	590	550
5	225	600	560
5	230	607	567
5	235	620	580
5	240	640	600
5	245	670	630
5	250	686	646
3	253	700	660
3	256	718	678
3	259	723	683
3	262	734	694
3	265	760	720
3	268	773	733
3	271	790	750
3	274	807	767
3	277	820	780
3	280	838	798
3	283	854	814
3	286	880	840

Table E14: Values of DCP blows against the penetration readings (mm)

A	B	C	D
CH: 1+300	--	--	--
No. Of Blows	Sum of No. Of Blows	Penetration (mm)	Corrected Penetration (mm)
0	0	40	0
5	5	60	20
5	10	86	46
5	15	110	70
5	20	136	96
5	25	160	120
5	30	188	148
5	35	211	171
5	40	234	194
3	43	256	216
3	46	274	234
3	49	294	254
3	52	316	276
3	55	338	298
3	58	360	320
3	61	381	341
2	63	404	364
2	65	420	380
2	67	434	394
2	69	450	410
2	71	464	424
2	73	483	443
2	75	500	460
2	77	516	476
2	79	534	494
2	81	540	500
5	86	561	521
5	91	576	536
5	96	594	554
5	101	605	565
5	106	616	576
5	111	626	586
5	116	646	606
5	121	666	626
5	126	686	646
5	131	700	660
5	136	710	670
5	141	726	686
5	146	741	701
5	151	766	726
5	156	790	750
5	161	812	772
5	166	840	800
5	171	869	829
5	176	884	844

Table E15: Values of DCP blows against the penetration readings (mm)

A	B	C	D
CH:1+400	--	--	--
No. Of Blows	Sum of No. Of Blows	Penetration (mm)	Corrected Penetration (mm)
0	0	40	0
5	5	50	10
5	10	62	22
5	15	80	40
5	20	93	53
5	25	105	65
5	30	118	78
5	35	131	91
5	40	148	108
5	45	163	123
5	50	174	134
3	53	197	157
3	56	220	180
3	59	238	198
3	62	256	216
3	65	277	237
3	68	297	257
3	71	312	272
3	74	332	292
3	77	354	314
3	80	380	340
3	83	400	360
3	86	420	380
3	89	442	402
3	92	463	423
3	95	486	446
3	98	512	472
3	101	530	490
2	103	544	504
2	105	560	520
2	107	580	540
2	109	600	560
2	111	620	580
2	113	641	601
2	115	667	627
2	117	690	650
2	119	720	680
2	121	750	710
2	123	780	740
2	125	820	780
2	127	860	820

Table E16: Values of DCP blows against the penetration readings (mm)

A	B	C	D
CH:1+500	--	--	--
No. Of Blows	Sum of No. Of Blows	Penetration (mm)	Corrected Penetration (mm)
0	0	40	0
5	5	53	13
5	10	62	22
5	15	73	33
5	20	89	49
5	25	104	64
10	35	120	80
10	45	136	96
10	55	154	114
10	65	170	130
10	75	190	150
10	85	206	166
10	95	225	185
10	105	246	206
10	115	267	227
10	125	289	249
10	135	308	268
10	145	326	286
5	150	346	306
5	155	363	323
5	160	384	344
5	165	402	362
5	170	424	384
5	175	444	404
5	180	464	424
5	185	493	453
5	190	519	479
5	195	540	500
5	200	564	524
5	205	592	552
5	210	620	580
5	215	645	605
5	220	667	627
5	225	680	640
5	230	708	668
5	235	720	680
3	238	742	702
3	241	762	722
3	244	781	741
3	247	801	761
3	250	832	792
3	253	850	810
3	256	890	850

Table E17: Values of DCP blows against the penetration readings (mm)

A	B	C	D
CH:1+600	--	--	--
No. Of Blows	Sum of No. Of Blows	Penetration (mm)	Corrected Penetration (mm)
0	0	44	0
5	5	69	25
5	10	76	32
5	15	88	44
5	20	94	50
5	25	112	68
10	35	121	77
10	45	136	92
10	55	146	102
10	65	170	126
10	75	190	146
10	85	206	162
10	95	225	181
10	105	246	202
10	115	267	223
10	125	289	245
5	130	308	264
5	135	326	282
5	140	346	302
5	145	363	319
5	150	384	340
5	155	402	358
5	160	424	380
5	165	444	400
5	170	464	420
5	175	493	449
5	180	519	475
5	185	540	496
5	190	564	520
5	195	592	548
5	200	620	576
5	205	645	601
5	210	667	623
5	215	680	636
5	220	700	656
5	225	712	668
5	230	732	688
5	235	752	708
5	240	772	728
5	245	793	749
5	250	812	768
5	255	832	788
5	260	857	813

Table E18: Values of DCP blows against the penetration readings (mm)

A	B	C	D
CH:1+700	--	--	--
No. Of Blows	Sum of No. Of Blows	Penetration (mm)	Corrected Penetration (mm)
0	0	45	0
5	5	64	19
5	10	79	34
5	15	95	50
5	20	125	80
3	23	132	87
3	26	148	103
3	29	162	117
3	32	175	130
3	35	186	141
3	38	200	155
3	41	211	166
3	44	225	180
3	47	240	195
3	50	252	207
3	53	273	228
3	56	293	248
3	59	312	267
3	62	334	289
3	65	360	315
3	68	382	337
3	71	410	365
3	74	428	383
3	77	452	407
3	80	474	429
3	83	500	455
3	86	527	482
3	89	554	509
3	92	582	537
3	95	609	564
3	98	627	582
3	101	642	597
3	104	668	623
3	107	694	649
2	109	719	674
2	111	740	695
2	113	760	715
2	115	781	736
2	117	804	759
2	119	830	785
2	121	845	800
2	123	861	816

Table E19: Values of DCP blows against the penetration readings (mm)

A	B	C	D
CH:1+800--	--	--	--
No. Of Blows	Sum of No. Of Blows	Penetration (mm)	Corrected Penetration (mm)
0	0	42	0
5	5	57	15
5	10	71	29
5	15	83	41
5	20	98	56
5	25	111	69
5	30	120	78
5	35	135	93
5	40	170	128
5	45	190	148
5	50	211	169
5	55	236	194
5	60	264	222
5	65	290	248
5	70	310	268
5	75	330	288
5	80	350	308
5	85	372	330
5	90	401	359
5	95	430	388
5	100	461	419
5	105	496	454
5	110	546	504
5	115	580	538
3	118	610	568
2	120	630	588
2	122	650	608
2	124	670	628
2	126	689	647
2	128	706	664
2	130	726	684
2	132	741	699
2	134	759	717
2	136	779	737
2	138	796	754
2	140	812	770
2	142	826	784
2	144	841	799
2	146	856	814

Table E20: Values of DCP blows against the penetration readings (mm)

A	B	C	D
CH1+900	--	--	--
No. Of Blows	Sum of No. Of Blows	Penetration (mm)	Corrected Penetration (mm)
0	0	45	0
5	5	58	13
5	10	67	22
5	15	73	28
5	20	80	35
5	25	86	41
5	30	93	48
5	35	101	56
5	40	111	66
5	45	122	77
5	50	135	90
10	60	154	109
10	70	176	131
10	80	201	156
10	90	216	171
10	100	231	186
10	110	243	198
10	120	255	210
10	130	267	222
10	140	282	237
10	150	292	247
5	155	304	259
5	160	316	271
5	165	326	281
5	170	340	295
5	175	357	312
5	180	372	327
5	185	390	345
5	190	408	363
5	195	426	381
5	200	446	401
5	205	470	425
5	210	490	445
5	215	516	471
3	218	528	483
3	221	547	502
3	224	564	519
3	227	584	539
3	230	598	553
3	233	618	573
3	236	637	592
3	239	665	620
3	242	699	654
3	245	730	685
2	247	750	705
2	249	801	756
2	251	831	786
2	253	870	825

Table E21: Values of DCP blows against the penetration readings (mm)

A	B	C	D
CH:2+000	--	--	--
No. Of Blows	Sum of No. Of Blows	Penetration (mm)	Corrected Penetration (mm)
0	0	40	0
5	5	57	17
5	10	64	24
5	15	72	32
10	25	81	41
10	35	89	49
10	45	102	62
10	55	114	74
10	65	129	89
10	75	138	98
10	85	156	116
10	95	184	144
10	105	207	167
10	115	231	191
5	120	248	208
5	125	262	222
5	130	282	242
5	135	302	262
5	140	320	280
5	145	336	296
5	150	352	312
5	155	375	335
5	160	398	358
5	165	410	370
5	170	423	383
5	175	435	395
5	180	450	410
5	185	472	432
5	190	495	455
5	195	520	480
5	200	540	500
5	205	563	523
5	210	582	542
5	215	601	561
5	220	621	581
5	225	645	605
5	230	674	634
5	235	702	662
5	240	725	685
5	245	751	711
5	250	772	732

Table E22: Values of DCP blows against the penetration readings (mm)

A	B	C	D
CH:2+100	**CH:2+100**	--	--
No. Of Blows	Sum of No. Of Blows	Penetration (mm)	Corrected Penetration (mm)
0	0	40	0
5	5	55	15
5	10	66	26
5	15	77	37
5	20	86	46
5	25	92	52
5	30	104	64
5	35	114	74
5	40	120	80
5	45	126	86
5	50	138	98
5	55	147	107
5	60	162	122
5	65	179	139
5	70	194	154
5	75	214	174
5	80	238	198
5	85	264	224
5	90	290	250
5	95	316	276
5	100	345	305
5	105	379	339
3	108	395	355
3	111	414	374
3	114	424	384
3	117	437	397
3	120	446	406
3	123	454	414
5	128	465	425
5	133	484	444
5	138	504	464
5	143	526	486
5	148	548	508
5	153	581	541
3	156	601	561
3	159	621	581
3	162	640	600
3	165	661	621
3	168	684	644
3	171	707	667
3	174	737	697
3	177	767	727
3	180	798	758
3	183	832	792
3	186	854	814

Table E23: Values of DCP blows against the penetration readings (mm)

A	B	C	D
CH:2+200	--	--	--
No. Of Blows	Sum of No. Of Blows	Penetration (mm)	Corrected Penetration (mm)
0	0	43	0
5	5	58	15
5	10	70	27
5	15	84	41
5	20	100	57
5	25	114	71
5	30	122	79
5	35	136	93
5	40	146	103
5	45	157	114
5	50	162	119
5	55	172	129
5	60	184	141
5	65	200	157
5	70	216	173
5	75	236	193
5	80	254	211
3	83	273	230
3	86	296	253
3	89	319	276
3	92	342	299
3	95	364	321
3	98	390	347
3	101	404	361
3	104	415	372
3	107	426	383
3	110	435	392
3	113	446	403
3	116	456	413
3	119	462	419
3	122	471	428
5	127	484	441
5	132	494	451
5	137	504	461
5	142	510	467
5	147	524	481
5	152	536	493
5	157	550	507
5	162	564	521
5	167	578	535
5	172	598	555
5	177	616	573
5	182	637	594
5	187	657	614
5	192	682	639
5	197	704	661
5	202	722	679
5	207	742	699
5	212	767	724
3	215	794	751
3	218	812	769
3	221	824	781
3	224	844	801
3	227	862	819

Table E24: Values of DCP blows against the penetration readings (mm)

A	B	C	D
CH:2+300	--	--	--
No. Of Blows	Sum of No. Of Blows	Penetration (mm)	Corrected Penetration (mm)
0	0	45	0
5	5	54	9
5	10	64	19
5	15	73	28
5	20	82	37
5	25	88	43
5	30	99	54
5	35	106	61
5	40	115	70
5	45	124	79
5	50	130	85
5	55	138	93
5	60	147	102
5	65	160	115
5	70	172	127
5	75	184	139
5	80	196	151
5	85	208	163
5	90	220	175
5	95	236	191
5	100	252	207
5	105	272	227
2	107	284	239
2	109	296	251
2	111	309	264
2	113	321	276
2	115	336	291
2	117	347	302
2	119	358	313
2	121	370	325
2	123	382	337
2	125	394	349
2	127	407	362
2	129	420	375
2	131	432	387
2	133	446	401
2	135	462	417
2	137	476	431
2	139	486	441
2	141	496	451
5	146	517	472
5	151	536	491
5	156	556	511
5	161	572	527
5	166	584	539
5	171	604	559
5	176	618	573
5	181	635	590
5	186	656	611
5	191	675	630
5	196	697	652
5	201	716	671
5	206	737	692
5	211	756	711
5	216	774	729
5	221	790	745
5	226	812	767
5	231	832	787
5	236	854	809

Table E25: Values of DCP blows against the penetration readings (mm)

A	B	C	D
CH:2+400	--	--	--
No. Of Blows	Sum of No. Of Blows	Penetration (mm)	Corrected Penetration (mm)
0	0	48	0
5	5	54	6
5	10	64	16
5	15	73	25
5	20	82	34
5	25	88	40
5	30	99	51
3	33	106	58
3	36	115	67
3	39	124	76
3	42	130	82
3	45	138	90
3	48	147	99
3	51	160	112
3	54	172	124
3	57	184	136
5	62	196	148
5	67	208	160
5	72	220	172
5	77	236	188
5	82	252	204
5	87	272	224
10	97	284	236
10	107	296	248
10	117	309	261
10	127	321	273
10	137	336	288
10	147	347	299
10	157	358	310
10	167	370	322
10	177	382	334
10	187	394	346
10	197	407	359
10	207	420	372
10	217	432	384
10	227	446	398
10	237	462	414
10	247	476	428
10	257	486	438
10	267	496	448
5	272	517	469
5	277	536	488
5	282	556	508
5	287	572	524
5	292	584	536
5	297	604	556
5	302	618	570
5	307	635	587
5	312	656	608
5	317	675	627
5	322	697	649
5	327	716	668
5	332	737	689
5	337	756	708
5	342	774	726
5	347	790	742
5	352	812	764
5	357	832	784
5	362	854	806

Table E26: Values of DCP blows against the penetration readings (mm)

A	B	C	D
CH:2+500--	--	--	--
No. Of Blows	Sum of No. Of Blows	Penetration (mm)	Corrected Penetration (mm)
0	0	42	0
5	5	59	17
5	10	80	38
5	15	102	60
10	25	127	85
10	35	154	112
5	40	162	120
5	45	180	138
5	50	197	155
5	55	201	159
5	60	238	196
5	65	257	215
5	70	282	240
5	75	300	258
5	80	316	274
5	85	337	295
5	90	367	325
5	95	386	344
5	100	406	364
5	105	425	383
5	110	443	401
5	115	466	424
5	120	487	445
5	125	513	471
5	130	534	492
5	135	565	523
5	140	586	544
5	145	606	564
5	150	624	582
5	155	646	604
5	160	674	632
3	163	691	649
3	166	709	667
3	169	726	684
3	172	742	700
3	175	762	720
3	178	780	738
3	181	796	754
3	184	812	770
3	187	834	792
3	190	853	811

Table E27: Values of DCP blows against the penetration readings (mm)

A	B	C	D
CH:2+600	--	--	--
No. Of Blows	Sum of No. Of Blows	Penetration (mm)	Corrected Penetration (mm)
0	0	44	0
10	10	70	26
10	20	86	42
10	30	104	60
10	40	124	80
10	50	145	101
10	60	165	121
10	70	182	138
10	80	199	155
10	90	214	170
10	100	231	187
10	110	248	204
10	120	265	221
5	125	282	238
5	130	301	257
5	135	320	276
5	140	338	294
5	145	360	316
5	150	378	334
5	155	394	350
5	160	411	367
5	165	427	383
5	170	442	398
5	175	460	416
5	180	475	431
5	185	494	450
5	190	517	473
3	193	540	496
3	196	567	523
3	199	582	538
3	202	601	557
3	205	616	572
3	208	640	596
3	211	658	614
3	214	678	634
3	217	698	654
3	220	721	677
3	223	741	697
3	226	761	717
3	229	780	736
3	232	800	756
3	235	837	793
3	238	858	814

Table E28: Values of DCP blows against the penetration readings (mm)

A	B	C	D
CH:2+700--	--	--	--
No. Of Blows	Sum of No. Of Blows	Penetration (mm)	Corrected Penetration (mm)
0	0	40	0
5	5	56	16
5	10	64	24
5	15	70	30
5	20	79	39
5	25	90	50
5	30	100	60
5	35	106	66
10	45	120	80
10	55	137	97
10	65	154	114
10	75	170	130
10	85	184	144
10	95	194	154
10	105	206	166
10	115	215	175
10	125	226	186
10	135	237	197
10	145	246	206
10	155	254	214
10	165	263	223
10	175	273	233
10	185	282	242
10	195	292	252
10	205	300	260
10	215	308	268
10	225	320	280
10	235	326	286
10	245	340	300
10	255	357	317
10	265	370	330
10	275	390	350
5	280	410	370
5	285	430	390
5	290	450	410
5	295	467	427
5	300	481	441
5	305	504	464
5	310	521	481
5	315	542	502
5	320	568	528
5	325	594	554
5	330	617	577
5	335	638	598
5	340	662	622
5	345	687	647
5	350	713	673
5	355	742	702
4	359	776	736
4	363	816	776
4	367	860	820
4	371	891	851

Table E29: Values of DCP blows against the penetration readings (mm)

A	B	C	D
CH:2+800	--	--	--
No. Of Blows	Sum of No. Of Blows	Penetration (mm)	Corrected Penetration (mm)
0	0	40	0
5	5	57	17
5	10	80	40
5	15	95	55
5	20	111	71
5	25	125	85
5	30	137	97
5	35	154	114
5	40	170	130
5	45	184	144
5	50	194	154
5	55	206	166
5	60	215	175
5	65	226	186
5	70	237	197
5	75	246	206
5	80	254	214
5	85	263	223
5	90	273	233
5	95	282	242
5	100	292	252
5	105	300	260
5	110	308	268
5	115	320	280
5	120	326	286
5	125	340	300
10	135	357	317
10	145	370	330
10	155	390	350
10	165	410	370
10	175	430	390
10	185	450	410
5	190	467	427
5	195	481	441
5	200	504	464
5	205	521	481
5	210	542	502
5	215	568	528
5	220	594	554
5	225	617	577
5	230	638	598
5	235	662	622
5	240	687	647
5	245	713	673
5	250	742	702
5	255	776	736
5	260	816	776
5	265	860	820
4	269	891	851

Table E30: Values of DCP blows against the penetration readings (mm)

A	B	C	D
CH:2+900	--	--	--
No. Of Blows	Sum of No. Of Blows	Penetration (mm)	Corrected Penetration (mm)
0	0	40	0
5	5	56	16
5	10	66	26
5	15	77	37
5	20	92	52
5	25	106	66
5	30	124	84
5	35	142	102
5	40	157	117
5	45	177	137
5	50	205	165
5	55	231	191
5	60	252	212
5	65	302	262
3	68	320	280
3	71	351	311
3	74	384	344
3	77	425	385
5	82	457	417
5	87	500	460
5	92	554	514
5	97	600	560
5	102	650	610
5	107	699	659
5	112	735	695
5	117	770	730
5	122	800	760
5	127	830	790
5	132	853	813
5	137	868	828
5	142	899	859
5	147	929	889

Table E31: Values of DCP blows against the penetration readings (mm)

A	B	C	D
CH 3+000	--	--	--
No. Of Blows	Sum of No. Of Blows	Penetration (mm)	Corrected Penetration (mm)
0	0	40	0
5	5	56	16
5	10	66	26
5	15	77	37
5	20	92	52
5	25	106	66
5	30	124	84
5	35	142	102
5	40	157	117
5	45	177	137
5	50	182	142
5	55	194	154
5	60	204	164
5	65	214	174
5	70	225	185
5	75	236	196
5	80	246	206
5	85	256	216
3	88	270	230
3	91	281	241
3	94	292	252
3	97	304	264
3	100	314	274
3	103	322	282
3	106	332	292
2	108	340	300
2	110	356	316
2	112	367	327
2	114	382	342
2	116	393	353
2	118	406	366
2	120	416	376
2	122	427	387
2	124	437	397
2	126	450	410
2	128	463	423
2	130	475	435
2	132	492	452
2	134	507	467
2	136	521	481
2	138	539	499
2	140	556	516
2	142	579	539
2	144	605	565
2	146	628	588
2	148	650	610
2	150	676	636
2	152	698	658
2	154	718	678
2	156	728	688
2	158	765	725
2	160	784	744
2	162	801	761
2	164	817	777
2	166	831	791
2	168	844	804
2	170	859	819
2	172	878	838

Table E32: Values of DCP blows against the penetration readings (mm)

A	B	C	D
CH3+100	--	--	--
No. Of Blows	Sum of No. Of Blows	Penetration (mm)	Corrected Penetration (mm)
0	0	44	0
5	5	54	10
5	10	70	26
5	15	87	43
5	20	104	60
5	25	117	73
5	30	128	84
5	35	137	93
5	40	146	102
10	50	156	112
10	60	165	121
10	70	174	130
10	80	182	138
10	90	194	150
10	100	204	160
10	110	214	170
10	120	225	181
10	130	236	192
10	140	246	202
10	150	256	212
5	155	270	226
5	160	281	237
5	165	292	248
5	170	304	260
5	175	314	270
5	180	322	278
5	185	332	288
5	190	340	296
5	195	356	312
5	200	367	323
5	205	382	338
5	210	393	349
5	215	406	362
5	220	416	372
5	225	427	383
5	230	437	393
5	235	450	406
5	240	463	419
5	245	475	431
5	250	492	448
5	255	507	463
5	260	521	477
5	265	539	495
5	270	556	512
5	275	579	535
3	278	605	561
3	281	628	584
3	284	650	606
3	287	676	632
3	290	698	654
3	293	718	674
3	296	728	684
3	299	765	721
3	302	784	740
3	305	801	757
3	308	817	773
3	311	831	787
3	314	844	800
3	317	859	815
3	320	878	834

Table E33: Values of DCP blows against the penetration readings (mm)

A	B	C	D
CH3+200	--	--	--
No. Of Blows	Sum of No. Of Blows	Penetration (mm)	Corrected Penetration (mm)
0	0	40	0
5	5	52	12
5	10	64	24
5	15	79	39
5	20	92	52
5	25	110	70
5	30	131	91
5	35	157	117
3	38	171	131
3	41	192	152
3	44	211	171
3	47	231	191
3	50	249	209
3	53	261	221
3	56	274	234
3	59	287	247
3	62	300	260
3	65	310	270
3	68	321	281
3	71	331	291
3	74	340	300
3	77	351	311
5	82	368	328
5	87	389	349
5	92	404	364
5	97	417	377
5	102	431	391
5	107	452	412
5	112	468	428
5	117	484	444
5	122	501	461
5	127	526	486
5	132	557	517
3	135	579	539
3	138	601	561
3	141	638	598
3	144	681	641
1	145	700	660
1	146	720	680
1	147	730	690
1	148	746	706
1	149	757	717
1	150	777	737
1	151	802	762
2	153	840	800
2	155	880	840

Table E34: Values of DCP blows against the penetration readings (mm)

A	B	C	D
CH3+300	--	--	--
No. Of Blows	Sum of No. Of Blows	Penetration (mm)	Corrected Penetration (mm)
0	0	40	0
5	5	62	22
5	10	82	42
5	15	101	61
5	20	121	81
5	25	144	104
5	30	169	129
5	35	190	150
5	40	206	166
5	45	217	177
5	50	232	192
5	55	248	208
5	60	268	228
5	65	289	249
5	70	308	268
5	75	338	298
5	80	368	328
5	85	385	345
5	90	398	358
5	95	412	372
5	100	425	385
5	105	437	397
5	110	451	411
5	115	470	430
5	120	490	450
5	125	515	475
5	130	535	495
3	133	555	515
3	136	572	532
3	139	592	552
3	142	614	574
3	145	632	592
3	148	652	612
3	151	675	635
3	154	696	656
3	157	716	676
3	160	741	701
3	163	768	728
3	166	796	756
3	169	825	785
3	172	868	828
3	175	890	850

Table E35: Values of DCP blows against the penetration readings (mm)

A	B	C	D
CH3+400	--	--	--
No. Of Blows	Sum of No. Of Blows	Penetration (mm)	Corrected Penetration (mm)
0	0	42	0
5	5	60	18
5	10	77	35
10	20	94	52
10	30	112	70
10	40	140	98
5	45	152	110
5	50	164	122
5	55	175	133
5	60	185	143
5	65	194	152
5	70	204	162
10	80	222	180
10	90	239	197
10	100	259	217
10	110	290	248
5	115	304	262
5	120	321	279
5	125	337	295
5	130	356	314
5	135	377	335
5	140	400	358
3	143	410	368
3	146	422	380
3	149	434	392
3	152	445	403
3	155	456	414
3	158	472	430
3	161	484	442
3	164	490	448
3	167	506	464
3	170	517	475
3	173	530	488
3	176	538	496
3	179	554	512
3	182	564	522
3	185	576	534
3	188	590	548
3	191	604	562
3	194	617	575
3	197	634	592
3	200	651	609
3	203	670	628
3	206	690	648
3	209	711	669
3	212	735	693
3	215	756	714
3	218	770	728
3	221	794	752
3	224	814	772
3	227	832	790
3	230	850	808
3	233	870	828

Table E36: Values of DCP blows against the penetration readings (mm)

A	B	C	D
CH3+500	--	--	--
No. Of Blows	Sum of No. Of Blows	Penetration (mm)	Corrected Penetration (mm)
0	0	40	0
5	5	62	22
5	10	89	49
5	15	116	76
5	20	132	92
5	25	150	110
5	30	174	134
5	35	195	155
5	40	217	177
5	45	226	186
5	50	245	205
5	55	268	228
5	60	292	252
5	65	310	270
5	70	360	320
5	75	401	361
5	80	432	392
3	83	468	428
3	86	498	458
3	89	540	500
3	92	576	536
3	95	606	566
3	98	642	602
3	101	686	646
3	104	709	669
3	107	726	686
3	110	740	700
3	113	754	714
3	116	766	726
3	119	781	741
3	122	796	756
3	125	810	770
3	128	822	782
3	131	844	804
3	134	864	824
3	137	880	840

Table E37: Values of DCP blows against the penetration readings (mm)

A	B	C	D
CH3+600	--	--	--
No. Of Blows	Sum of No. Of Blows	Penetration (mm)	Corrected Penetration (mm)
0	0	42	0
5	5	60	18
5	10	75	33
5	15	90	48
5	20	104	62
5	25	122	80
5	30	142	100
5	35	164	122
5	40	184	142
5	45	200	158
5	50	215	173
5	55	234	192
5	60	254	212
5	65	277	235
5	70	300	258
5	75	328	286
5	80	367	325
3	83	387	345
3	86	404	362
3	89	422	380
3	92	444	402
3	95	462	420
3	98	481	439
3	101	510	468
3	104	532	490
3	107	551	509
3	110	574	532
3	113	610	568
3	116	644	602
3	119	671	629
3	122	700	658
3	125	730	688
3	128	760	718
3	131	790	748
3	134	816	774
3	137	840	798
3	140	870	828

Table E38: Values of DCP blows against the penetration readings (mm)

A	B	C	D
CH3+700	--	--	--
No. Of Blows	Sum of No. Of Blows	Penetration (mm)	Corrected Penetration (mm)
0	0	52	0
5	5	66	14
5	10	81	29
5	15	100	48
5	20	120	68
5	25	136	84
5	30	151	99
5	35	167	115
5	40	180	128
5	45	195	143
5	50	210	158
5	55	222	170
5	60	237	185
5	65	261	209
3	68	275	223
3	71	294	242
3	74	316	264
3	77	339	287
3	80	357	305
3	83	371	319
3	86	398	346
3	89	410	358
3	92	432	380
3	95	456	404
3	98	479	427
3	101	500	448
3	104	530	478
3	107	551	499
5	112	576	524
5	117	600	548
5	122	620	568
5	127	635	583
5	132	656	604
5	137	674	622
5	142	694	642
5	147	716	664
5	152	740	688
5	157	766	714
5	162	790	738
5	167	820	768
5	172	841	789
5	177	870	818

Table E39: Values of DCP blows against the penetration readings (mm)

A	B	C	D
CH3+800	--	--	--
No. Of Blows	Sum of No. Of Blows	Penetration (mm)	Corrected Penetration (mm)
0	0	42	0
5	5	63	21
5	10	89	47
5	15	118	76
5	20	130	88
5	25	150	108
5	30	170	128
5	35	192	150
5	40	210	168
5	45	222	180
5	50	235	193
5	55	242	200
5	60	260	218
5	65	270	228
5	70	286	244
5	75	300	258
5	80	320	278
5	85	340	298
5	90	364	322
5	95	400	358
5	100	431	389
5	105	459	417
5	110	489	447
5	115	508	466
3	118	530	488
3	121	550	508
3	124	570	528
3	127	589	547
3	130	604	562
3	133	621	579
3	136	636	594
3	139	654	612
3	142	668	626
3	145	682	640
3	148	700	658
3	151	712	670
3	154	726	684
3	157	739	697
3	160	754	712
3	163	772	730
3	166	791	749
3	169	811	769
3	172	829	787
3	175	850	808
3	178	870	828

Table E40: Values of DCP blows against the penetration readings (mm)

A	B	C	D
CH3+900	--	--	--
No. Of Blows	Sum of No. Of Blows	Penetration (mm)	Corrected Penetration (mm)
0	0	45	0
10	10	60	15
10	20	74	29
10	30	92	47
10	40	114	69
10	50	144	99
10	60	171	126
10	70	192	147
10	80	212	167
10	90	230	185
10	100	248	203
10	110	268	223
10	120	291	246
5	125	311	266
5	130	334	289
5	135	355	310
5	140	376	331
5	145	394	349
5	150	408	363
5	155	426	381
5	160	442	397
5	165	461	416
5	170	478	433
5	175	498	453
5	180	524	479
5	185	542	497
5	190	560	515
5	195	574	529
5	200	589	544
5	205	604	559
5	210	621	576
5	215	642	597
2	217	662	617
2	219	675	630
2	221	686	641
2	223	722	677
2	225	738	693
2	227	754	709
2	229	771	726
2	231	781	736
2	233	785	740
2	235	801	756
2	237	823	778
2	239	846	801
2	241	870	825

Table E41: Values of DCP blows against the penetration readings (mm)

A	B	C	D
CH4+000	--	--	--
No. Of Blows	Sum of No. Of Blows	Penetration (mm)	Corrected Penetration (mm)
0	0	46	0
5	5	72	26
5	10	104	58
5	15	112	66
5	20	136	90
5	25	151	105
5	30	167	121
5	35	182	136
5	40	195	149
5	45	209	163
5	50	222	176
5	55	234	188
5	60	251	205
5	65	270	224
5	70	292	246
3	73	307	261
3	76	324	278
3	79	341	295
3	82	360	314
3	85	380	334
3	88	396	350
3	91	420	374
3	94	438	392
3	97	453	407
3	100	470	424
3	103	486	440
3	106	507	461
3	109	527	481
3	112	546	500
3	115	564	518
3	118	580	534
3	121	597	551
2	123	616	570
1	124	636	590
1	125	660	614
1	126	693	647
1	127	711	665
1	128	729	683
1	129	748	702
1	130	768	722
1	131	784	738
1	132	801	755
1	133	820	774
1	134	840	794
1	135	860	814
1	136	872	826

Table E42: Values of DCP blows against the penetration readings (mm)

A	B	C	D
CH4+100	--	--	--
No. Of Blows	Sum of No. Of Blows	Penetration (mm)	Corrected Penetration (mm)
0	0	40	0
5	5	57	17
5	10	71	31
5	15	82	42
5	20	92	52
5	25	100	60
5	30	112	72
5	35	120	80
5	40	130	90
5	45	141	101
5	50	152	112
5	55	162	122
5	60	180	140
5	65	192	152
3	68	207	167
3	71	225	185
3	74	242	202
3	77	260	220
3	80	276	236
3	83	299	259
3	86	321	281
3	89	344	304
3	92	364	324
3	95	389	349
3	98	414	374
3	101	444	404
3	104	461	421
3	107	482	442
3	110	498	458
3	113	512	472
3	116	524	484
3	119	540	500
3	122	551	511
3	125	570	530
3	128	584	544
3	131	600	560
3	134	612	572
3	137	627	587
3	140	640	600
3	143	652	612
3	146	664	624
3	149	678	638
3	152	692	652
3	155	700	660
3	158	712	672
3	161	732	692
3	164	752	712
3	167	762	722
3	170	772	732
3	173	784	744
3	176	796	756
3	179	808	768
3	182	820	780
3	185	831	791
3	188	846	806
3	191	854	814
3	194	867	827
3	197	888	848

Table E43: Values of DCP blows against the penetration readings (mm)

A	B	C	D
CH4+200	--	--	--
No. Of Blows	Sum of No. Of Blows	Penetration (mm)	Corrected Penetration (mm)
0	0	44	0
5	5	64	20
5	10	85	41
5	15	98	54
5	20	110	66
5	25	120	76
5	30	129	85
5	35	140	96
5	40	148	104
5	45	160	116
5	50	172	128
5	55	185	141
5	60	204	160
5	65	218	174
5	70	234	190
5	75	250	206
5	80	267	223
5	85	284	240
5	90	302	258
5	95	318	274
5	100	338	294
5	105	356	312
5	110	370	326
5	115	384	340
5	120	395	351
5	125	408	364
5	130	421	377
5	135	440	396
5	140	454	410
5	145	470	426
5	150	489	445
5	155	509	465
5	160	531	487
5	165	556	512
5	170	584	540
5	175	612	568
5	180	642	598
5	185	684	640
3	188	711	667
3	191	752	708
3	194	772	728
3	197	801	757
3	200	831	787
3	203	852	808
3	206	890	846

Table E44: Values of DCP blows against the penetration readings (mm)

A	B	C	D
CH4+300	--	--	--
No. Of Blows	Sum of No. Of Blows	Penetration (mm)	Corrected Penetration (mm)
0	0	46	0
10	10	67	21
10	20	80	34
10	30	100	54
10	40	121	75
10	50	137	91
10	60	149	103
10	70	160	114
10	80	172	126
10	90	188	142
10	100	200	154
10	110	218	172
10	120	236	190
5	125	247	201
5	130	264	218
5	135	280	234
5	140	301	255
5	145	322	276
5	150	347	301
5	155	363	317
5	160	380	334
5	165	401	355
5	170	414	368
5	175	430	384
5	180	450	404
5	185	464	418
5	190	484	438
5	195	502	456
5	200	520	474
5	205	538	492
5	210	548	502
5	215	560	514
5	220	568	522
5	225	580	534
5	230	591	545
5	235	601	555
5	240	618	572
5	245	634	588
5	250	648	602
5	255	660	614
5	260	670	624
5	265	681	635
5	270	693	647
5	275	707	661
5	280	720	674
5	285	734	688
5	290	745	699
5	295	755	709
5	300	765	719
5	305	788	742
5	310	790	749
5	315	812	766
5	320	830	784
5	325	842	796
5	330	860	814
5	335	870	824

Table E45: Values of DCP blows against the penetration readings (mm)

A	B	C	D
CH4+400	--	--	--
No. Of Blows	Sum of No. Of Blows	Penetration (mm)	Corrected Penetration (mm)
0	0	45	0
5	5	70	25
5	10	96	51
5	15	120	75
5	20	137	92
5	25	152	107
5	30	164	119
5	35	186	141
5	40	207	162
5	45	220	175
5	50	240	195
5	55	254	209
5	60	267	222
5	65	280	235
5	70	292	247
5	75	307	262
5	80	310	265
5	85	320	275
5	90	340	295
5	95	345	300
5	100	350	305
5	105	365	320
5	110	381	336
5	115	397	352
5	120	416	371
5	125	440	395
5	130	460	415
5	135	482	437
5	140	512	467
3	143	530	485
3	146	544	499
3	149	561	516
3	152	582	537
3	155	596	551
3	158	610	565
3	161	620	575
3	164	642	597
3	167	665	620
3	170	686	641
3	173	708	663
3	176	727	682
3	179	748	703
3	182	768	723
3	185	787	742
3	188	805	760
3	191	822	777
3	194	841	796
3	197	863	818

Table E47: Values of DCP blows against the penetration readings (mm)

A	B	C	D
CH4+600	--	--	--
No. Of Blows	Sum of No. Of Blows	Penetration (mm)	Corrected Penetration (mm)
0	0	40	0
5	5	58	18
5	10	74	34
5	15	88	48
5	20	104	64
5	25	120	80
5	30	134	94
5	35	151	111
5	40	165	125
5	45	184	144
5	50	200	160
5	55	214	174
5	60	230	190
5	65	245	205
5	70	260	220
5	75	274	234
5	80	288	248
5	85	293	253
5	90	310	270
5	95	324	284
5	100	348	308
5	105	368	328
5	110	384	344
5	115	401	361
5	120	428	388
5	125	440	400
5	130	460	420
5	135	484	444
5	140	511	471
5	145	538	498
5	150	567	527
5	155	594	554
5	160	624	584
5	165	654	614
5	170	690	650
5	175	730	690
5	180	772	732
3	183	804	764
3	186	831	791
3	189	840	800

Table E48: Values of DCP blows against the penetration readings (mm)

A	B	C	D
CH4+700	--	--	--
No. Of Blows	Sum of No. Of Blows	Penetration (mm)	Corrected Penetration (mm)
0	0	40	0
5	5	52	12
5	10	60	20
5	15	68	28
5	20	77	37
5	25	91	51
5	30	105	65
5	35	120	80
5	40	138	98
5	45	156	116
5	50	172	132
5	55	189	149
5	60	209	169
5	65	228	188
5	70	248	208
5	75	272	232
5	80	295	255
5	85	320	280
5	90	348	308
5	95	364	324
5	100	384	344
5	105	396	356
5	110	410	370
5	115	425	385
5	120	444	404
5	125	468	428
5	130	494	454
5	135	524	484
5	140	552	512
5	145	589	549
3	148	616	576
3	151	635	595
3	154	656	616
3	157	674	634
3	160	696	656
3	163	721	681
3	166	751	711
3	169	776	736
3	172	804	764
3	175	832	792
3	178	859	819
1	179	870	830

Table E49: Values of DCP blows against the penetration readings (mm)

A	B	C	D
CH4+800	--	--	--
No. Of Blows	Sum of No. Of Blows	Penetration (mm)	Corrected Penetration (mm)
0	0	40	0
5	5	62	22
5	10	90	50
5	15	112	72
5	20	132	92
5	25	154	114
5	30	176	136
5	35	188	148
5	40	210	170
10	50	235	195
10	60	254	214
10	70	272	232
10	80	291	251
10	90	310	270
10	100	331	291
10	110	350	310
10	120	364	324
10	130	380	340
10	140	400	360
5	145	419	379
5	150	450	410
5	155	472	432
5	160	510	470
5	165	522	482
5	170	556	516
5	175	570	530
5	180	584	544
3	183	601	561
5	188	617	577
5	193	638	598
5	198	654	614
5	203	672	632
5	208	690	650
5	213	709	669
5	218	728	688
5	223	746	706
5	228	774	734
5	233	800	760
5	238	820	780
5	243	850	810
5	248	875	835

Table E50: Values of DCP blows against the penetration readings (mm)

A	B	C	D
CH4+900	--	--	--
No. Of Blows	Sum of No. Of Blows	Penetration (mm)	Corrected Penetration (mm)
0	0	40	0
10	10	68	28
10	20	96	56
10	30	118	78
10	40	130	90
10	50	144	104
10	60	159	119
10	70	171	131
10	80	186	146
10	90	197	157
10	100	210	170
5	105	219	179
5	110	236	196
5	115	248	208
5	120	265	225
5	125	280	240
5	130	300	260
5	135	310	270
5	140	320	280
5	145	336	296
5	150	362	322
5	155	386	346
5	160	406	366
5	165	426	386
5	170	446	406
5	175	463	423
5	180	478	438
5	185	495	455
5	190	512	472
5	195	532	492
5	200	559	519
5	205	590	550
5	210	613	573
5	215	634	594
5	220	650	610
5	225	670	630
5	230	687	647
5	235	703	663
5	240	713	673

Table E51: Values of DCP blows against the penetration readings (mm)

A	B	C	D
CH5+000	--	--	--
No. Of Blows	Sum of No. Of Blows	Penetration (mm)	Corrected Penetration (mm)
0	0	40	0
5	5	56	16
5	10	80	40
5	15	104	64
5	20	125	85
5	25	151	111
5	30	177	137
5	35	207	167
5	40	232	192
5	45	252	212
10	55	268	228
10	65	280	240
10	75	300	260
10	85	310	270
10	95	320	280
10	105	346	306
10	115	362	322
10	125	386	346
10	135	406	366
10	145	426	386
10	155	446	406
10	165	463	423
10	175	478	438
10	185	495	455
5	190	512	472
5	195	532	492
5	200	559	519
5	205	590	550
5	210	613	573
5	215	634	594
5	220	650	610
5	225	662	622
5	230	687	647
5	235	700	660
5	240	713	673
5	245	723	683

Table E52: Values of DCP blows against the penetration readings (mm)

A	B	C	D
CH5+100	--	--	--
No. Of Blows	Sum of No. Of Blows	Penetration (mm)	Corrected Penetration (mm)
0	0	40	0
10	10	52	12
10	20	70	30
10	30	96	56
10	40	126	86
10	50	137	97
10	60	148	108
10	70	172	132
10	80	190	150
10	90	220	180
5	95	250	210
5	100	268	228
5	105	282	242
5	110	292	252
5	115	312	272
5	120	331	291
5	125	357	317
5	130	390	350
5	135	409	369
5	140	424	384
5	145	442	402
5	150	466	426
5	155	486	446
5	160	492	452
5	165	512	472
5	170	532	492
5	175	559	519
5	180	590	550
2	182	613	573
2	184	634	594
2	186	650	610
2	188	670	630
2	190	687	647
2	192	703	663
2	194	713	673
2	196	723	683

Table E53: Values of DCP blows against the penetration readings (mm)

A	B	C	D
CH5+200	--	--	--
No. Of Blows	Sum of No. Of Blows	Penetration (mm)	Corrected Penetration (mm)
0	0	40	0
5	5	61	21
5	10	79	39
5	15	97	57
5	20	112	72
5	25	128	88
5	30	137	97
5	35	150	110
5	40	161	121
5	45	170	130
5	50	184	144
5	55	193	153
5	60	204	164
5	65	210	170
5	70	222	182
5	75	248	208
5	80	268	228
5	85	287	247
5	90	314	274
5	95	337	297
5	100	350	310
5	105	358	318
5	110	364	324
5	115	390	350
5	120	409	369
5	125	424	384
5	130	442	402
5	135	466	426
3	138	486	446
3	141	509	469
3	144	522	482
3	147	532	492
3	150	559	519
3	153	590	550
3	156	613	573
3	159	634	594
3	162	650	610
3	165	670	630
3	168	687	647
3	171	703	663
3	174	713	673
3	177	723	683